ISTANBUL TECHNICAL UNIVERSITY ★ GRADUATE SCHOOL

FORMATION OF ANTHOCYANIN-RICH BLACK CARROT EXTRACT LOADED POTATO PROTEIN PARTICLES BY TERNARY COMPRESSED CO_2-ETHANOL-WATER MIXTURE EXTRACTION AND PGSS-DRYING

Ph.D. THESIS

Merve YAVUZ DÜZGÜN

Department of Food Engineering

Food Engineering Programme

AUGUST 2021

ISTANBUL TECHNICAL UNIVERSITY ★ GRADUATE SCHOOL

FORMATION OF ANTHOCYANIN-RICH BLACK CARROT EXTRACT LOADED POTATO PROTEIN PARTICLES BY TERNARY COMPRESSED CO_2-ETHANOL-WATER MIXTURE EXTRACTION AND PGSS-DRYING

Ph.D. THESIS

Merve YAVUZ DÜZGÜN
(506142501)

Department of Food Engineering

Food Engineering Programme

Thesis Advisor: Prof. Dr. Beraat ÖZÇELİK

AUGUST 2021

İSTANBUL TEKNİK ÜNİVERSİTESİ ★ LİSANSÜSTÜ EĞİTİM ENSTİTÜSÜ

ÜÇLÜ SIKIŞTIRILMIŞ CO_2-ETANOL-SU KARIŞIMI EKSTRAKSİYONU VE PGSS-KURUTMA İLE ANTOSİYANİNCE ZENGİN KARA HAVUÇ ÖZÜTÜ YÜKLÜ PATATES PROTEİNİ PARTİKÜLLERİ OLUŞUMU

DOKTORA TEZİ

Merve YAVUZ DÜZGÜN
(506142501)

Gıda Mühendisliği Anabilim Dalı

Gıda Mühendisliği Programı

Tez Danışmanı: Prof. Dr. Beraat ÖZÇELİK

AĞUSTOS 2021

Merve YAVUZ DÜZGÜN, a Ph.D. student of ITU Graduate School student ID 506142501 successfully defended the dissertation entitled "FORMATION OF ANTHOCYANIN-RICH BLACK CARROT EXTRACT LOADED POTATO PROTEIN PARTICLES BY TERNARY COMPRESSED CO_2-ETHANOL-WATER MIXTURE EXTRACTION AND PGSS-DRYING", which she prepared after fulfilling the requirements specified in the associated legislations, before the jury whose signatures are below.

Thesis Advisor :	**Prof. Dr. Beraat ÖZÇELİK** Istanbul Technical University	.....
Jury Members :	**Prof. Dr. Gürbüz GÜNEŞ** Istanbul Technical University	.....
	Assoc. Prof. Dr. Sibel ULUATA Inönü University	.....
	Assoc. Prof. Dr. Aslı CAN KARACA Istanbul Technical University	.....
	Dr. Ceren DAŞKAYA DİKMEN Pladis Global	.....

Date of Submission : 8 July 2021
Date of Defense : 16 August 2021

To my beloved family,

FOREWORD

Firstly, I acknowledge that this thesis was supported by the Research Fund of ITU with a project number of MDK-2018-41534. The part of the thesis was also supported by TUBITAK through the programme named 2214-A - International Research Fellowship Programme for PhD Students with an application number of 1059B141700764.

I would like to express my sincere heartfelt gratitude to my supervisor and mentor, Prof. Dr. Beraat ÖZÇELİK for all her contributions, support, patience, and guidance. Her understanding attitude and enthusiasm have been motivational throughout the research.

The part of this thesis was conducted at Ruhr University. It is my privilege to express my thanks to Prof. Dr. Eckhard WEIDNER for accepting me to study the PGSS system for one year in his laboratory. I am also thankful to Dr. Sabine KARETH for her guidance. The other part of the thesis on the coacervation was conducted on Hohenheim University. I am also grateful to Prof. Dr. Jochen WEISS who accepted me to conduct a study for a semester in his laboratory under his valuable supervision. My special thanks to Dr. Benjamin ZEEB for his guidance and help.

I am thankful to my workfellows Cansu TOPKAYA, Eda ŞENSU, and Eda Nur AYAR for their contribution to laboratory studies. I want to extent my thanks to Evren DEMİRCAN who always there to help, Ceren DAŞKAYA DİKMEN for her friendship and my research group members Ümit ALTUNTAŞ, Mine GÜLTEKİN ÖZGÜVEN and Kadriye Nur KASAPOĞLU for motivational support. My special thanks are attended to my office-mate, Gülay ÖZKAN for her support and friendship. I would also thank to all members of ITU Food Engineering Department.

I am also grateful to all members of the Particle Technology Department at Ruhr University Bochum who are always there to help. My special thanks are to Mark-Andre WÜSTKAMP for his help in all kinds of laboratory issues. I am also thankful to Dr. Alina HANU and Khalil AOUN for their help with the PGSS-drying system. My special thanks are to Dr. Kristen GRÜBEL and Dr. Vincent BÜRK for their support and friendship during my one-year stay abroad.

I am deeply grateful to my mom Nilüfer YAVUZ and my dad Ali YAVUZ, they have given unconditional care, support and always believed in me. Under their wisdom, constant encouragement, motivations, and endless guidance, I have reached this level.

Lastly, and most importantly I would like to thank my husband Okan Onur DÜZGÜN for his great support, patience, being stood by me through all struggles and understanding attitude. I would like to dedicate this thesis to him, to my mom and to my dad.

I did not forget you my little one, you began to give power to your mom already now, thank you to you too.

August 2021

Merve YAVUZ DÜZGÜN
(Food Engineer, M. Sc)

TABLE OF CONTENTS

Page

ABBREVIATIONS

ANOVA : Analysis of Variance
AC-CUPRAC : Antioxidant Capacity measured by CUPRAC assay
AC-DPPH : Antioxidant Capacity measured by DPPH assay
AR : Anthocyanin Retention
BCE : Black Carrot Extract
CCD : Central Composite Design
CUPRAC : Cupric Reducing Antioxidant Capacity
DB : Degree of Blockiness
DE : Degree of Esterification
DPPH : 1,1-Diphenyl-2-picrylhydrazyl
DSC : Differential Scanning Calorimetry
ECP : Emulsified Core-Particles
EE : Encapsulation Efficiency
FDP : Freeze-dried Particles
FT-IR : Fourier Transform Infrared Spectroscopy
NECP : Non-emulsified Core-Particles
PGSS : Particles from Gas-Saturated Solutions
PGSSDP : PGSS-dried Particles
PPI : Potato Protein Isolate
RSM : Response Surface Methodology
SEM : Scanning Electron Microscopy
SFE : Supercritical Fluid Technology
TAC : Total Antioxidant Capacity
TMAC : Total Monomeric Anthocyanin Content
TFC : Total Flavonoid Content
TPC : Total Phenolic Content

LIST OF TABLES

Page

LIST OF FIGURES

Page

FORMATION OF ANTHOCYANIN-RICH BLACK CARROT EXTRACT LOADED POTATO PROTEIN PARTICLES BY TERNARY COMPRESSED CO_2-ETHANOL-WATER MIXTURE EXTRACTION AND PGSS-DRYING

SUMMARY

Black carrot anthocyanins have importance for food industry as it is a natural colorant and possesses health beneficial effects regarding the functional food and beverages. Anthocyanins are conventionally extracted by using organic solvents such as methanol, acetone or water with small amount of hydrochloric acid or formic acid. These methods are problematic due to the residues of organic solvents remaining in extracts that are associated with food safety or due to the degradation of anthocyanins at high temperatures which required for acidified water extraction. Due to these problems, it is crucial to develop novel methods which are environmentally sustainable and efficient, resulting in high yields. The extraction using sub- and supercritical carbon dioxide (sc-CO_2) has been growing as an alternative to conventional extraction, as it can potentially fulfill these demands. The anthocyanin- rich extracts are still very labile to different environmental conditions. Encapsulation or complexation with different biopolymers of bioactive compounds provides a good solution before the incorporation of these valuable compounds in food and beverages. Complex coacervation is one of the encapsulation methods which finds a widespread relevance in functional biomaterials consisting the food and beverage area. It is a physicochemical process that be conducted at mild temperatures without high pressures. The other process applied in this thesis for the purpose of complexation was Particles from Gas saturated Solutions–Drying. It could enable a successful drying and micronization of aqueous solutions at operation temperatures significantly below the minimum temperatures required by conventional spray-drying, making it a suitable technique for the processing of thermally-sensitive materials.

This thesis contained four work-packages. In the first work package, potato protein isolate was characterized in terms of solubility, surface charge and phase separation. Potato protein - pectin complexes were then formed, and the impact of the pectin source, degree of esterification and the biopolymer ratio on the complex coacervation was investigated. The complexes were characterized in terms of surface charge, viscosity, microstructure and phase separation. Potato protein and potato protein complexes were studied to form the wall material which will be studied in the third and the fourth work packages. In the second work package, core material to be used was studied. Pressurized ternary solvent of CO_2-water-ethanol mixtures was employed to derive anthocyanin-rich extracts from black carrots. The effect of process parameters which are pressure, temperature and ethanol-water ratio were investigated and the optimum values were found using RSM with response variables of total monomeric anthocyanin, total flavonoid, total phenolic content and total antioxidant capacity. In the third part of the thesis, coacervation was employed to formulate black carrot extract - potato protein - pectin particles with and without emulsification step via the freeze-drying. The effect of core-to-wall ratio and the wall material concentration was studied. The last part included the production of potato protein

particles loaded with black carrot extract via the PGSS-Drying. The effect of process parameters which are pressure, temperature and nozzle size was investigated. Spray-drying and freeze-drying were also applied to produce particles for comparison with commercial counterparts. The particles obtained with complex coacervation - freeze-drying and PGSS-drying was characterized in terms of moisture, hygroscopicity, encapsulation efficiency, particle size, morphology and thermal properties.

The protein-pectin ratio and degree of esterification of pectin substantially influenced the interaction behavior and phase separation of the protein-pectin mixtures. Citrus pectin at a high degree of esterification (DE 70) was selected for further studies as it gives complexes at a lower viscosity. The complexes generated at a protein-pectin ratio of 2.5 had approximately zero surface charge, indicating a strong interaction between protein and pectin. Thus, the protein-pectin ratio and pectin to be used in further encapsulation study was decided. In the second part of the study, RSM was applied to produce core material which is anthocyanin-rich black carrot extract at the optimum conditions. The optimized process parameters were estimated to be the pressure of 304 bar, the temperature of 52ºC and the ethanol-water ratio of 48/52. Extraction using these optimum parameters gave the highest total monomeric anthocyanin content (123 mg/L), total phenolic content (62 mg/100mL), total flavonoid content (44 mg/100mL), CUPRAC (473 mg/100mL) and DPPH (120 mg/100mL) antioxidant capacity. The experimental values were coherent with those predicted, thus expressing the fitness of the model and the success of CCD in the optimization of extraction conditions. In the third part of the thesis, anthocyanin-rich black carrot extract was complexed with potato protein - citrus pectin DE 70 successfully with or without emulsification step. Black carrot extract loaded potato protein particles (BCE-PPI) without the incorporation of pectin was also generated. Hygroscopicity of non-emulsified core particles were ranged between 18.13 - 28.65% (w/w, dry basis) while it was 10.15-17.49% (w/w, dry basis) for emulsified core particles. BCE-PPI particles had similar hygroscopicity values with the non-emulsified core particles. It seems that CP incorporation did not have any positive effect on hygroscopicity. In general, ECP could be regarded as non-hygroscopic while NECP was found slightly hygroscopic. The mean particle diameter of powders ranged from 65.05 to 152.47 μm. Despite an increasing trend with an increasing core-to-wall ratio for the PPI-CP complexed with BCE without emulsification, the difference in measurements was not statistically significant ($p > 0.05$). However, ECP showed lower particle size values with increased wall concentration at the constant core-to-wall ratio. EE of NECP and ECP was between 69.26 - 82.84% and 85.48 - 90.15% while AR was between 79.08 - 102.16% and 53.90 – 83.37%, respectively. In general, for both NECP and ECP, the increased core-to-wall and wall material concentration did not affect EE and AR significantly ($p > 0.05$). Only a small increase was observed for NECP5 in comparison to NECP4 which has lower core-to-wall ratio at the same wall material concentration. Regarding ECP, a decreasing trend was observed at increasing core-to-wall ratio for both low and high wall material concentration. According to DSC thermograms, microcapsules obtained with double emulsion showed a sharp and narrow peak while the non-emulsified microcapsules gave a large and broad peak. Moreover, a slight difference was observed in melting peak temperatures of ECP and NECP. The melting peaks ranged between 133.38- 146.36ºC for ECP and 118.24 – 128.1ºC for NECP. DSC thermograms proved that the black carrot extract was successfully encapsulated in potato protein – pectin complexes as its thermal behavior was not observed in the produced particles. FT-IR spectra of ECP proved the complexation between PPI and CP as 2961 cm^{-1}, 2931 cm^{-1} and 2874 cm^{-1} of PPI disappeared, a new peak formed at

1539 cm^{-1} and a shift was seen in the amide I band of PPI from 1453 cm^{-1} to 1456 cm^{-1}. This new peak was also observed in NECP probably due to interaction between PPI, CP and BCE which was supported by ζ-potential measurements. Large and irregular particles were observed in SEM micrographs which is suitable with particle size measurements. In the last part of the thesis, PGSS-drying was employed to produce black carrot extract – potato protein particles. It was found that GLR and spray tower temperature were two decisive parameters on the final moisture content of particles. The experiments giving particles with moisture content under 10% were regarded as successful and further experiments were conducted on these particles. The hygroscopicity of the produced particles was ranged from 18.79% to 24.94% (w/w, dry basis) which could be regarded as slightly hygroscopic according to the conventional criteria. The mean particle size values D[4,3] and d50 were ranged between 9.28 – 14.97 μm and 8.04 - 11.56 μm, respectively. PGSS-dried particles did not show any significant difference ($p > 0.05$) with SDP and FDP, indicating the possibility of powder production with PGSS having the similar particle size values with commercial powdered products. EE of particles obtained at different parameters were between 69.49 - 81.78%, while it was 78.58% and 84.80% for FDP and SDP, respectively. Except the PGSSDP5 which was produced with the highest GLR, EE did not differ significantly ($p > 0.05$) between all samples including FDP and SDP. AR was found in a narrow range (84.02 ± 1.34 – 87.27 ± 4.09%) for PGSS-dried particles which was probably due to the spray tower temperature lower than 42.73 ± 0.61°C. There was no statistical difference ($p > 0.05$) between PGSS-dried particles and FDP. However, SDP had lower AR than other samples. DSC thermograms showed that crystal transition peaks of BCE were not observed in PPI-BCE particles regardless of the applied drying process which was corroborating the amorphous state of the BCE when it is complexed with PPI. In general, it indicated the success of encapsulation and improved thermal properties of particles. FT-IR results suggested that BCE was not only incorporated in the carrier's matrix through physical interaction but also with the formation of chemical bond indicating a more efficient encapsulation. This was confirmed by ζ-potential measurements, PPI-BCE particles had significantly lower values compared to individual PPI had. Based on the SEM micrographs, PGSSDP were smaller than SDP, but they formed agglomerates very easily composed by partially fused spheres, producing much larger clusters. *In vitro* bioaccessability indicated that the encapsulation with PPI via freeze-drying, spray-drying and PGSS-drying did not affect the anthocyanin gastric release significantly ($p > 0.05$) as compared to release from black carrot extract. However, intestinal conditions caused a high decomposition of anthocyanins in un-encapsulated black carrot extract. Encapsulation with PPI caused slightly higher release of TMA from the particles produced by freeze-drying and spray-dried particles which are PGSSDP1, PGSSDP2, PGSSDP3 and PGSSDP4.

ÜÇLÜ SIKIŞTIRILMIŞ CO_2-ETANOL-SU KARIŞIMI EKSTRAKSİYONU VE PGSS-KURUTMA İLE ANTOSİYANİNCE ZENGİN KARA HAVUÇ ÖZÜTÜ YÜKLÜ PATATES PROTEİNİ PARTİKÜLLERİ OLUŞUMU

ÖZET

Sağlıklı beslenme tercihlerinin artması ile fonksiyonel gıdalara olan talep dünya çapında artış göstermiştir. Fonksiyonel gıdaların üretim yöntemlerinden biri, ürünü biyoaktif bileşenlerle zenginleştirmektir. Bunun için ilk adım, ilgili biyoaktif bileşeni verimli bir yöntem kullanarak elde etmektir. İkinci adım, bileşenin doğrudan gıda veya içeceğe eklenmesi bazı sorunlara yol açabileceğinden, biyoaktif bileşenin kapsüllenmesi olabilmektedir. Proses veya depolama koşullarına duyarlılık ve/veya metabolizma sırasında düşük biyoyararlanım bu sorunlar arasında sayılabilir. Biyoaktif bileşenler fonksiyonel gıdalara enkapsüle edilmiş formda eklenerek, bu bileşenlerin biyoyararlanımları ve proses koşullarına karşı kararlılığı arttırılabilmektedir. Siyah havuç antosiyaninleri, doğal renklendirici özellikleri ve sağlığa yararlı etkileri nedeniyle gıda endüstrisi için önem arz etmektedir. Antosiyaninler geleneksel olarak metanol ve aseton gibi organik çözücüler veya az miktarda hidroklorik asit veya formik asit içeren su kullanılarak özütlenir. Bu yöntemler, gıda güvenliği ile ilişkili olarak özütlerde kalan organik çözücü kalıntıları ve/veya asitlendirilmiş su ekstraksiyonu için gerekli olan yüksek sıcaklıklarda antosiyaninlerin bozunması gibi bazı sorunlara neden olur. Bu sorunlardan dolayı, yüksek verimle sonuçlanan, sürdürülebilir ve verimli yeni yöntemler geliştirmek önem taşımaktadır. Alt- ve süper-kritik karbondioksit (sub- and sc-CO_2) kullanılarak yapılan ekstraksiyon (özütleme işlemi), bu talepleri karşılayabileceğinden, geleneksel ekstraksiyona önemli bir alternatif oluşturmaktadır. Bununla beraber, antosiyanin açısından zengin özütler, farklı çevresel koşullara karşı kararsızdır. Biyoaktif bileşenlerin yiyecek ve içeceklere dahil edilmesinden önce, çeşitli biyopolimerler ile kapsülleme işlemi uygun bir çözüm sunar. Kompleks koaservasyon, yiyecek ve içecek alanını da kapsayan fonksiyonel biyomateryallerde yaygın olarak geçerlilik bulan enkapsülasyon yöntemlerinden biridir. Yüksek basınçlar olmadan ılıman koşullarda gerçekleştirilebilen fizikokimyasal bir işlemdir. Tezde, enkapsülasyon amacıyla uygulanan bir diğer işlem Gazla Doymuş Çözeltilerden Parçacıklar – Kurutma olmuştur. Bu işlem, geleneksel püskürtmeli kurutmanın gerektirdiği minimum sıcaklıkların önemli ölçüde altındaki çalışma sıcaklıklarında, sulu çözeltilerin başarılı bir şekilde kurutulmasını ve mikronizasyonunu sağlayabilir, bu da işlemi termal olarak hassas malzemelerin işlenmesi için özel olarak uygun bir teknik haline getirmektedir.

Bu tez dört bölümden oluşmaktadır. Birinci kısımda, patates proteini izolatı çözünürlük, yüzey yükü ve faz ayrımı açısından karakterize edilmiştir. Daha sonra patates proteini - pektin kompleksleri oluşturulmuş ve pektin kaynağının, esterleşme derecesinin ve biyopolimer oranının kompleks koaservasyon üzerindeki etkisi araştırılmıştır. Kompleksler; yüzey yükü, viskozite, mikro yapı ve faz ayrımı açısından karakterize edilmiştir. Üçüncü ve dördüncü bölümlerde kullanılacak olan duvar materyalini oluşturmak için patates proteini ve patates proteini kompleksleri çalışılmıştır. İkinci kısımda, kullanılacak olan çekirdek material üzerinde çalışılmıştır.

Siyah havuçlardan antosiyanin açısından zengin özütler elde etmek için sıkıştırılmış CO_2-su-etanol karışımından faydalanılmıştır. Basınç, sıcaklık ve etanol-su oranı gibi proses parametrelerinin etkisi araştırılmış ve yanıt değişkenleri olan toplam monomerik antosiyanin, toplam flavonoid, toplam fenolik içerik ve toplam antioksidan kapasite ile RSM kullanılarak optimum değerler bulunmuştur. Tezin üçüncü bölümünde, dondurarak kurutma yoluyla siyah havuç özütü - patates proteini - pektin partikülleri emülsifikasyon işlemine tabi tutularak veya tutulmadan koaservasyon yöntemi ile formüle edilmiştir. Çekirdek-duvar materyali oranı ve duvar malzemesi konsantrasyonunun etkisi incelenmiştir. Son kısım, PGSS-drying yoluyla siyah havuç özütü yüklü patates proteini parçacıklarının üretimini içermiştir. Basınç, sıcaklık ve nozül boyutu parametrelerinin etkisi araştırılmıştır. Üçüncü ve dörüdncü kısımlarda elde edilen partiküller nem, higroskopiklik, kapsülleme verimliliği, partikül boyutu, morfoloji ve termal özellikler açısından karakterize edilmiştir.

Çalışmanın ilk kısmında, patates proteini çözeltisinin ζ-potansiyeli değerinin, pH 8'den 3'e düşürüldüğünde, negatiften (−1,05 mV) pozitife (+23,7 mV) doğru değiştiği gözlenmiştir. Patates proteinin izoelektrik noktası pH 7-8 aralığında belirlenmiştir. En düşük çözünürlük (53,52%) alkali koşullarda pH 8'de elde edilirken, düşen pH ile birlikte çözünürlük de artış göstermiştir ve en yüksek çözünürlüğe pH 3'te ulaşılmıştır (92,99%). Üzerinde çalışılan pektin türlerinin (elma pektini DE35, elma pektini DE70, narenciye pektini DE35, narenciye pektini DE70) tümü pH 3-8 aralığında negatif yüzey yükü göstermiştir. Tüm pektin türlerinin daha yüksek pH değerlerinde daha yüksek negatif yüzey yüküne sahip olduğu ve pH 3,5 civarında karboksilik asit gruplarının pKa değerlerinden dolayı net negatif yüzey yükünde keskin bir düşüş olduğu görülmüştür. Protein ve pektin türlerinin karakterizasyonu sonrası, kompleks oluşumu için pH 3 değeri seçilmiştir, bu pH değerinde iki biyopolimer de (protein ve polisakkarit) en yüksek çözünürlük değerine ve yaklaşık olarak eşit seviyede mutlak yüzey yüküne sahip olmuştur. Protein-pektin oranı ve pektinin esterleşme derecesi, protein-pektin karışımlarının etkileşimlerini ve faz ayrılmasını büyük ölçüde etkilemiştir. Komplekslerin mutlak yüzey yükü, elektronötralite (ζ-potansiyel = 0 mV) elde edilene kadar protein oranı ile azalırken, daha yüksek protein-pektin oranları, daha yüksek pozitif yüzey yüküne sahip kompleksler üretilmesine yol açmıştır. Yüksek DE değerine sahip pektinler ile oluşturulan kompleksler için 2,5'e yakın bir protein-pektin oranında nötr yüzey yükü elde edilirken, AP DE35 ve CP DE35 ile oluşturulan kompleksler için yük nötralizasyonu için sırasıyla 1 ve 1,67 protein-pektin oranları gerekmiştir. Daha düşük viskozitede kompleks oluşumu sağladığından ileri çalışmalar için narenciye pektini DE70 ve protein-pektin arasında güçlü bir etkileşimi sağlayan biyopolimer oranı 2,5 değeri seçilmiştir. Çalışmanın ikinci bölümünde, antosiyanin bakımından zengin siyah havuç özütlerinin optimum koşullarda üretilmesi için Yüzey Cevap Metodu ile çalışılmıştır. Cevap parametreleri olan toplam monomerik antosiyanin, toplam fenolik, toplam flavonoid ve toplam antioksidan değerleri arasında yüksek korelasyon değerleri ($p < 0,05$) bulunmuştur. Ekstraksiyon basıncı cevap parametreleri üzerinde istatistiksel açıdan önemli bir etkiye sahip olmuştur ($p < 0,0001$, $p < 0,0005$). Basınç etkisinin ikinci dereceden katsayıları da tüm cevaplar üzerinde istatistiksel olarak anlamlı olarak bulunmuştur. Yine ekstraksiyon sıcaklığının cevap parametreleri üzerindeki etkisi hem birinci hem de ikinci dereceden katsayılar için istatistiksel olarak anlamlı olarak elde edilmiştir. Etanol-su oranı ise cevap parametreleri üzerinde birinci dereceden istatistiksel olarak anlamlı bir etkiye sahip olmazken, ikinci dereceden katsayılar istatistiksel olarak önemli olarak bulunmuştur. Optimize edilmiş proses parametreleri 304 bar basınç, 52°C sıcaklık, 48/52 etanol/su oranı olarak elde edilmiştir. Bu optimum parametreler kullanıldığında

toplam monomerik antosiyanin içeriği 123 mg/L, toplam fenolik içeriği 62 mg/100mL, toplam flavonoid içeriği 44 mg/100mL, CUPRAC değeri 473 mg/100mL ve DPPH değeri 120 mg/100mL olarak bulunmuştur. Deneysel değerlerin, Yüzey Cevap Metodu ile tahmin edilen değerler ile uyumlu olması modelin uygunluğunu ve CCD'nin ekstraksiyon koşullarını optimizasyonundaki başarısını ifade etmiştir. Yüksek Basınç Sıvı Kromotografisi ile optimum değerlerde elde edilen özütte antosiyanin karakterizasyonu yapılmıştır. Özütte, ticari özütle uyumlu olarak siyanidin-3-ksilosil-glukosil-galaktozid, siyanidin-3-ksilosil galaktozid, sinapik asitle açillenmiş siyanidin-3-ksilosil-glukosil-galaktozid, kumarik asitle açillenmiş siyanidin-3-ksilosil-glukosil-galaktozid ve ferulik asitle açillenmiş siyanidin-3-ksilosil-glukosil-galaktozid bulunmuştur. Optimum değerlerde elde edilen açillenmiş antosiyanin % 62,48 olarak bulunurken, ticari özütte bu değer % 60,34 olarak elde edilmiştir. Antosiyanin bakımından zengin siyah havuç özütü, patates proteini - narenciye pektini DE 70 ile emülsifikasyona tabi tutularak veya tutulmadan başarılı bir şekilde enkapsüle edilmiştir. NECP'nin su çekme özelliği %18,13– 28,65 (w/w, kuru bazda) arasında değişirken, ECP için bu değer %10,15 – 17,49 (w/w, kuru bazda) arasında olmuştur. BCE-PPI partiküllerinin su çekme özelliği (higroskopiklik), NECP ile benzerlik göstermiştir. Görünüşe göre, CP eklenmesi higroskopiklik üzerinde herhangi bir olumlu etki yaratmamıştır. Genel olarak, NECP hafif higroskopik bulunurken, ECP higroskopik olmayan olarak kabul edilebilir. Tozların ortalama partikül çapı 65,05 µm ile 152,47 µm arasında değişmiştir. NECP için partikül boyutu, artan çekirdek-duvar materyali oranı ile artan bir eğilime sahip olmakla beraber, ölçümlerdeki fark istatistiksel olarak anlamlı olmamıştır ($p>0,05$). Bununla birlikte, ECP, sabit çekirdek-duvar materyali oranında artan duvar materyali konsantrasyonu ile daha düşük partikül boyutu değerleri göstermiştir. NECP ve ECP için sırasıyla EE değerleri %69,26 - 82,84 ile %85,48 - 90,15 iken AR sırasıyla %79,08 - 102,16 ile %53,90 - 83,37 arasındadır. Genel olarak, hem NECP hem de ECP için, artan çekirdek-duvar materyali oranı ve duvar malzemesi konsantrasyonu, EE ve AR'yi önemli ölçüde etkilememiştir ($p > 0,05$). Yalnızca NECP5, NECP4'e göre artış göstermiştir. Ek olarak, ECP için, hem düşük hem de yüksek duvar materyali konsantrasyonu için artan çekirdek-duvar materyali oranı ile azalma eğilimi gözlenmiştir. DSC termogramlarına göre, ECP keskin ve dar bir tepe noktası gösterirken, NECP geniş bir tepe noktası vermiştir. ECP için erime tepe noktaları 133,38 - 146,36°C, NECP için 118,24 - 128,1°C arasında değişmiştir. DSC termogramlarında, siyah havuç özütünün patates proteini – pektin ile enkapsüle edildiğinde kendine özgü termal davranışı gözlemlenmemiş ve bundan dolayı başarılı bir şekilde kapsüllendiği kanıtlanmıştır. ECP'ye ait FT-IR spektrumlarında 2961 cm^{-1}, 2931 cm^{-1} and 2874 cm^{-1} dalga boylarında elde edilen PPI pikleri gözlemlenmemiş ve bu şekilde PPI ve CP arasındaki kompleksleşme kanıtlanmıştır. Bununla beraber, 1539 cm^{-1} dalga boyunda yeni bir pik oluşmuş ve amid I bandında 1453 cm^{-1}'den 1456 cm^{-1}'e bir kayma gerçekleşmiştir. Bu yeni zirve, muhtemelen, ζ-potansiyel ölçümleri tarafından da desteklenen PPI, CP ve BCE arasındaki etkileşimden dolayı NECP'de de gözlenmiştir. Hem NECP, hem de ECP için, partikül boyutu ölçümleri ile uyumlu olarak, SEM görüntülerinde büyük ve düzensiz partiküller gözlenmiştir. Tezin son bölümünde, siyah havuç özütü – patates proteini partikülleri üretmek için PGSS-kurutma kullanılmıştır. GLR (Gas-Sıvı oranı) ve püskürtme kulesi sıcaklığının, partiküllerin nihai nem içeriği üzerinde iki belirleyici parametre olduğu bulunmuştur. Nem içeriği %10'un altında olan partiküller veren denemeler başarılı olarak kabul edilmiş ve bu partiküller üzerinde daha ileri deneyler yapılmıştır. Üretilen partiküller, ticari ürün kriterlerine göre hafif higroskopik partiküller olarak kabul edilmiştir, partiküllerin su çekme özelliği %18,79 ile %24,94

(w/w, kuru baz) arasında değişmiştir. Ortalama partikül boyutu değerleri D[4,3] ve d50 sırasıyla 9,28 – 14,97 μm ve 8,04 - 11,56 μm arasında değişmiştir. PGSS ile üretilmiş partiküller, partikül boyutu bakımından SDP ve FDP ile önemli bir fark göstermemiştir ($p > 0,05$). Farklı parametrelerde elde edilen partiküllerin kapsülleme verimliliği %69,49 - 81,78 arasında iken, FDP ve SDP için sırasıyla %78,58 ve %84,80 olarak gerçekleşmiştir. EE değerleri için, en yüksek GLR değeri ile üretilen PGSSDP5 dışında; FDP ve SDP dahil tüm numuneler arasında önemli ölçüde farklılık gözlemlenmemiştir ($p > 0,05$). AR, muhtemelen, tüm denemelerde 42,73°C'den daha düşük olan püskürtme kulesi sıcaklığından dolayı PGSS ile kurutulmuş partiküller için dar bir aralıkta (%84,02 – 87,27) bulunmuştur. PGSS ile kurutulmuş partiküller ile FDP arasında istatistiksel bir fark ($p > 0,05$) bulunmamıştır. Bununla birlikte, SDP, diğer numunelere göre daha düşük AR oranına sahip olmuştur. DSC termogramlarında, uygulanan kurutma işleminden bağımsız olarak, BCE'nin amorf yapısını gösteren pikler, PPI ile kompleks haline getirildiğinde gözlemlenmemiştir. Bu durum, kapsüllemenin başarısını ve partiküllerin iyileştirilmiş termal özelliklerini göstermiştir. FT-IR sonuçları ile, BCE'nin yalnızca fiziksel etkileşim yoluyla taşıyıcının matrisine dahil edilmediği, aynı zamanda daha verimli bir kapsüllemeyi gösteren bir kimyasal bağ oluşumunun varlığı gözlemlenmiştir.

1. INTRODUCTION

The demand for functional foods has increased worldwide due to the rising healthy diet preferences. Functional foods can be produced by enrichment with bioactive compounds. To achieve this, the first step is to extract the interested bioactive compound using an efficient method. The second step could be the encapsulation of bioactive compound as the direct addition could have some disadvantages. These could be the degradation of the bioactive compound due to sensitivity to process and/or storage conditions and low bioavailability during metabolism. Encapsulation is used to increase the bioavailability and stability of bioactive compounds when added in encapsulated form to functional foods.

Black carrots are good source of anthocyanin pigments, it was reported that they contain 1750 mg kg^{-1} fresh weight and 45.4 mg kg^{-1} to 17.4 g kg^{-1} dry matter. Besides, black carrots contain a high amount of nutraceutical components and possess high antioxidant activity. Anthocyanins are natural colorants that give the bright red color to various plants. Besides their coloring properties, the interest in anthocyanins has increased due to their reducing activity on the risk of coronary heart disease, cancer and stroke. However, anthocyanins are easily degraded due to their high reactivity and convert to unfavorably colorless or brown colored compounds. They were reported to be vulnerable to temperature, pH, oxygen, ascorbic acid and hydrogen peroxide [1]. Thus, it is important to develop new procedures with novel technologies to increase the anthocyanin extraction yield and extraction rates to minimize the degradation during the process. Sub- and Supercritical Fluid Extraction (SFE) using carbon dioxide in combination with water and/or alcohol is an attractive alternative to conventional extraction as it is an environmentally-friendly process serving a high efficient extraction [2].

As previously mentioned, an efficient extraction may not be sufficient to preserve the stability of anthocyanins to be used in functional foods or in the purpose of usage as a colorant. The complex coacervation is one of the methods to encapsulate bioactive compounds. It is defined as phase separation phenomenon, which renders the

formation of electrostatic complexes between oppositely charged biopolymers leading to a charge neutralization. In the presence of a protein and a cationic polysaccharide in a solution, soluble complexes are initially formed at a first critical pH (pH_c), and then soluble complexes start to aggregate into the coacervate phase at a second lower critical pH ($pH_{\varphi 1}$) which finally converts into a precipitation. When pH decreases down to the third critical pH ($pH_{\varphi 2}$), complexes dissociate into a soluble state due to the charge loss of proteins. The values of pH_c and $pH_{\varphi 1}$ changes with pI of the protein, the biopolymer ratio, the ionic strength and the molar masses of the biopolymers as well [3]. Coacervates are usually dried with freeze-drying to protect the structure of them.

Protein-phenolic complex formation is another method for formation of complexes with anthocyanins in accordance with the aim of stability and bioaccessability increase. Phenolic compounds may interact with proteins both reversibly and irreversibly. In reversible interactions, usually non-covalent forces such as hydrogen bonding, hydrophobic bonding and van der Waals forces are involved [4, 5], whereas, in irreversible interactions, covalent bonds are formed between the polyphenols and proteins [6]. Protein-phenolic complex formation is generally dried by spray-drying and to some extent by freeze-drying. However, these drying processes have disadvantages relating to cost of process and the quality of particles.

Supercritical fluids have been studied especially in pharmaceutical science for the encapsulation with a spray dryer-like system [11, 12]. Supercritical CO_2 has high solvent power and diffusivity which enables encapsulation or micronization at high pressures. In addition, it is regarded as green solvent and easily removed from the capsules/composites by rapid expansion [7]. PGSS is one of the supercritical encapsulation processes where supercritical CO_2 dissolves in or forms a mixture with the substrates or solutions and then the mixture passes through a nozzle and rapidly expands enabling the formation of fine solid particles or droplets [8]. It allows the use of a wide range of substances (polymers, resins, waxes, surface-active components, and pharmaceuticals) as it does not require solubility in sc-CO_2 and it was tested in the pilot and technical size on various classes of substances. In addition, organic solvents are not required for the PGSS process [9]. The commonly used techniques which are freeze-drying and spray-drying have some disadvantages. The disadvantages of freeze-drying are high energy input and long processing times. For the spray dryer, the

most important drawback is the degradation of bioactive compound due to high temperature during processing [10]. It is possible to overcome these disadvantages by using supercritical systems for encapsulation purposes.

In the purpose of encapsulation, proteins are common to be employed as wall materials. The interest in plant-derived proteins has increased because of rising awareness about healthy life and the fact that their production is environmentally friendly and more economic compared to animal derived products. The use of plant proteins in encapsulation also emerges as a part of the 'green' trend rising in the pharmaceutical, cosmetic and food industries. Plant proteins are preferred by consumers due to being less allergenic and mostly not containing GMOs, however most of plant proteins have a different isoelectric point from animal proteins and their solubility in water could be quite low. Potato proteins are gaining an interest as a new source as they exhibit high solubility and possessing different fractions with different isoelectric points.

1.1 Purpose of Thesis

The main objective of this thesis was to investigate the production of anthocyanin-rich black carrot extract loaded potato protein based particles. To achieve this aim, the following objectives were followed;

The objective of first work package of this thesis was to characterize the potato protein and potato protein - pectin complexes as wall materials. To derive a more robust wall material, the formation of potato protein – pectin complexes was chosen. The solubility and surface charge are the two key factors for the characterization of proteins to be used in protein polysaccharide complexes. The impact of pectin source, pectins' DE and biopolymer ratio were the selected parameters to form complexes more efficiently. Surface charge, microstructure, and viscosity were important factors in characterization of complexes.

The second objective of thesis was to produce the anthocyanin-rich extract using pressurized ternary solvents of CO_2 – ethanol – water. The parameters of pressure, temperature and ethanol-water ratio was selected to reveal the effect of process parameters on the extraction of black carrots. To determine the optimum values of extraction parameters for total anthocyanin content (TMAC), phenolic content (TPC),

total flavonoid content (TFC), and antioxidant activity, RSM design was selected to be employed.

The objective of the third work package was to produce potato protein - pectin particles loaded with anthocyanin rich black carrot extract by freeze-drying. The presence of an emulsification step, the wall material concentration and the core-to-wall ratio were selected as parameters to investigate the hygroscopicity, encapsulation efficiency, anthocyanin retention, particle size, thermal properties, FT-IR characteristics and morphology of produced particles.

In the last work package of thesis, the formation of black carrot extract loaded potato protein particles with PGSS-drying was investigated. The objective was to reveal the effect of process parameters on the properties of particles regarding the residual moisture, hygroscopicity, encapsulation efficiency, anthocyanin retention, particle size, FT-IR characteristics, morphology, thermal characteristics and bioaccessability. The nozzle size, temperature and pressure were selected to investigate the effect of process on the characteristics of the particles.

2. LITERATURE

2.1 Supercritical Extraction

2.1.1 Definition of supercritical fluids

As it is known, pure compounds are found in three states: solid, liquid or vapor. The state of any substance is characterized based on a critical point, which consists of specific pressure and temperature value. If a component reaches a higher pressure and temperature levels than its critical point by heating and compressing, its physical properties change and it passes to a fourth state called as “supercritical fluid”.

As an example, Fig. 2.1 presents the pressure and temperature diagram for CO_2. The distinct boundaries divide the diagram into three regions representing the three main stages of compounds. Along these curves, two phases are in equilibrium and the three states coexist at the triple point. The “vaporization – liquefaction” curve terminates at the “critical point” with a critical temperature T_c and a critical pressure P_c. The critical temperature (T_c) is such a temperature for each gas that no matter how high the pressure is applied above this temperature; the gas cannot be liquefied. Additionally, the critical pressure (P_c) is defined as the minimum pressure required liquefying a gas at critical temperature. A supercritical fluid is a fluid with a temperature and pressure higher than T_c and P_c [11].

In Table 2.1, critical properties of several supercritical fluids were shown. In the supercritical phase, the fluids carry intermediate thermo-physical properties between that a liquid and a gas. They have liquid-like densities and they behave as liquid solvents, whereas they can also fill their containers as gasses and have gas-like viscosities. Due to these hybrid properties, the supercritical fluids have unique capabilities. For instance, as a result of their relatively low viscosities, supercritical fluids can penetrate into the solids quickly, dissolve the materials and diffuse out of the solid with the extracted material, rapidly. This ability of supercritical fluids can develop the extraction efficiencies and ameliorate the extraction time. Additionally, as it is shown in the pressure – temperature diagram (Fig. 2.1), there is no liquid/gas phase

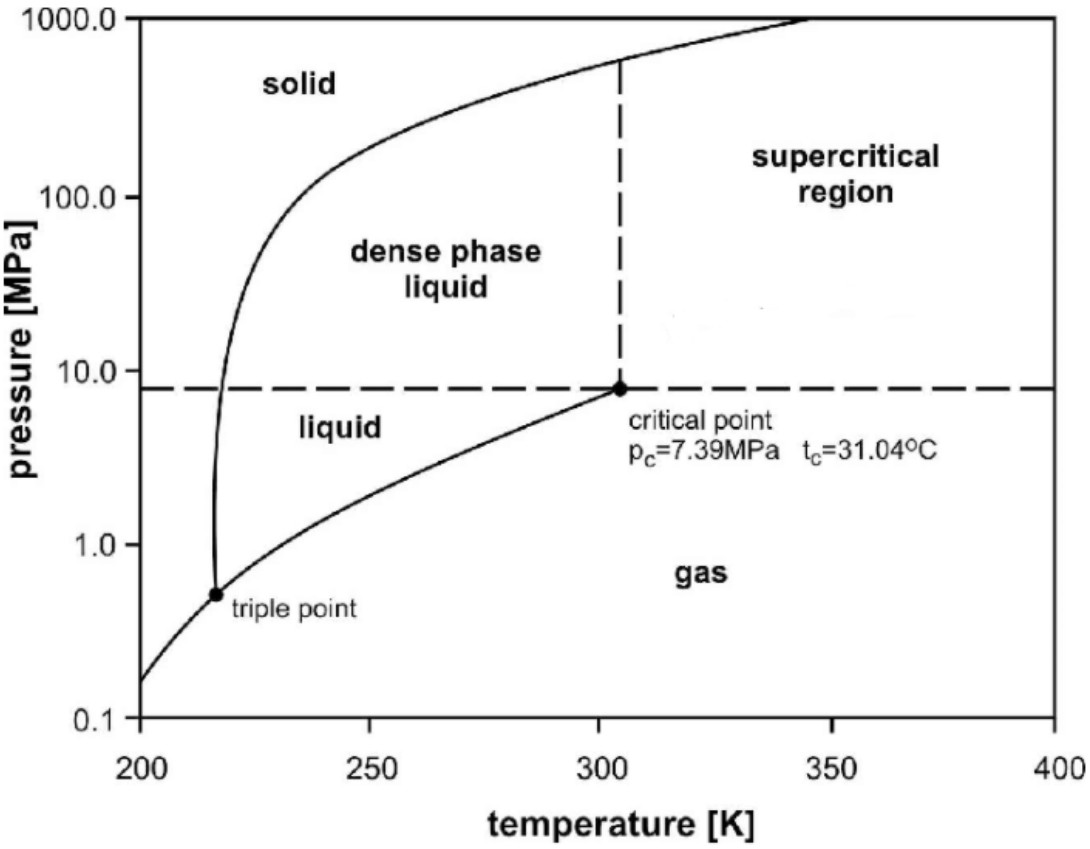

Figure 2.1 : Pressure-temperature phase diagram for CO_2 [12].

Table 2.1 : Critical properties of various solvents [13].

Supercritical Fluid	Molecular Weight	Critical Temperature	Critical Pressure	Critical Density
	g/mol	K	MPa (atm)	g/cm^3
Carbon dioxide (CO_2)	44.01	304.1	7.38 (72.8)	0.469
Water (H_2O)	18.05	647.096	4.60 (45.4)	0.322
Methane (CH_4)	16.04	190.4	4.87 (48.1)	0.162
Ethane (C_2H_6)	30.07	305.3	4.25 (41.9)	0.203
Propane (C_3H_6)	44.09	369.8	5.04 (49.7)	0.217
Ethylene (C_2H_4)	28.05	282.4	4.60 (45.4)	0.215
Propylene (C_3H_6)	42.08	364.9	4.60 (45.4)	0.232
Methanol (C_3H_5OH)	32.04	512.6	8.09 (79.8)	0.272
Ethanol (C_2H_5OH)	46.07	513.9	6.14 (60.6)	0.276
Acetone (C_3H_6O)	58.08	508.1	4.70 (46.7)	0.278

boundary in supercritical region. This situation makes supercritical fluids to gain an important feature called “tunability” which is an ability to change the properties to be more liquid – or more gas – like by changing the pressure and temperature [14].

On the other hand, most of the supercritical fluids act like non-polar solvents showing a solid affection with lipids and hydrocarbons, yet a feeble liking with oxygenated or hydroxylated particles; it is conceivable to tune their extremity by including a polar co-solvent (ethanol or light alcohols, esters or ketones) [15].

Solvent power which is referred as the ability to dissolve other substance is one of the most important point in supercritical fluid applications. The solvent power of the supercritical fluids varies continuously with density. By changing the temperature and pressure, the density of supercritical fluids can be brought to a point where they are able to dissolve high amounts of a solute. da Ponte and Zakrzewska [16] states that if a high density (high pressure) is used, the solvent power will increase and as a result higher amounts of solvents will be dissolved. On the contrast, when a low density is obtained due to low pressure or high temperature, the solubility in supercritical fluid will be decreased because of the reduced solvent power [16].

2.1.2 Properties of supercritical carbon dioxide

Some of the supercritical fluids have been listed in Table 2.1. Among these compounds, supercritical CO_2 has so far been the most widely utilized fluid. The pressure – temperature phase diagram of CO_2 is shown in Fig. 2.1, including the critical points of 7.39 MPa, 304 K / 31.1 °C and 73.8 bar [17].

CO_2 frequently used in the studies due to being non-toxic and chemically inert, less expensive, readily available at higher purities, odorless, non-explosive, non-flaming and not corrosive. It has high solvent power due to its symmetrical structure and not including any dipole moments. It is a good solvent because it can mix easily with low molecular weight hydrocarbons and organic compounds and shows bacteriostatic effect. It also possesses higher volatility compare with other fluids and it is advantageous in terms of energy consumption. Celiktas et al. [18] states that since pure CO_2 has a non-polar characteristic, it behaves more selective during the extraction of substances having low molecular weight or compounds with weak polarities such as lipids, cholesterols, aldehydes, ethers and ketones. On the other hand, that the

solubility of high molecular weight materials and polar groups like hydroxyls, carboxyls, polysaccharides, amino acids and proteins are low in CO_2.

2.1.3 Supercritical fluid extraction system

Supercritical fluid extraction (SFE) is mainly described as a process of separating one component from another by using a supercritical fluid as an extraction solvent. In addition to improve the extraction efficiency and increase the solubility, co-solvents can also be used. While CO_2 is mostly preferred solvent for this process, alcohols like methanol and ethanol are most commonly used co-solvents. These co-solvents have higher polar characteristics which could increase the solvation power.

According to Sapkale et al. [19], an ideal separation technique should cause none or minor losses or degradation in recovering of the analyte; should not produce wastes that have to be eliminated; should be rapid, inexpensive, and not difficult to use. However, they mention that conventional extraction methods could not meet with some of these criteria, such that they require longer operating time, more expensive solvents and an additional concentration step. The use of supercritical fluids in the extraction was discovered over two decades ago, and it became a well-known environmentally friendly, convenient and effective method which has begun to be preferred instead of conventional extraction methods.

Supercritical CO_2 extraction method provides a good deal of advantageous when it is compared to conventional extraction methods using liquid solvents. First of all, unlike liquid extraction techniques, no solvent residue can be encountered as a result of this method, since CO_2 can be easily removed from the extract [19]. As it is highlighted before, it is also non-toxic, environmentally friendly and recoverable. Furthermore, since the diffusivities of the supercritical fluids are faster than in liquids and there is no surface tension, the solvent penetrates into the solid matrix easily and the duration of the extraction process becomes shorter [19]. Besides, this method provides opportunity to extract components having high boiling point at relatively low temperatures. Most importantly, the compounds sensitive to the temperature can be extracted with a minimal damage.

As Mohamed and Mansoori [20] have referred in their review, today there are many studies conducting on supercritical fluid technology, and it has started to be identified as a potent analytical method with a lot of benefits and comparable efficiencies to the

already existing methods. Over the time, the use of supercritical extraction method is expanding, and today it is possible to encounter with its applications in many different industries such as food, medicine and cosmetics. In Mohamed and Mansoori [20]'s review, it is mentioned that SFE technology is employed with various ways in food industry, such as in obtaining edible fats and oils, purification of solid matrices, separation of tocopherols and other antioxidants, clean-up of herb medicines and food products from pesticides, detoxification of shellfish and concentration of fermentation broth and fruit juices [21-24].

A supercritical fluid extraction system consists of basically a pump for CO_2, an extraction vessel where the sample to be extracted is placed, a restrictor to maintain the pressure inside the system and a collecting vessel where obtained extract is kept as it is shown in the Fig. 2.2. The system starts operating with pumping of the fluid into a heating zone. When it reaches to the supercritical conditions by heating, it passes through the extraction vessel, diffuses into the solid matrix and dissolves the compounds to be extracted. The dissolved compounds are transferred to the separator at low pressure and obtained from collection vessel. At the end of the process, the CO_2 can be cooled, recompressed and recycled, or released to the air [19]. On the purpose of maintaining the pressure inside the system, a simple restrictor or a back-pressure regulator can be used depending on the scale of the systems. The adiabatic expansion of CO_2 can result in extreme cooling and if there is any water or other extracted material left in the sample, they can freeze inside the restrictors or valves which may lead to breakages. Therefore, for the both scale of systems, heat supply could be required [19].

2.2 Encapsulation

Microencapsulation technology supplies the food industry with two key applications. The technique is widely applied for ensuring stability for the active ingredient in food products. The dominant principle is achieving desirable product stability which can be managed by controlling the structural design of the microcapsule that gives improved performance in food products. Another major use of microencapsulation technology is to form an aimed physicochemical change in sensory perception in the food product at the targeted time or by applying an adequate triggering mechanism. A better understanding of the molecular and physico-chemical interactions between the active

ingredient and the material composition is crucial for the creation of such a dynamic system [26].

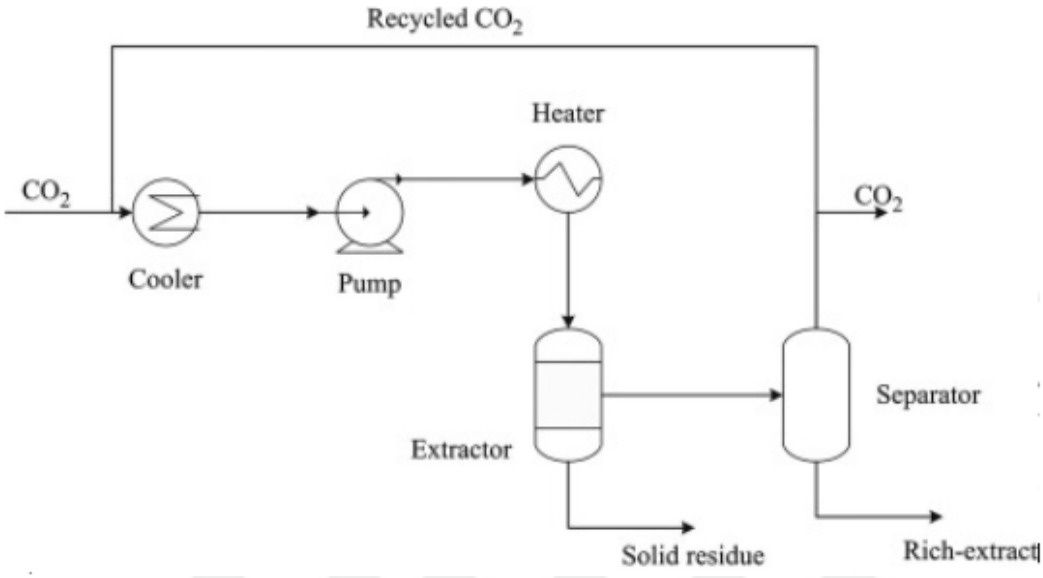

Figure 2.2 : Simplified flow diagram of the supercritical fluid extraction with CO_2 [25].

Encapsulation is a process that can be explained as entrapping one substance within another one, so we have to produce particles with diameters of a few nm to a few mm. The component which is encapsulated can be defined as the core material, the active agent, fill, internal phase or payload phase. The component which is used to encapsulate can be named the coating, membrane, shell, carrier material, wall material, external phase or matrix. The carrier material of encapsulates used in food products should be food grade and have the ability to build a barrier between the active agent and its surroundings [27].

The stability and release of the active ingredients are significantly affected by the morphological configuration of the matrix wall or by microsphere morphology, where the active ingredient is embedded in a number of small discrete droplets or particles that are spread in the matrix material. Different structural configurations of microencapsulated systems are presented in Fig. 2.3. In addition, it shows how the active ingredient is spreaded in the matrix polymer. It should be noted here that both microcapsule and microsphere morphologies must be free of defects, pin holes, or high curvatures to favor the stability since the presence of defects can cause oxidative or hydrolytic degradation over longer periods of time [26].

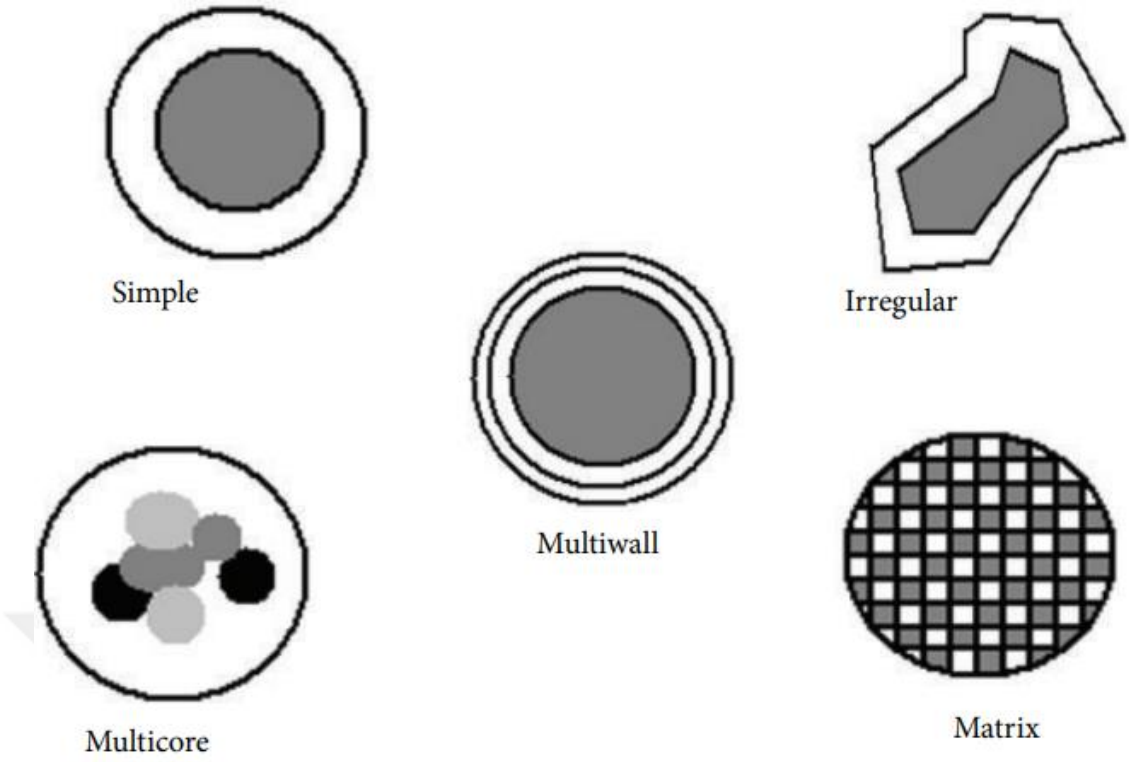

Figure 2.3 : Various forms of microcapsule used in the food industry [28].

Microencapsulation can be applied for different purposes (i) it can be applied to protect sensitive substances from the surrounding environment, (ii) to hide the organoleptic properties like color, taste, odor of the substance, (iii) to provide a controlled release of the drug substance, (iv) to ensure a safe handling of the toxic materials, (v) to get targeted release of the drug (vi) to avoid variable side effects, like gastric irritation of the drug, e.g. aspirin was the first drug which is used to avoid gastric irritation [29].

The selection of adequate wall material is a significant point since it affects both encapsulation efficiency and stability of microencapsulation. The ideal wall material should have the following characteristics:

- Simple workability and good rheological property at high concentration.
- Possibility to disperse or emulsify the active material and stabilize the produced emulsion.
- Chemical non-reactivity with the active core materials to be encapsulated during processing.
- Ability to enclose and carry the active material within its structure during processing or storage.

- Ability to release the solvent or other materials used completely during the process of encapsulation under drying or other desolventization conditions.
- Ability to ensure maximum protection of active material from environmental conditions (e.g., oxygen, heat, light, and humidity).
- Solubility of the used solvents should be acceptable to food industry (e.g. water and ethanol).

Different techniques are available for the encapsulation of core materials. In general, the techniques are classified into three types: chemical methods, physico-chemical methods and physico-mechanical methods (Table 2.2). These mentioned techniques are largely used for the microencapsulation of several pharmaceutics. Among these processes, fluidized bed or air suspension method, coacervation and phase separation, spray-drying and spray-congealing, pan coating and solvent evaporation methods are widely used. Table 2.3 illustrates microencapsulation processes and their uses [29].

2.3 Complex Coacervation

Coacervation is called phase separation process which can be induced by varying medium parameters such as pH, ionic strength, temperature and solubility under the controlled conditions. In this technique, the phase which is rich in colloid is known as the coacervate phase, but the one having very little amounts of colloid is known as the equilibrium phase [30]. Depending on the polymer systems used, coacervation techniques are divided into two types which are simple and complex coacervation. The simple coacervation process involves the use of single polymer and coacervates are formed under the action of dehydration or "water deficit". Mechanism favored by the

Table 2.2 : Different techniques applied for microencapsulation [13].

Chemical processes	Physico-chemical processes	Physico-mechanical process
Interfacial polymerization	Coacervation and phase separation	Spray-drying and congealing
In situ polymerization	Sol-gel encapsulation	Fluid bed coating
Poly condensation	Supercritical CO_2 assisted microencapsulation	Pan coating
		Solvent evaporation

Table 2.3 : Microencapsulation processes and their applicability [13].

Microencapsulation process	Nature of the core material	Approximate particle size (μm)
Air suspension	Solids	5–5000*
Coacervation and phase separation	Solids and liquids	2–5000*
Multi-orifice centrifugation	Solids and liquids	1–5000*
pan coating	Solids	600–5000*
Spray-drying and congealing	Solids and liquids	600
Solvent evaporation	Solids and liquids	5–5000*

*The 5000 μm size is not a particle size limitation. The methods are also applicable for macro-coating

addition of a salt or desolvation liquid (also named coacervation agent or inducing agent) into the reaction medium. An example of simple coacervation process is the phase separation of gelatin by using sodium sulfate salt (Na_2SO_4) or by the addition of ethanol into its solution. However, in complex coacervation processes, two or more oppositely charged polymers are involved where an ionic interaction takes place between them which leads to a phase separation. Mostly, these polymers are proteins and polysaccharides. The major factor that controls the complex coacervation is the electrostatic interaction between the charged macromolecules. In addition, van der Waals intermolecular force hydrophobic interactions in dipolar proteins and nucleic acids and hydrogen bonds also play a significant role in the complex coacervation process [30].

The term coacervate was used in 1623 for the first time and coacervation process was first described in 1911 by F.W.Z. Tiebackx, but more systematically studied by Bungenberg de Jong and Kruyt during the 1920s and 1940s. They used gelatin and gum Arabic as model biopolymers. Barrette Green was the one who reported the industrial application of coacervation for the production of carbonless duplicating paper in 1950s. Recently, coacervation is described as one of the most effective techniques of micro/nano encapsulation applied in the food and pharmaceutical industries. Encapsulation process by coacervation method involves the deposition of the coacervated polymer around the active ingredient (core) leading to the precipitation of the encapsulated core.

Complex coacervation in food ingredient encapsulation primarily involves the use of two oppositely charged biopolymers, primarily proteins and polysaccharides, that are able to form a complex shell around the core material. Proteins are either of animal origin such as gelatin, whey proteins, egg albumin and silk fibroin, or of plant origin such as soy protein, pea protein, wheat protein, lentil protein and chia protein. Similarly, polysaccharides include alginate, chitosan, gum Arabic, pectin, agar, carrageenan and carboxymethyl cellulose (CMC). Both gelatin and gum Arabic are defined as the historic biopolymers. Nowadays, varieties of new pairs of biopolymers have been applied for complex coacervation for encapsulation of different hydrophobic and hydrophilic food and agricultural nutrients and chemicals [30]. The complex coacervation process is described as a three-phase system, which consist of the solvent, the active material and the coating material. This process is made up of four steps: (a) preparation of an aqueous solution that is made up of two or more polymers. The preparation of this solution always takes place at the temperature above the gelling temperature or/and above the isoelectric point of the protein; (b) then a hydrophobic phase is mixed with the aqueous solution of one polymer, usually protein solution, and homogenizing the resultant mixture, thus a stable emulsion is produced; (c) changing the pH and temperature to an aimed level to induce coacervation and phase separation; and (d) lastly, hardening of the polymer matrix using elevated temperature, desolvation agent, or cross-linker as illustrated in Fig. 2.4 [30].

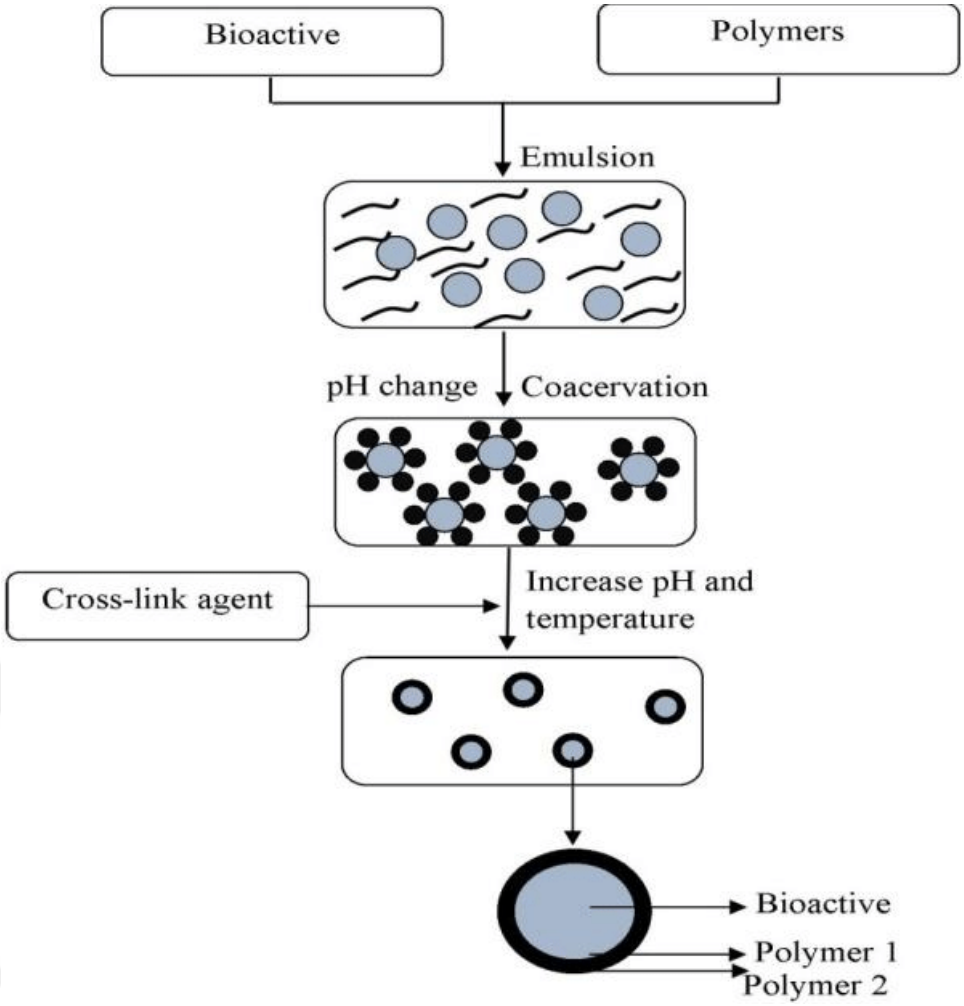

Figure 2.4 : Schematic representation of complex coacervation process applied in encapsulation of active ingredients [32].

In general, the coacervation can be initiated either by decreasing the temperature or by altering pH or by dilution or addition of a salt (known as a coacervation agent). Thus, the formation of very fine coacervate particles leads to a turbid appearance in the medium. This stage of coacervation is usually defined as micro-coacervation. When coacervation process is continued, the micro particles bind together leading to formation of larger particles. The produced larger particles have a higher density and so they settle at the bottom of the container. After a period of time, obviously visible two-phase system is formed which is called macro-coacervation.

Microcapsules are characterized by their core-shell architecture which could be generally mono-nucleated or multi-nucleated. In both core-shell types, the small core is completely surrounded by a uniform coating of the polymer matrix [30]. The complex coacervation technique is applicable because of its simplicity, low cost, scalability and reproducibility in encapsulation of food ingredients that yields high

encapsulation efficiency even at very high payload (up to 99%). It has been proved that the characteristics of shell materials used in the encapsulation process largely affects the core stability, process efficiency and degree of protection of active components [30].

2.4 Freeze-Drying

Freeze-drying is one the commonly used processes in pharmaceutical, enzyme stabilization and food applications in order to convert solutions into solid materials [33]. It is mostly used for dehydration of foodstuffs where water is eliminated under reduced pressure and at sub-zero temperatures by sublimation [34]. This process is achieved by three main steps: the solution is firstly frozen at extremely low temperature ranged between -70 to -80°C. The solution is then partially dried by reducing the pressure which is defined as the initial drying. Lastly, in the secondary drying process, the remained water is extracted. The main advantage of freeze-drying process is the use of water instead of organic solvent [33]. By means of such mild drying conditions, color, flavour and antioxidant content of dried foods or food components could be preserved at high level. In addition, drying at sub-zero temperatures inhibits most of microbial reactions and enzymatic browning, as well [34]. The main disadvantages of freeze-drying are the high energy needed, the long processing time, and the open porous structure which prevents to obtain an efficient barrier between the active material and its surroundings. In addition, it is 30–50 times more expensive as compared to spray-drying [27].

2.5 Spray-Drying

Spray-drying is a well-designed technique for the transformation of liquids into stable and simply applied powders in food industry. It is recorded that about 90% of microencapsulates are prepared by spray-drying [35].

The steps of the spray-drying are following: Feeds enter the atomizer through the feed pump, which is normally a peristaltic pump. The atomizer can be one-/two-fluid nozzle or centrifugal atomizer. This component breaks down the liquid feed that is pumped inside the drying chamber into small droplets. Simultaneously, a heated drying gas (normally air) is pumped into the drying chamber in parallel (sometimes in a counter-

current style) to the atomized droplets. Inside this chamber, atomized droplets are dried within a few seconds under the action of hot gas then fall to the bottom of the chamber. Later, these droplets are sucked into the cyclone, which is connected to the exit fan. Dried particles are separated from the drying air by a filter and gathered at the bottom of the container. Drying gas is removed from the spray dryer by an exhaust fan [19].

Spray-drying is one of the most applicable encapsulation techniques for different food ingredients. It can be applied directly for hydrophilic ingredients and indirectly for lipophilic ingredients after an emulsification step. It is possible to encapsulate viable microorganisms, such as probiotics, and other compounds, such as enzymes and bioactive phenolics by spray-drying, to increase the product yield and encapsulation efficiency. Several parameters related to feed composition can be adjusted which are total solid content, viscosity, surface tension and concentration of wall and core materials. The other important aspect to be optimized are the process parameters which are inlet and outlet temperatures, the flow rate and humidity of the drying gas, feed flow rate and atomizer pressure and speed [36].

2.6 PGSS-Drying

PGSS (Particle from Gas Saturated Solutions) is a high-pressure technique which can produce powders that are difficult to be formed by classical methods like milling, spray-drying, or crystallization. In the last years, PGSS process was applied to produce micronized single components and to encapsulate different active compounds. In this technique, the target substance or the mixture of substances to be powderized are transformed into a sprayable form by liquefaction/dissolution. To achieve this, the substance or mixture of substances are melt or dissolved in a liquid solvent, or dispersed in a melt or solution which follows by a saturation of the melt/solution/dispersion with the CO_2 gas. PGSS process is made up of the following steps, (1) the substance to be powderized is melted (2) it is mixed with supercritical CO_2 (3) it expands into the spray tower where solid particles are formed. Under the effect of reduced solubility by the expansion, the increased volume of the disappearing gas leads to the transformation of liquid into droplets. Due to the Joule-Thomson effect the gas cools down and the droplets solidify. Therefore, fine particles can be produced which are collected on the bottom of the spray tower.

Composites can also be produced by the following strategy: Both shell and core materials are melted and pumped through the static mixer, where supercritical CO_2 is introduced. The mixture is then expanded through a nozzle into a spray tower at ambient pressure. Micro-meter sized powders with a high loading of dispersed phase as well as a distribution-controlled particle size can be produced [37].

PGSS-drying of aqueous solutions is advantageous as compared to spray-drying by means of reduced thermal degradation and contamination of the product. The technique takes place in a closed system inertized with CO_2, and only static mixer is carried out at high temperature [37].

Different powder properties can be achieved by changing the process parameters. The process parameters that have an influence on the final product are following:

Pre-expansion temperature: The droplets solidification time, the morphology and the size of the obtained particles can be altered by the pre-expansion temperature. The viscosity of the employed substances and the solubility of carbon dioxide varies depending on the temperature. As the temperature increases, the viscosity of the sprayed substances decreases.

Pre-expansion pressure: The pre-expansion pressure affects the solubility of carbon dioxide in the sprayed materials and influences the spraying of the mixture. Higher pre-expansion pressure could lead to finer droplets or smaller particle size and lower bulk density. In addition, with a higher pre-expansion pressure, better solubility of carbon dioxide in the sprayed materials can be achieved.

Spray tower temperature: The temperature of the spray tower influences the solidification time of the droplets obtained after spraying. An increase in temperature results in an increased possibility of agglomeration and thus higher particle size and bulk density of the powder.

Gas to liquid ratio (GLR): Further important parameter that influences the characteristics of the obtained powder is the GLR. The GLR is defined as a mass flow ratio of CO_2 to that of feed (equation 2.1).

$$\mathrm{GLR} = \frac{\dot{m}_{CO_2}}{\dot{m}_{\mathrm{Feed}}} \tag{2.1}$$

Based on Joule-Thomson effect, a higher GPR will results in a faster cooling and solidification of the droplets in the spray tower and therefore a lower residual moisture, smaller particle size and decreased bulk density.

2.7 Black Carrot Extract

According to historical data, carrots were originated from Afghanistan before the 10th century and the first carrots have yellow and purple colored roots. Then the next 600 years, cultivation spread over east (Asia) and west (Europe). Although, black carrot was known as a good culinary source, yellow and purple/black rooted carrots replaced by white and then orange rooted carrots in time [38, 39]. Just as there are several different colors of carrots, black carrots can be different within themselves in terms of their flesh, peel and xylem color. Antonina, Deep Purple, Indigo, Maroon, Purple Dragon, Cosmic Purple, Purple Dutch, Beta Sweet, and Purple Haze are the names of some different black carrots according to their types [40].

Black carrot juice and concentrate are used as natural colorants in milk, ice cream, jam-marmalade, cake, fruit juice, alcoholic beverages, and canned food processing areas. In Turkey, main usage area of black carrot is Shalgam juice production. In addition, there are some companies that produces black carrot concentrates. Besides, increasing demand on natural food colorants give rise to black carrot anthocyanins usage in food industry with a wide application area due to being more stable compared to that of other plants [41].

2.8 Potato Protein Isolate

The potato starch industry produces large quantities of a by-product known as potato fruit juice, which is expensive to dispose due to its high levels of contaminants and has low economic value when employed as animal feed and fertilizer. As potato fruit juice is rich in proteins, minerals and free amino acids, the valorization of this by-product into ingredients with high added value would have a significant economic and environmental effect. Hence, the extraction of proteins from potato fruit juice is of high interest. The production of starch from 1000 kg of potatoes produces 5-12 m^3 of juice with 30-41% (dry basis) protein content which makes it a good source for the production of potato protein isolate (PPI) [42, 43].

Isolation of proteins from the juice with their preserved functional properties is a challenge due to aqueous nature of potato fruit juice and its complex composition. The common industrial techniques for producing PPI are combinations of thermal coagulation at temperatures of 75 °C to 120 °C and acidic precipitation [43]. While thermic/acid precipitation generates a high protein yield, it results frequently the complete loss of protein functionality, and thus limits its application to animal feed. Further extraction techniques have been studied for the recovery of functional proteins, including salt, acid, ethanol, ammonium sulfate ($(NH_4)_2SO_4$) precipitation, carboxymethyl cellulose (CMC) complex formation and chromatographic techniques. Nevertheless, contradictory results have been obtained on the efficiency of these techniques for the isolation of potato proteins. These differences could be due to the use of different potato varieties and potato fruit juice preparation methods [42].

Potato proteins contain a balanced amino acid composition and a high percentage of lysine (~8%) [43], which is missing in other plants. They are generally considered at higher quality than major plants (e.g. vegetable and cereal proteins). Furthermore, it is comparable to that of whole egg, whey and egg protein. Potato proteins are usually divided into three fractions: Patatin (up to 40%), protease inhibitors (~50%) and other high molecular weight proteins (~10%). The patatin fraction as dimer glycoprotein has a molecular weight of 40-45 kDa and is available in many isoforms. With respect to its health-beneficial properties, patatin exhibits antioxidant capacity and lipid-acyl hydrolase (LAH) activity. In addition, patatin has excellent foaming and emulsifying properties, which may vary depending on the specific patatin forms or potato tubers of the different cultivars. With a molecular weight of 5 to 25 kDa, the protease inhibitors have proven to have beneficial properties such as anti-carcinogenic, anti-microbial and saturating action by releasing the hunger inhibitor cholecystokinin. Functionally, the protease inhibitor fraction is soluble over a wide pH range, while patatin has a minimal solubility at pH 4 [43].

2.9 Pectin

Pectin is an anionic cell-wall polysaccharide which is composed of a backbone of (1→4) α-D-galacturonosyl residues interrupted with typically a 10% substitution of (1→2)-α-L-rhamnopyranosyl residues [44]. Generally, the main sources for commercial pectin production are apple pomace and citrus peel [45]. Apple pectins

(AP) and citrus pectins (CP) have different functional properties due to their structural differences. Pectins are classified based on two parameters: the degree of methyl esterification of the carboxyl group and the distribution of these methyl-esters along the pectin backbone. The ratio of methyl-esterified galacturonic acid groups to total galacturonic acid groups is termed as the degree of esterification (DE). High-methoxy pectins have ≥ 50% DE, whereas low methoxy pectins have < 50% DE [46]. The other parameter which is related to distribution of the methyl-esters is represented as the degree of blockiness (DB). A high DB value means that the methyl-esters are distributed in a block-wise manner while low DB value corresponds a random distribution [47].

3. THE IMPACT OF ESTERIFICATION DEGREE AND SOURCE OF PECTINS ON COMPLEX COACERVATION

3.1 Introduction

Complex coacervation is separation of a solution into two liquid phases in an aqueous colloidal media that caused by the interaction of two oppositely charged biopolymers. The coacervate is defined as the more concentrated phase in the mixture, while the other phase is called equilibrium solution [48]. The behavior of two oppositely charged biopolymers in a solution mainly depends on the pH of the solution. It was reported that three critical pH values determine the behavior of complex formation: pH_c corresponds to the formation of initial soluble complexes, these soluble complexes aggregated into the coacervate phase at $pH_{\phi 1}$ and $pH_{\phi 2}$ causes the dissociation of complexes into a soluble state due to charge loss of biopolymer [49]. The values of pH_c and pH_ϕ change with isoelectric point of the protein, the biopolymer ratio, the ionic strength and the molar masses of the biopolymers [50].

Biopolymer complexes or coacervates have been utilized in food industry as they can be used as encapsulation wall materials for delivery of bioactive components in food matrices [51]. Moreover, it is possible to improve dispersion stability, texture and interfacial properties as well as the sensorial characteristics via the masking of odd flavor [52].

The usage of complex coacervates in food industry has increased due to its high encapsulation efficiency and mild processing conditions. It is mainly utilized for encapsulation of hydrophobic compounds, however, addition of a double emulsion step at the beginning of process could make possible the encapsulation of hydrophilic compounds [53]. Up to now, complex coacervation has been used for microencapsulation of various active agents such as casein hydrolysate, sweet orange oil, propolis, lycopene, ascorbic acid, aspartame, Miglyol, tuna oil and probiotic Lactobacillus casei 431, astaxanthin, nisin and avocado extract and algal oil.

Plant proteins are known to have potential positive health effects such as decreasing the plasma cholesterol, decreasing coronary heart disease development and controlling calorie intake. They can provide an essential high quality protein in a concentrated form for specially designed low-calorie/high-nutrient-density meals [54]. In addition, mixtures of plant proteins serve as a well-balanced source of amino acids to meet human physiological needs [55].

Potato proteins are by-products of starch production and its nutritional value has been shown to be greater than that of other vegetable or cereal proteins and casein while being comparable to that of egg protein [56-59]. Potato proteins are divided into three major fractions which are patatins, protease inhibitors and remainder proteins. Patatins (35-40%) are glycoproteins with a molecular weight around 40 kDa, having a pI at 4.8-5.2. The protease inhibitors (25-50%) are diverse group of proteins with a molecular weight of 7-21 kDa and the pI varying between 5–8. The remainder proteins (~10%) are enzymes with different high molecular weights [60, 61]. In contrast, pectin is α-D-galacturonosyl residues interrupted with typically a 10% substitution of (1→2)-α-L-rhamnopyranosyl residues [62]. Generally, the main sources for commercial pectin production are apple pomace and citrus peel [63]. Degree of esterification (DE) and degree of blockiness (DB) are two factors affecting the functionality of pectins.

According to our knowledge, there are no studies investigating the effect of biopolymer ratio and usage of different sources of pectin with varying DE on complex formation of potato proteins. In addition, the pectin's origin could also have an influence, as the degree of blockiness that affects protein pectin interactions is highly depended on the pectin source. All biopolymers were individually characterized in terms of solubility and surface charge.

3.2 Materials and Methods

3.2.1 Materials

Food grade potato protein isolate was donated by Döhler GmbH (Darmstadt, Germany). Potato protein isolate contained (min.) 90% protein, (max.) 9% moisture, (max.) 5% ash (max.) and 0.5% sulphite according to specification provided by manufacturer. Apple pectin with 71% DE (AP DE71, Pectin Classic AU-L 051/15), apple pectin with 35% DE (AP DE35, Pectin Classic AU-L 051/15), citrus pectin with 70% DE (CP DE70, Pectin Classic CU-L 053/15) and citrus pectin with 35% DE (CP

DE35, Pectin Classic CU-L 054/15) were supplied from Herbstreith & Fox KG (Neuenbürg, Germany) and used without further purification. Bradford reagent Roti®-Quant, analytical grade sodium hydroxide (NaOH), and hydrochloric acid (HCl) were obtained from Carl Roth GmbH+Co. KG (Karlsruhe, Germany). All samples were prepared in double-distilled water and all concentrations are expressed in mass percentage (% w/w).

3.2.2 Biopolymer solution preparation

Powdered potato protein isolate (0.5% w/w) and pectins (0.5% w/w) were dissolved in double-distilled water and stirred at ambient temperature overnight to ensure complete hydration. After hydration, the biopolymer solutions were adjusted to pH 3.0 – 8.0 using HCl and/or NaOH (0.1 M, 1 M).

3.2.3 Biopolymer complex formation

The biopolymer complexes were generated based on the method described in our previous study [52]. The potato protein isolate (1%, w/w) and pectin (1%, w/w) solutions were initially adjusted to pH 3 using HCl and/or NaOH (0.1 M, 1 M). A series of complex dispersions were generated with different protein-pectin ratios (0.33-5.00). All biopolymer dispersions were mixed for at least 2 min at ambient temperature on a stirrer plate (mixing speed 100 rpm) to ensure evenly distributed dispersions. The final concentration of protein was 0.25% w/w and the pectin concentration was between 0.05-0.75% w/w in complexes.

3.2.4 ζ-potential

The ζ-potential of individual biopolymer dispersions (0.5%, w/w) at pH 3-8 and complex biopolymer dispersions (0.3-1%, w/w) at pH 3 were measured by using a Laser-Doppler-micro-electrophoresis device (Zetasizer Nano-ZS, Malvern Instruments, Malvern, UK). Samples were diluted to a biopolymer concentration of 0.05% with double-distilled water to ensure uniform and spherical shape of complex droplets and then loaded into an appropriate cuvette. The ζ-potential was determined by measuring the direction and velocity that the droplets moved in the electric field applied. All measurements were carried out at 25 °C. The Smoluchowski equation was utilized to calculate the ζ-potential according to equation 3.1.

$$\nu_E = 4\pi\varepsilon_0\varepsilon_r \frac{\zeta}{6\pi\mu}(1+\kappa r) \quad (3.1)$$

where ν_E is the mobility, ζ is the ζ-potential, ε_0 and ε_r are the relative dielectric constant and the electrical permittivity of a vacuum, respectively, μ is the solution viscosity, r is the particle radius and κ is the Debye–Hückel parameter. The ζ-potential measurements were conducted on two replicates of freshly prepared samples with four readings on each replicate.

3.2.5 Solubility

The solubility of the protein was determined using a method published previously [64]. In brief, protein solution (2%) in double-distilled water were prepared with stirring at ambient temperature for 2 hours to ensure a complete hydration. pH values were adjusted from 3 to 8 using 0.1 M and 1 M HCl and/or NaOH and samples were centrifuged for 30 min at 36 000 rpm (Biofuge 28 RS, Heraeus Sepatech, Germany). The protein concentration in the supernatant after centrifugation was measured with microplate procedure of Coomassie Brilliant Blue reagent which is a modificated procedure of Bradford assay [65]. 5 µL of the supernatant and 250 µL of Coomassie reagent mixed for 30 seconds and incubated for 10 min. The absorbance of mixtures was measured at 595 nm using a spectrophotometer (BioTek Synergy 2 Multi-Mode Reader, Winooski, USA). Quantification was carried out using a calibration curve (0–25 µg mL^{-1}) obtained with albumin.

3.2.6 Viscosity

The flow behavior of individual and complex dispersions was analyzed using a modular compact oscillatory rheometer (Anton Paar, Stuttgart, Germany) which was equipped with a coaxial cylinder (CC-27, cup diameter: 28.92 mm, bob diameter: 26.66 mm). Flow curves were recorded by increasing the shear rate of the coaxial cylinder system equilibrated to 25 °C logarithmically from 1.0 to 300 s^{-1}. The viscosity η was calculated as the slope of the shear stress vs. strain curve and plotted as a function of protein-pectin ratio at a shear rate $\gamma = 203\ s^{-1}$.

3.2.7 Microstructure

Microstructure of samples was assessed by light microscopy. Micrographs were taken with an axial-mounted Canon Powershot G10 digital camera (Canon, Tokyo, Japan)

mounted on an Axio Scope optical microscope (A1, Carl Zeiss Microimaging GmbH, Göttingen, Germany). The images presented are representative examples of the samples investigated during the study.

3.2.8 Visual observation

The individual and complex biopolymer dispersions stored for 24 h at room temperature and phase separation behavior was observed using a digital camera (PowerShot SX200 IS, Canon, Tokyo, Japan).

3.2.9 Rheological measurements

The flow behavior of single and complex dispersions was analyzed using a modular compact oscillatory rheometer (Anton Paar, Stuttgart, Germany). The rheometer was equipped with a coaxial cylinder (CC-27, cup diameter: 28.92, bob diameter: 26.66 mm). Flow curves were recorded by increasing the shear rate of the coaxial cylinder system equilibrated to 25 °C logarithmically from 1.0 to 300 s^{-1}. The viscosity η was calculated as the slope of the shear stress vs. strain curve and plotted as a function of pectin concentration at a shear rate γ = 203 s^{-1}.

3.2.10 Statistical analysis

All measurements were repeated at least three times using duplicate samples. Means and standard deviations were calculated from these measurements using Excel (Microsoft, Redmond, WA, USA). A Fisher test with a confidence interval of 95 was used to evaluate the statistical differences (Minitab® 16 Statistical Software, Minitab Inc. State College, Pennsylvania, USA). Pearson correlation coefficient and p-value was found by Excel – Data Analysis (Microsoft, Redmond, WA, USA). For microscopic imaging, representative images were chosen from amongst at least five similar images.

3.3 Results and Discussion

3.3.1 Physicochemical characterization of individual biopolymers

The impact of pH (3-8) on the ζ-potential of potato protein and pectin solutions (0.5% w/w) in distilled water was investigated (Fig. 3.1). The ζ-potential of potato protein solution changed from negative (−1.05 ± 0.09 mV) to positive (+23.7 ± 1.74 mV) as

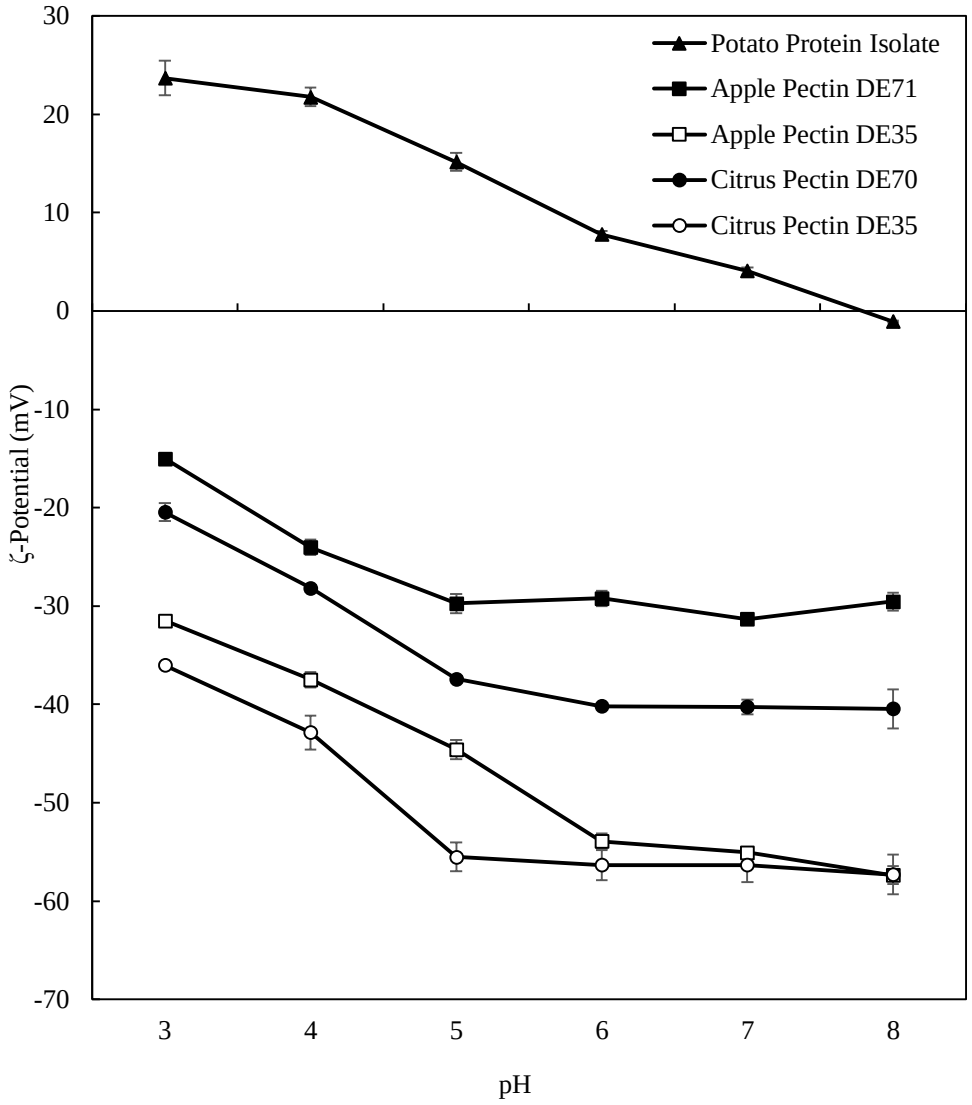

Figure 3.1 : Impact of pH on ζ-potential of PPI, AP DE71, AP DE35, CP DE70, CP DE35.

the pH was decreased from 8 to 3. As the pH decreases, carboxyl groups and amino groups of the protein undergo a gradual protonation which results a change in electrostatic repulsion pattern [66]. The measured pI of potato protein was between pH 7-8 which shows that the potato protein samples used in this study mostly consisted of protease inhibitors, that were reported to have a varying pI between 5-8 [60, 67].

In addition, the lowest solubility (53.52 ± 1.00%) for potato protein solution was measured under alkaline conditions (pH 8) whereas a gradual increase was observed with decreasing pH reaching a maximum value (92.99 ± 2.03%) at pH 3 (Table 3.1). A statistical evaluation confirmed that solubility was directly dependent on net ζ-potential values ($r = 0.922$; $p > 0.01$) proving the effect of alteration in electrostatic

repulsion on the solubility with a change in degree of surface charge. It was mentioned that increased net surface charge can overcome various attractive forces (e.g., van der Waals, hydrophobic and depletion) which contributes to the solubility at acidic pH [68, 69]. Near the pI, the repulsive electrostatic interactions between molecules are of very low magnitude so that protein molecules form aggregates [70].

Table 3.1 : Solubility (%) of potato protein ($c_{biopolymer}$ 0.5%) as a function of pH (3 - 8).

pH (±0.05)	Solubility (%)
3	92.99 ± 2.03
4	91.05 ± 3.23
5	60.74 ± 0.34
6	62.12 ± 1.61
7	55.50 ± 0.45
8	53.52 ± 1.00

In contrast, all pectins tested had negative surface charge over the entire pH range (Fig. 1) – a typical pH-depended behavior for that type of hydrocolloid. It can be clearly seen that all pectin types had higher negative surface charge at higher pH values and there is a sharp decrease in net negative surface charge due to p*K*a values around 3.5 of carboxylic acid groups. The carboxylic acid groups would be uncharged (–COOH) at the values lower than p*K*a while they can be fully charged ($–COO^-$) at high pH values [71]. However, significant differences between pectins with various DE was observed. As such, pectins with a low DE had a higher net negative surface charge over the whole pH range regardless of origin due to a larger number of dissociated carboxylic acid groups [72]. The differences in ζ-potential plots of pectins with the same DE and from different sources could be due to block-wise distribution of free carboxylic acid groups in citrus pectin [73, 74]. It was previously reported that the most ordered pectin in terms of non-esterified carboxylic acid groups has the net highest negative ζ-potential among pectins with the same DE [74].

Based on the characterized properties of individual biopolymers, we chose pH 3 for the formation of complexes. At this pH both biopolymers (protein and polysaccharides) showed a high solubility and nearly equal net surface charge values which potentially promotes electrostatic attraction [75, 76].

3.3.2 Physicochemical characterization of complexes

In general, it was demonstrated that the complex formation was promoted under conditions where the biopolymers carry opposite charges, whereas the pH-value, protein-pectin ratio, and the pectin type could be used to modulate the size and morphology of the complexes formed. ζ-potential measurements have been used as a rough measure in the study as it is the commonly used method to evaluate the complex formation between oppositely charged biopolymers [30]. Viscosity measurements, microstructure images and visual observations were used to characterize the complexes formed.

3.3.3 Impact of biopolymer ratio

The purpose of this set of experiments was to determine an optimum protein-pectin ratio to generate complexes. As such, potato protein and various pectin types were mixed under acidic conditions (pH 3) at different protein-pectin ratios ranging between 0.33-5, whereas the overall protein concentration (0.25 %) was kept constant. The impact of protein-pectin ratio on the surface charge of complexes is shown in Fig. 3.2. The net negative surface charge of the complexes decreased with protein proportion until achieving electro-neutrality (ζ-potential = 0 mV), whereas higher protein-pectin ratios produced complexes with higher positive surface charge. At the point of electro-neutrality, all negative sites of pectin are saturated by positive sites of potato protein. Neutral surface charge was obtained at near to a protein-pectin ratio of 2.5 for the complexes formed with high DE pectins. Protein-pectin ratios of 1 and 1.67 were required for charge neutralization for the complexes formed by AP DE35 and CP DE35, respectively. The ζ-potential values of the mixtures turned to positive at higher protein-pectin ratios, which can be explained by low amount of carboxylic groups of pectins in solution to interact with amino groups of protein. It was indicated that, protein-pectin ratio controls the equilibrium of macromolecule charges and thus the degree of electrostatic interactions and the extent of self-aggregation during complex formation [77]. Sanchez et al. [78] also stated that the structure of coacervates is affected by biopolymer mixing ratio.

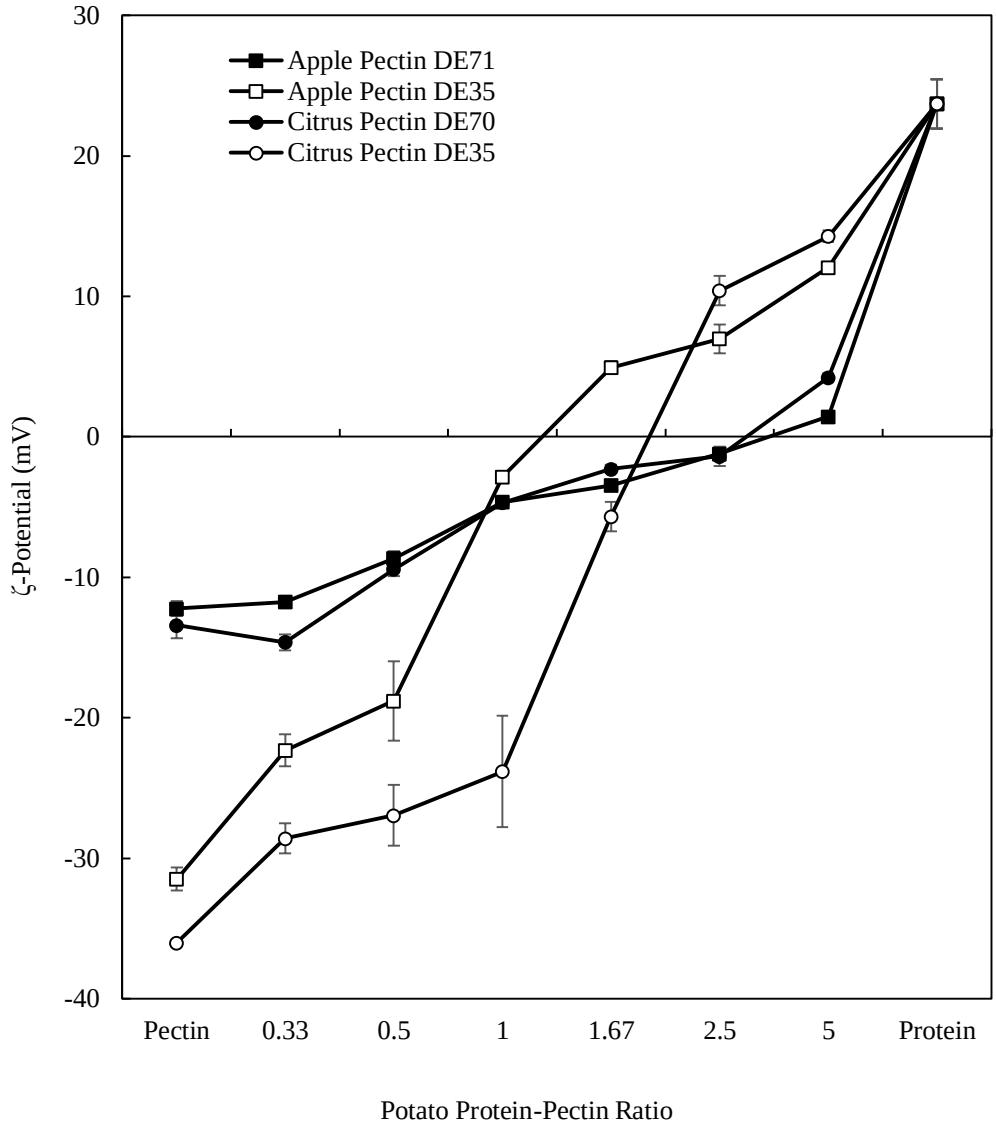

Figure 3.2 : ζ-potential of complexes ($c_{protein}$ 0.25%) of PPI / different pectin types as a function of protein-pectin ratio generated at pH 3.

ζ-potential results were supported by visual observations of the mixtures as a function of protein-pectin ratio (0.33-5) (Fig. 3.3). For samples with lower ζ-potential values (< 20mV), phase separation and precipitation could be observed, while at higher values (> 20 mV) stable coacervates with a turbid appearance formed. Kim and Wicker [79] also stated that insufficient pectin concentration results in bridging flocculation while too high pectin concentration cause a strong increase in viscosity preventing the precipitation. In addition, microscopic images showed that intensity of interaction between biopolymers was enhanced by the protein-pectin ratio (Fig. 3.4). The complexes at the ratio of 0.33 showed dispersed small aggregates while larger clusters with a firmer appearance were observed for those complexes generated at ratio of 1, 2.5 and 5. There were dispersed small aggregates which probably resulted from

protein-protein interactions at high protein-pectin ratio. Wang et al. [73] explained complex formation at high protein-pectin ratio with binding of protein separately on the pectin chain network and aggregation of some protein dimers with each other to form small protein domains. In addition, all complexes at different protein-pectin ratio showed various morphology rather than uniform and spherical shape. It was explained by Ducel et al. [80] by the concentration of biopolymers. They indicated that, some particles agglomerate and coalesce which results in an increase in the size of coacervates (more than 50 μm) and cause different morphologies at a concentration of 10 g/L while small spherical droplets of coacervates were obtained with a mean size around 10 μm at a concentration of 1g/L.

3.3.4 Impact of pectins' DE

As it is seen in Fig. 3.2, the surface charge pattern of the complexes was clearly affected by DE of pectins. The slope of surface charge plot of complexes generated with low DE pectins was higher than complexes formed with high DE pectins. Higher protein-pectin ratios required for net ζ-potential values < 10 mV in the complexes generated with low DE pectins. This is probably due to higher amount of galacturonic acid content of low DE pectins. In addition, previous literature [81, 82] indicated that the difference in water affinity between protein and pectin decrease when the pectin is less hydrophilic which is possible when it has lower DE. It was reported that when both biopolymers have similar and low water affinity, they do not show a tendency to dissolve in water as an individual biopolymer, instead their compatibility to each other increase and stronger interactions are formed [83]. We assumed that, plant proteins which contains relatively higher hydrophobic amino acids than animal proteins could make stronger interactions with pectins with low DE. It was also stated by Einhorn-Stoll et al. [81] that compatibility of sodium caseinate which is a relatively hydrophobic protein has increased when pectin with low DE has used for complexation.

Visual observations also demonstrated that DE of pectins clearly affects the complex formation especially at higher protein-pectin ratios (Fig. 3.3). All complexes at the protein-pectin ratio of 0.33 promoted a turbid appearance without visible sedimentation. However, high DE pectins caused a precipitation at the ratio of 0.5 in

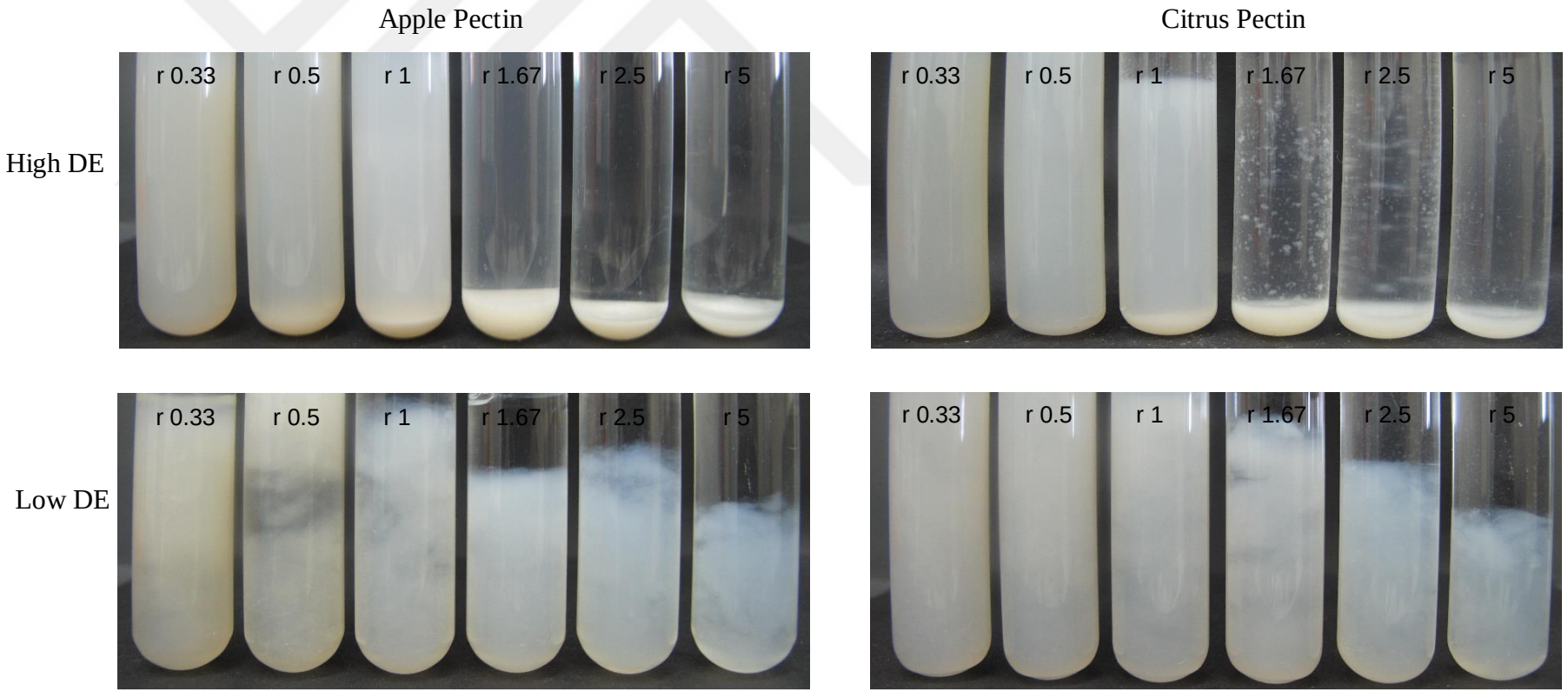

Figure 3.3 : Images of complexes complexes ($c_{protein}$ 0.25%) of PPI / different pectin types as a function of protein/pectin ratio generated at pH 3.

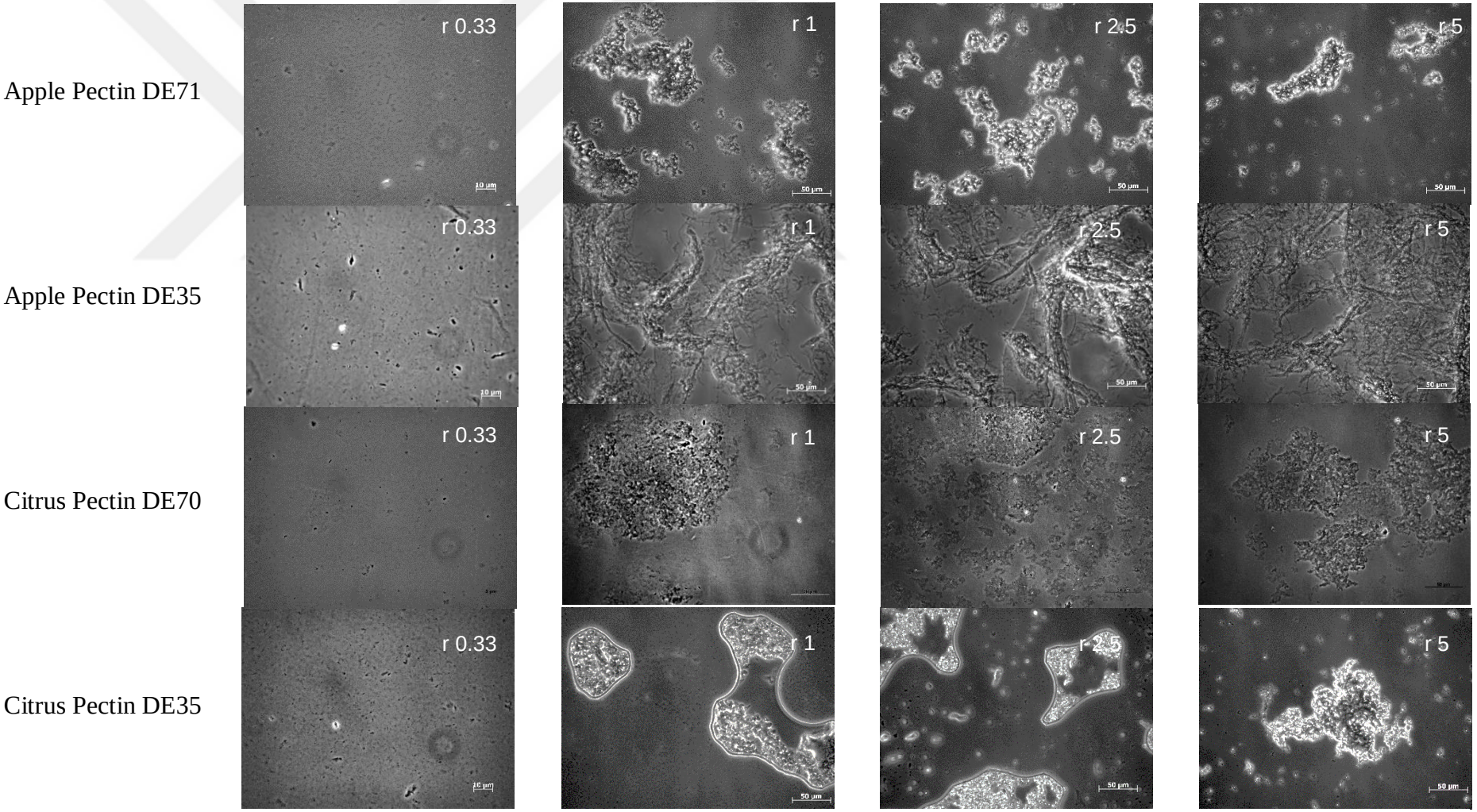

Figure 3.4 : Microscopic images of complexes generated at different protein to pectin ratios (0.33 – 1 – 2.5 – 5.0) with AP DE71, AP DE35, CP DE70 and CP DE35.

addition to a turbid supernatant. At higher protein-pectin ratios, the complexes generated with high DE pectins looked more like a precipitate than a coacervate while there was a cloudy phase separation formed with low DE pectins. This is probably due to viscous structure of low DE pectins interfering with the sedimentation of coacervate [84]. Microscopic images (Fig. 3.4) supported the visual observation that large number of small features in microscopic images gave a low degree of phase separation in visual observation while small number of large features lead to precipitation or coacervation. Protein-pectin mixtures obtained with low DE pectin had a different visual observation and microscopic images than the mixtures obtained with high DE. This could be due to the presence of hydrogen bonding between pectin chains and minor contribution of hydrophobic interactions to electrostatic interactions in complexes formed with low DE. These interactions could be neglected for the complexes generated with high DE due to their high hydrophilicity [85].

3.3.5 Impact of pectin source

The pectin source also had an effect on complexation and the viscosity of the formed complexes. The degree of blockiness, molecular weight and neutral sugar side chains could be the influencing factors depending on the source of pectins.

As can be seen from Fig. 3.2, surface charge patterns were similar for complexes formed with high DE pectins, irrespective of their origin. For low DE pectins, however, clear differences could be seen. Even though the DE of CP DE35 and AP DE35 was the same, the complexes formed with the latter reached to neutralization at a lower protein-pectin ratio. This could be explained by differences in degree of blockiness values in these two pectins.

The distribution of carboxylic acid groups was largely studied in relation to the formation of gels in the presence of Ca^{2+}. It was reported in several studies that pectins with low DE which are able to form gel in the presence of Ca^{2+} have higher gelling properties when those have higher amount of block-wise distributed carboxylic acid groups. Block-wise distribution of reactive sites generates a local charge concentration and hold Ca^{2+} ions in place in gel structure [86-92]. Lutz et al. [74] explained that, the block-wise arrangement allows stronger and more effective intermolecular interactions, probably because the sequence of carboxylic acids permits better contact

between the pectin chains and better utilization of the carboxylic acid groups is provided.

As such, it was indicated that pectins having a higher local charge density might form complexes with proteins which could withstand harsher environmental conditions [93]. Warnakulasuriya et al. (2013) [94] also found that dispersions including pectins with high DB gave higher OD values meaning the formation of more complexes with pea protein isolate. In addition, we recently demonstrated that protein pectin complexes grew in size with decreasing temperatures, increasing degree of charge density and decreasing pectin concentration [95].

It was indicated that citrus pectin shows a block-wise esterification due to its partial demethylation by native pectin esterase prior to processing [74, 93, 96]. However, for complexes formed with low DE pectins, higher differences in ζ-potential were observed. A reason for this could be the higher sensitivity of low DE pectins than that of high DE pectins to cationic charge groups when they possess a block-wise distribution [97]. Besides the degree of blockiness, Warnakulasuriya et al. [94] mentioned that neutral sugar side chains could also have an important role on complex coacervation by means of hydrogen bonding or hydrophobic interactions.

Based on the viscosity measurements, complexes formed with apple pectin had a higher viscosity than citrus pectin with the same DE at lower protein-pectin ratios (Fig. 3.5). Wang et al. [73] indicated that, viscosity of pectin solutions increase with molecular weight and neutral sugar side chains at similar galacturonic acid contents. However, neutral sugar side chains appeared to be predominant factor affecting the viscosity in our case as apple pectin has lower molecular weight but higher neutral sugar side chains than citrus pectin. This finding was supported by Wang et al. [73] and Renard et al. [98] who observed a higher viscous shares for apple pectin than citrus pectin.

3.4 Conclusion

The results of this study showed that the pectin type and degree of esterification had a clear impact on the association of potato protein-pectin complexes. Based on the measured surface charge, microscopic images and visual observation, it can be concluded that the ratio between protein and polysaccharide had also a substantial

effect on charge balance and therefore on the intensity of interactions. Citrus pectin proved to be better to prepare complexes as complex solutions had a lower viscosity. Moreover, high DE pectins provided less viscous complexes than low DE pectins which could make their utilization easier in food industry. The strongest interaction between PPI and citrus pectin with a high DE occurred at a protein-pectin ratio of 2.5:1. A further study could be conducted on microencapsulation of a bioactive compound using the prepared potato protein - pectin coacervates.

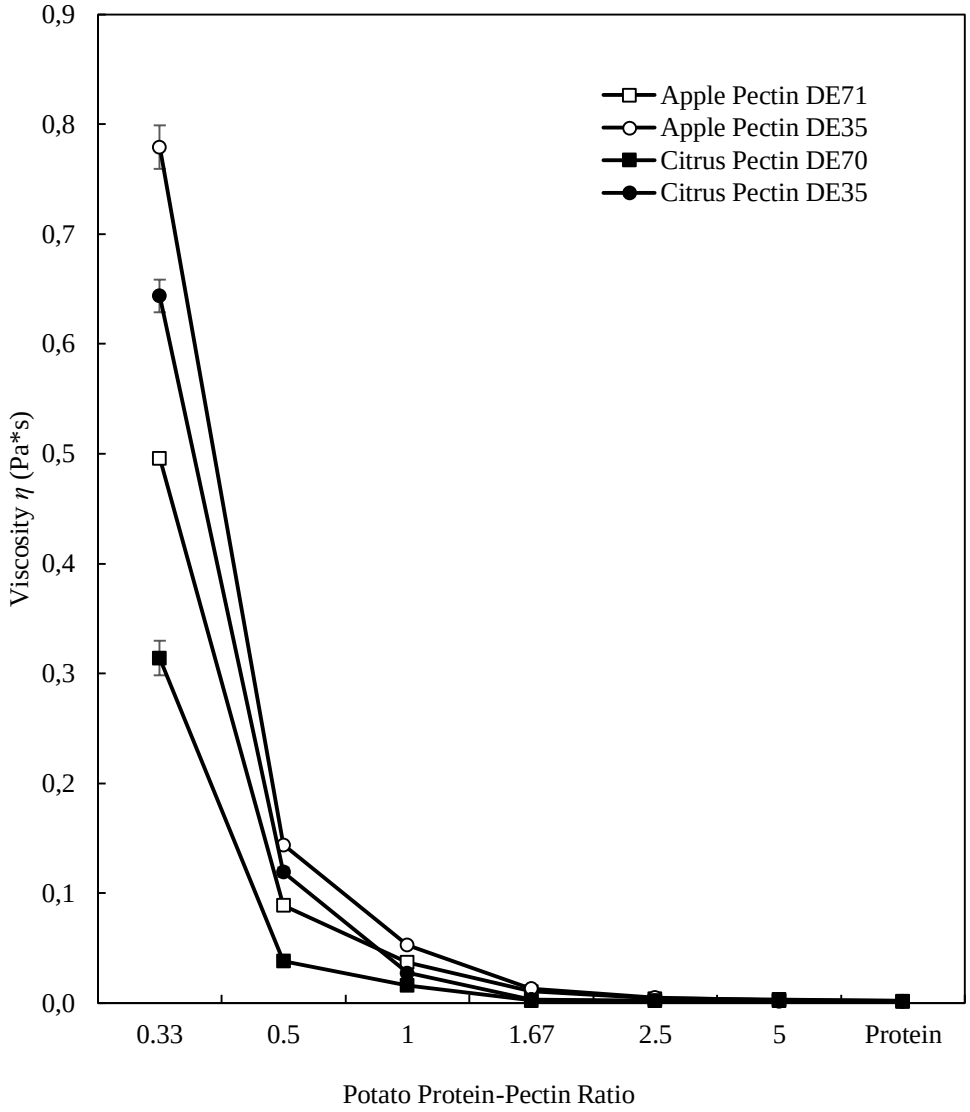

Figure 3.5 : Rheological properties (viscosity) of biopolymer samples as a function of apple pectin/protein ratio formed at pH 3 ($c_{protein}$ = 0.5%). Viscosity η shown at a shear rate $\gamma = 203\ s^{-1}$.

4. THE RSM OPTIMIZATION OF RECOVERY OF ANTHOCYANIN-RICH EXTRACTS FROM BLACK CARROTS USING TERNARY COMPRESSED MIXTURES OF CO_2-ETHANOL-WATER

4.1 Introduction

Black or purple carrot (Daucus carota ssp. sativus var. atrorubens Alef.) is an ancient root crop which originate from Turkey and the Middle and Far East [99]. Black carrots were reported to have anthocyanin content in the range of up to 1750 mg/kg fresh weight whereas 45.4 mg/kg to 17.4 g/kg dry matter [100]. Black carrot anthocyanins reported to have higher color stability to alterations in pH and temperature than those of other plants which makes black carrot extracts a good alternative for coloring confectionery, jellies, conserves, soft drinks, and fruit juices and nectars [1].

Anthocyanin-rich extracts are conventionally derived based on solid–liquid extraction using slightly acidified aqueous alcoholic solvents [101, 102]. Traditional extraction methods are fairly simple and have widespread use, however, they can be inadequate and time-consuming, consume large amount of organic solvents, and cause degradation of anthocyanins [103]. Therefore, the availability of novel technologies for the extraction of colorants, antioxidants or other bioactive compounds are being investigated to explore faster and environmental-friendly extraction procedures for high-quality extracts with reduced organic solvent consumption [101, 102]. CO_2 at sub- and supercritical conditions has drawn an increasing interest as an extraction solvent due to its high solvating power and being available, cost-effective, non-flammable, non-toxic, and easily removed from the obtained extracts. Moreover, the inert atmosphere provided in extraction system prevents the deterioration of phenolic compounds [104]. However, CO_2 has a nonpolar and lipophilic nature and is not able to extract compounds with strong polar functional group such as –OH and -COOH [105]. In addition, it was documented that compounds with the molecular weights higher than 400 are almost insoluble, anthocyanins have a molecular weight of ≈600 g/mol [105, 106]. Modifiers are used to overcome this problem such as ethanol, water

or mixtures of both [107]. The concentration of modifier can be used at a level where it is soluble in sc-CO_2, at the pressure and temperature used, so the mixture is considered supercritical [107, 108]. Another approach is to use higher amounts of water and/or ethanol where CO_2 is completely dissolved in the liquid phase, or the two-phase region, where liquid and vapor phases are in equilibrium [104, 108, 109]. The usage of CO_2-ethanol-water ternary compressed solvents for the extraction of phenolic compounds may provide the benefits of both sc-CO_2 extraction and solid liquid extraction which results in decreased solvent usage with increased mass transfer and the solubility [109].

Recently, several papers have been documented on the applicability of CO_2-ethanol-water mixtures to obtain anthocyanin-rich extracts from *Crocus sativus* petals [103], eggplants [110], *Syzygium cumini* fruit pulp [102], cranberry pomace [109], purple corn cob [111], blueberry residues [108], *Arrabidaea chica* [112], blackberry bagasse [113], elderberry pomace [104], and grape marc varieties [114]. However, there is no study on the optimization of extraction parameters using ternary solvents to produce anthocyanin-rich extracts from black carrots. Thus, the present study is considered the first effort aiming to investigate the effect of process parameters i.e. pressure, temperature and ethanol-water ratio on total anthocyanin content (TMAC), total flavonoid content (TFC), total phenolic content (TPC), and antioxidant activity and determine the optimum values of process parameters to extract phenolic compounds by CO_2-ethanol-water mixtures.

4.2 Materials and Methods

4.2.1 Chemicals and reagents

Liquid CO_2 (purity 99.5%) at 49.5 bar (15ºC) was supplied by Linde Gases (Istanbul, Turkey). For TMAC, TPA, TFA, antioxidant activity analyses measured by CUPRAC (AC-CUPRAC) and DPPH (AC-DPPH) and anthocyanin composition; cyanidin-3-glucoside (≥95%), neocuproine ($C_{14}H_{12}N_2$), 6-hydroxy-2,5,7,8-tetramethylchroman-2-carboxylic acid (Trolox), ammonium acetate (NH_4Ac), copper (II) chloride ($CuCl_2$), potassium metabisulfite ($K_2S_2O_5$), sodium acetate trihydrate ($CH_3COONa.3H_2O$), potassium chloride (KCl), sodium bicarbonate ($NaHCO_3$), methanol (≥99.9 %), ethanol (≥99.8 %), 1,1-diphenyl-2-picrylhydrazyl (DPPH), Folin-Ciocalteu phenol reagent, and gallic acid (≥98) were purchased from Sigma-Aldrich Chemie GmbH

(Steinheim, Germany). For all analysis, distilled water was used and all other reagents used were of analytical grade.

4.2.2 Conventional extraction

The freeze-dried black carrot samples were extracted using the method of Guldiken et al. [115] with some modifications. 0.3 gr of sample was dissolved in 30 ml of 75% ethanol-water mixture, which was adjusted to pH 3.5 with citric acid. The tubes were then placed in a thermostatic water bath at 50^{o}C and shaken at maximum speed for 3 hours. After this step, the tubes were placed in the ultrasonic bath for 15 minutes and then centrifuged at 5000 rpm for 10 minutes. The supernatant was separated by filter paper and collected for further analysis.

4.2.3 Ternary compressed fluid extraction

Ternary compressed fluid extraction experiments were conducted in a bench scale apparatus (SFE-500, Separex, Champigneulles, France). It consists of a high pressure vessel (500 mL) with sintered disks, a separator (max. 210 bar and 150^{o}C, 300 mL), high pressure CO_2 piston pump (max. 1000 bar, 5-100 g/min), high pressure co-solvent pump (max. 400 bar, 0.01 – 10 mL/min), an oven, a pre-heater, a cold exchanger and a condenser. The flow sheet of this plant is given in Fig. 4.1.

Liquid CO_2 is sub-cooled in the cold exchanger and then pressurized by a high pressure piston pump where flow rate can be regulated. The extraction pressure is adjusted manually by means of a back pressure valve. CO_2 and aqueous ethanol solutions are pre-heated through a heat exchanger before the extraction vessel. The extraction takes place in a high pressure vessel that is maintained at constant pressure and temperature which is placed in an oven. The extract is collected at the bottom of the separator and gas effluent is sent to the vent line. High pressure cyclonic separator is also adjusted to extraction temperature by an electrically heated jacket. Gaseous CO_2 is recycled from the separator to the pump through a condenser to be liquefied. An electronic interface (Nanodac^{TM} Eurotherm^{TM} Controller/Indicator/Data Logger) indicates the extraction vessel temperature, extraction vessel pressure, separator temperature and separator pressure.

Black carrots were supplied from a local producer in Adana and stored at −80 °C until analysis. All samples were ground to a fine powder (d = 200 μm) under liquid nitrogen

using a precooled grinder and then lyophilized. In each experiment, 10 g of feed material were placed between three layers of glass beads in the high pressure vessel. The glass beads were used for a uniform distribution of solvent flow and reducing the dead space in the vessel. When the desired temperature reached, the CO_2 and co-solvent pumps are opened and vessel was pressurized. The pressure was adjusted using a back pressure regulator. The flow rate of CO_2 and ethanol-water mixtures were set at 100 g/min and 10 mL/min, respectively, considering the limitations of the equipment. The volume and molar ratio of CO_2-ethanol-water mixture were calculated for all experiments and presented in Table 4.1. Extraction time was determined in preliminary experiments and keep constant at 40 min. The extract was collected in propylene tubes and stored at -80°C.

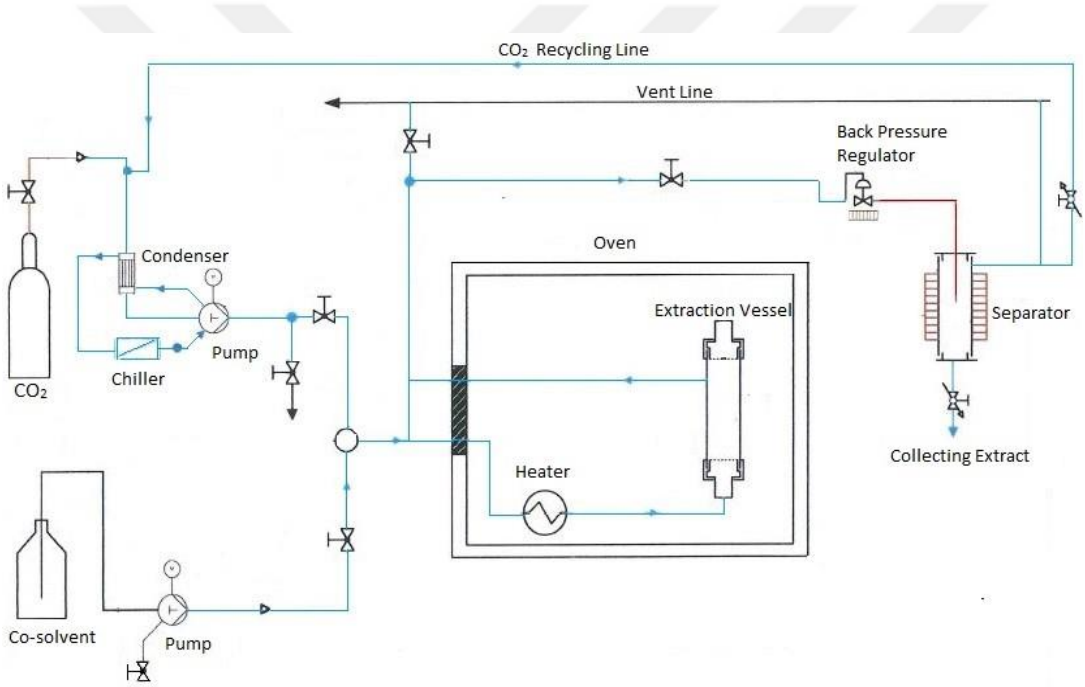

Figure 4.1 : Flow diagram for the SFE 500 apparatus.

The amount of dry matter was determined by removing the ethanol at 40°C using a rotary evaporator and then drying at 105°C until constant weight of the dry matter was obtained.

The densities of solvents at the conditions determined by RSM were calculated using TREND 4.0 (Thermodynamic Reference and Engineering Data) [116]. Even though there is no equation of state available in the literature for ternary CO_2-ethanol-water mixtures, a predictive combining rule which is the linear combining rule was applied. Thereby, the densities at different surface parameters were calculated to be able to

observe if there is any relation between the densities and the results of response variables.

4.2.4 Experimental design

Response Surface Methodology (RSM) accompanied by Central Composite Design (CCD) was used to determine the influence of selected process parameters and find optimal condition of variables for desirable responses. CCD was constructed by the Design Expert (Version 12.0.0, Stat-Ease Corporation, Minneapolis, MN, USA). As demonstrated in Table 4.2, the design comprises 20 trials from three independent variables at five levels of the system: pressure (100, 175, 250, 325, 400), temperature (20, 30, 40, 50, and 60^{o}C) and ethanol-water ratio in ethanol water mixtures (10/90, 30/70, 50/50, 70/30, 90/10). Six replicates of the center point were used to evaluate the process stability and inherent variability. All experiments were conducted in duplicate and the averages of results were taken as a response.

4.2.5 Total monomeric anthocyanins

The total monomeric anthocyanin content was determined in duplicate using the pH differential method (Giusti and Wrolstad, 2000). The appropriate dilution factor was determined by diluting with 0.025 M potassium chloride buffer, pH 1 until the absorbance of the sample at 520 nm is within the linear range of spectrophotometer (Biotek Instruments Inc., Vinooski, USA). Two dilutions of the samples were prepared, one with potassium chloride buffer, pH 1, and the other with sodium acetate buffer, pH 4.5, diluting each by the previously determined dilution factor. The samples were then equilibrated for 15 min and the absorbance of samples were measured at 520 nm and 700 nm. The results were expressed as cyanidin-3-glucoside equivalents per L extract by using the following formula:

$$\text{Total Monomeric Anthocyanin (mg/L)} = \frac{\text{A x MW x DF x 1000}}{\varepsilon \text{ x } 1} \tag{4.1}$$

$$A = (A_{520} - A_{700})_{pH1} - (A_{520} - A_{700})_{pH4.5} \tag{4.2}$$

where A is the absorbance, MW is the molecular weight of cyanidin-3-glucoside (449.2 g/mol), DF is the dilution factor, 1000 is the conversion factor from g to mg, ε

Table 4.1 : Volume fraction, molar fraction and density of ternary solvent mixtures for all experiments.

Pressure (bar)	Temperature (^oC)	EtOH Conc. in EtOH/W mixtures(% v/v)	Volume Fraction			Molar Fraction			Density of Solvent
			CO_2	EtOH	H_2O	CO_2	EtOH	H_2O	
250	40	50	0.92	0.04	0.04	0.8625	0.0325	0.1050	898.58
250	40	50	0.92	0.04	0.04	0.8625	0.0325	0.1050	898.58
250	40	50	0.92	0.04	0.04	0.8625	0.0325	0.1050	898.58
250	60	50	0.93	0.04	0.04	0.8625	0.0325	0.1050	818.43
250	20	50	0.91	0.04	0.04	0.8625	0.0325	0.1050	970.15
100	40	50	0.94	0.03	0.03	0.8625	0.0325	0.1050	711.35
175	30	70	0.92	0.06	0.02	0.8882	0.0469	0.0649	891.73
175	50	70	0.93	0.05	0.02	0.8882	0.0469	0.0649	791.63
250	40	90	0.92	0.07	0.01	0.9156	0.0621	0.0223	895.66
250	40	10	0.92	0.01	0.07	0.8152	0.0061	0.1787	903.56
250	40	50	0.92	0.04	0.04	0.8625	0.0325	0.1050	898.58
325	30	30	0.91	0.03	0.06	0.8382	0.0190	0.1429	968.26
400	40	50	0.91	0.04	0.04	0.8625	0.0325	0.1050	962.24
325	50	30	0.92	0.02	0.06	0.8382	0.0190	0.1429	904.96
175	50	30	0.93	0.02	0.05	0.8382	0.0190	0.1429	791.14
175	30	30	0.92	0.02	0.06	0.8382	0.0190	0.1429	894.97
325	50	70	0.92	0.06	0.02	0.8882	0.0469	0.0649	899.67
250	40	50	0.92	0.04	0.04	0.8625	0.0325	0.1050	898.58
250	40	50	0.92	0.04	0.04	0.8625	0.0325	0.1050	898.58
325	30	70	0.91	0.06	0.03	0.8882	0.0469	0.0649	963.61

Table 4.2 : Central Composite Design and the dry matter, total anthocyanins, total phenolics, total flavonoids and antioxidant capacities of the extracts.

Run	Parameters			Responses					
	Pressure (bar)	Temperature (°C)	Ethanol Conc. in Ethanol-Water Mixtures (%, v/v)	Dry Matter Content (%)	TMAC (mg/L)	TPC (mg/ 100mL)	TFC (mg/100mL)	AC-CUPRAC (mg/100 mL)	AC-DPPH (mg/100 mL)
1	250	40	50	8.80 ± 0.82	106.43 ± 2.01	49.16 ± 0.99	31.56 ± 1.52	389.15 ± 49.86	98.60 ± 16.88
2	250	40	50	9.54 ± 0.44	112.63 ± 1.67	59.96 ± 3.01	32.43 ± 3.13	414.44 ± 40.10	104.74 ± 18.54
3	250	40	50	9.19 ± 0.64	114.89 ± 16.36	56.39 ± 4.80	38.54 ± 1.33	434.91 ± 40.45	111.00 ± 10.93
4	250	60	50	8.73 ± 1.04	89.17 ± 11.59	52.57 ± 4.20	36.26 ± 3.41	398.32 ± 32.06	104.97 ± 18.70
5	250	20	50	2.72 ± 0.28	38.74 ± 3.25	19.56 ± 1.26	16.14 ± 2.28	251.30 ± 21.41	60.06 ± 3.79
6	100	40	50	2.07 ± 0.16	36.63 ± 3.60	16.90 ± 0.64	12.19 ± 0.47	149.80 ± 16.61	37.28 ± 1.40
7	175	30	70	4.16 ± 0.02	64.51 ± 4.29	19.97 ± 1.33	17.28 ± 1.80	247.91 ± 23.82	63.06 ± 5.77
8	175	50	70	5.19 ± 0.56	72.81 ± 6.53	26.89 ± 0.98	23.79 ± 0.38	309.70 ± 41.38	72.82 ± 3.55
9	250	40	90	2.57 ± 0.37	42.80 ± 0.51	15.15 ± 0.81	14.53 ± 0.57	162.44 ± 17.30	29.64 ± 1.60
10	250	40	10	3.46 ± 0.43	46.48 ± 2.57	13.40 ± 0.86	17.42 ± 0.66	164.73 ± 14.84	33.23 ± 2.41
11	250	40	50	8.31 ± 0.53	91.57 ± 5.68	44.24 ± 6.12	30.36 ± 0.95	384.34 ± 38.83	94.14 ± 20.18
12	325	30	30	4.41 ± 0.51	74.70 ± 13.26	33.81 ± 2.52	26.33 ± 0.38	302.91 ± 22.06	64.03 ± 1.70
13	400	40	50	9.44 ± 0.34	93.12 ± 4.55	48.87 ± 1.68	32.57 ± 5.41	389.49 ± 35.52	96.80 ± 12.28
14	325	50	30	8.56 ± 0.61	105.87 ± 13.80	43.40 ± 4.44	39.21 ± 3.98	416.31 ± 39.45	92.40 ± 9.67
15	175	50	30	4.20 ± 0.39	53.38 ± 8.77	22.36 ± 2.62	22.65 ± 3.13	292.05 ± 3.27	64.24 ± 5.41
16	175	30	30	3.37 ± 0.52	44.42 ± 2.05	18.08 ± 0.18	18.56 ± 1.52	216.06 ± 15.42	45.72 ± 2.70
17	325	50	70	11.43 ± 0.47	122.57 ± 7.25	65.58 ± 11.69	47.39 ± 1.90	455.40 ± 48.71	115.40 ± 12.61
18	250	40	50	10.04 ± 0.80	115.53 ± 2.49	57.16 ± 1.68	40.62 ± 4.27	424.45 ± 50.79	106.07 ± 19.47
19	250	40	50	10.51 ± 0.31	119.56 ± 6.72	54.44 ± 3.43	43.97 ± 0.28	452.64 ± 20.35	112.22 ± 9.05
20	325	30	70	5.04 ± 0.57	73.70 ± 9.28	35.24 ± 2.99	29.02± 1.71	357.31 ± 22.80	78.79 ± 6.01

is the molar extinction coefficient of cyanidin-3-glucoside (26900 L/(mol.cm)), and l is the path length (cm).

4.2.6 Anthocyanin profile in the optimized extract by HPLC

The extract obtained at the optimum conditions and commercial extract were analyzed by HPLC for the comparison of the anthocyanin profile and quantification using the method of Agcam et al. [117]. The extracts filtered by 0.45 µm PES syringe filter, and injected to high performance liquid chromatographer (Agilent 1260 Infinity Series, Agilent Technologies, Waldbronn, Germany) equipped with a diode array detector (DAD) and autosampler. 20 µL of supernatant was injected into the C18 (5 µm, 4.6 x 250 mm) Nucleodur (Macherey-Nagel, Düren, Germany) column at room temperature. The flow rate was 1.0 mL min^{-1} and detector was set to 520 nm. Formic acid-water (5:95, v/v, A) and ACN-phase A (80:20, v/v, B) were used as mobile phases. The mobile phase gradient elution was 95% A + 5% B at 0 min, 75% A + 25% B at 25 min, and 95% A + 5% B at 30 min. Individual anthocyanins in extract obtained at optimal conditions were quantified using a calibration curve of cyanidin 3-O-glucoside including a molecular weight correction factor [118].

4.2.7 Total flavonoid content

Total flavonoid content was determined according to method of Bouayed et al. [119]. At the onset of the experiment, 250 µL extract was diluted with 1.25 mL of distilled water and 75 µL of $NaNO_2$ solution (5% w/v) was added. After 5 min incubation, 150 µL of $AlCl_3$ solution (10% w/v) and subsequently, 500 µL of 1 M NaOH solution was introduced to the solution. The volume of the mixture was completed to 2.5 mL with distilled water. The absorbance was measured against blank at 510 nm. The results were expressed as mg catechin equivalent (CAE) per 100 mL extract.

4.2.8 Total phenolic content

Total phenolic content was determined based on the Folin–Ciocalteau method. Briefly, 1.5 mL of diluted Folin–Ciocalteau reagent (1:10, v/v) was added to 200 µL extract. Subsequently, 1.2 mL aqueous 7.5% sodium bicarbonate solution was added to this mixture. After 90 min incubation, absorbance was measured at 765 nm. Results were expressed as mg of gallic acid equivalents (GAE) per 100 mL extract.

4.2.9 Total antioxidant capacity

The total antioxidant capacity was estimated by two different assays; 1,1-diphenyl-2-picrylhydrazil (DPPH) and cupric ion reducing antioxidant capacity (CUPRAC) assays which were conducted based on the methods of Kumaran and Karunakaran [120] and Apak et al. [121], respectively.

To determine total antioxidant capacity with CUPRAC assay, 100 µL of sample was treated with 1 mL of ammonium acetate (pH 7), 1 mL of neocuproine solution (7.5×10^{-3} mol/L), 1 mL of copper (II) chloride solution (10^{-2} mmol/L) and 1 mL of distilled water. The mixture was then kept in the dark at room temperature for 25 min and the absorbance was measured at 450 nm.

DPPH assay was performed with 2 mL of DPPH solution (10^{-1} mmol/L) which was added to 100 µL of sample. The solution was then vortexed and kept in the dark at room temperature for 25 min. The absorbance was measured at 517 nm. The results of both CUPRAC and DPPH assays were expressed as mg TEAC per 100 mL extract.

4.2.10 Statistical analysis

4.2.10.1 Modeling of variables

The second order polynomial equation used to predict optimal point as a function of the independent variables along with the regression coefficient values are shown in equation 4.3 below:

$$Y=b_0+b_1x_1+b_2x_2+b_3x_3+b_{11}x_1^2+b_{22}x_2^2+b_{33}x_3^2+b_{12}x_1x_2 +b_{13}x_1x_3+b_{23}x_2x_3+\varepsilon \quad (4.3)$$

where Y is the predicted response; x_1, x_2 and x_3 the independent variables; b_0 a model constant; b_1, b_2 and b_3 the linear coefficients; b_{11}, b_{22} and b_{33} the quadratic coefficients; and b_{12}, b_{13} and b_{23} the cross-product coefficients. The statistical significance of the terms in the regression equations was evaluated by analysis of variance (ANOVA) for each response. The values of determination coefficient (R^2), adjusted determination coefficient (Adj. R^2), predicted determination coefficient (Pred. R^2), and CV % were obtained to check the quality of the fit polynomial model. The significances of all terms in the polynomial were determined statistically by evaluating the Lack of Fit F-

value and p-value. The aforementioned quadratic equation was employed to describe surfaces for the variables.

4.2.10.2 Optimization and verification procedures

The models fitted in the study were also utilized for numerical optimization using the desirability function which was represented in equation 4.4 below:

$$D=(d_1 d_2 \ldots d_m)^{1/m} \quad (4.4)$$

Where D is defined as the geometric mean of the individual desirability functions. The algorithm searches for response variable values where D converges to 1. m is the number of response variables. Design Expert Version 11 was used for numerical optimization. Optimization was aimed to maximize anthocyanins, total phenolics, total flavonoids and antioxidant activity. To evaluate the validity of the optimized conditions, experiments were conducted under optimum conditions. The average value of the experiments was compared with the predicted values of the optimized conditions and ascertain the accuracy and suitability of the optimum conditions and mathematical models.

4.3 Discussion

4.3.1 Model fitting

Extraction variables were selected as pressure, temperature, and ethanol-water ratio. The design for combined effects comprised of 20 experiments according to Table 4.2. The experimental values of extract yield, total monomeric anthocyanin, total phenolics, total flavonoids and antioxidant capacities of black carrot extracts at various experimental conditions were also shown in Table 4.2. The results of analysis of variance, goodness of fit and the adequacy of the models are presented in Table 4.3. The models had satisfactory R^2 and adjusted R^2 values. Predicted R^2 values were in reasonable agreement with the adjusted R^2; i.e. the difference was less than 0.2 for all responses. The model F values implied that the models were significant and the p values were less than 0.05. Lack of fit F values implied that the Lack of Fit is not significant relative to pure error.

Table 4.3 : Model summary and lack of fit values.

	R^2	Adj. R^2	Pred. R^2	CV %	F-value	p-value	Lack of Fit F-value	Lack of Fit p-value
Dry Matter Content	0.96	0.92	0.79	13.01	26.59	< 0.0001	1.25	0.40
TMAC	0.94	0.89	0.73	12.25	18.20	< 0.0001	0.93	0.53
TPC	0.95	0.89	0.75	14.96	19.08	< 0.0001	0.88	0.55
TFC	0.89	0.79	0.60	16.83	8.94	0.001	0.49	0.78
AC-CUPRAC	0.95	0.91	0.74	9.20	22.53	< 0.0001	1.65	0.30
AC-DPPH	0.96	0.92	0.75	10.21	24.54	< 0.0001	1.65	0.30

4.3.2 Optimization and model validation

The data obtained from experiments was used to reveal optimal conditions. All the response variables (TMAC, TPC, TFC, AC-DPPH and AC-CUPRAC) were kept at maximum and the independent variables (A, B, C) in range. Dry matter content was also targeted in range as the main goal was to derive maximum yield of phenolic compounds. The optimum conditions were generated using the numerical optimization technique by the software. Among all the optimum conditions, the one having higher desirability index (0–1) was selected. The experimental values were compared with predicted values based on the 95% predicted interval using the confirmation technique by the software.

4.3.3 Effect of extraction pressure on response variables

The effect of each extraction parameter was discussed on all response variables since high correlations ($p < 0.05$) were found between the response variables. The Pearson correlation coefficients were given in Table 4.4.

Table 4.4 : Pearson correlation coefficients between responses.

	AC-DPPH	AC-CUPRAC	TFC	TPC	TMAC
Dry Matter Content	0.95	0.94	0.95	0.97	0.97
TMAC	0.95	0.95	0.95	0.96	
TPC	0.96	0.95	0.94		
TFC	0.93	0.95			
AC-CUPRAC	0.98				

Three-dimensional (3D) plots showing the effect of extraction pressure on TMAC, TPA, TFA, AC-DPPH and AC-CUPRAC were given in Fig. 4.2. The plots were generated by setting one variable at the midpoint of the experimental range and changing the other two within the studied range.

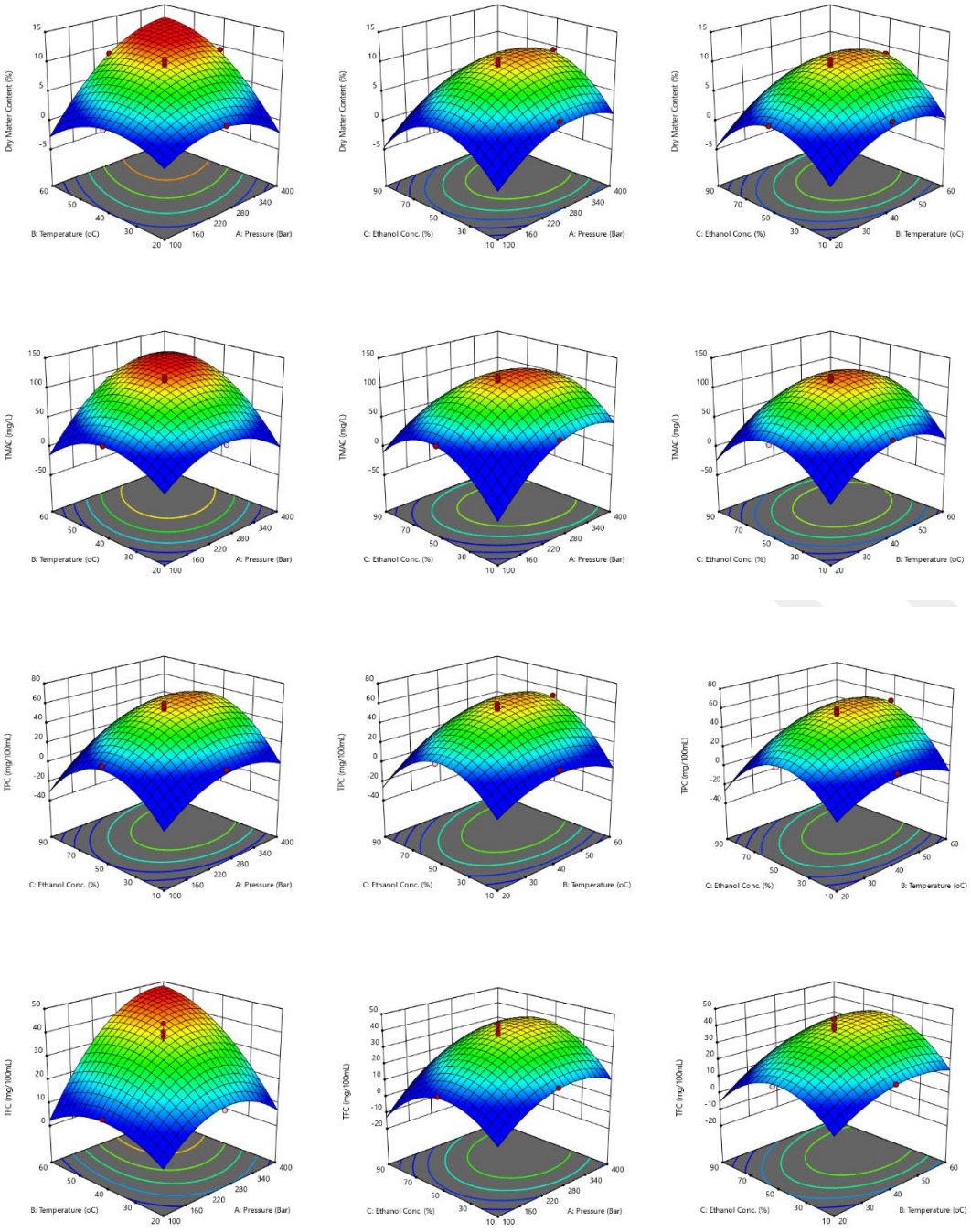

Figure 4.2 : Response surfaces of the dry matter, TMAC, TPC and TFC of black carrot extracts as a function of pressure, temperature and ethanol concentration (%) in ethanol-water mixture; other variables are held at the medium level.

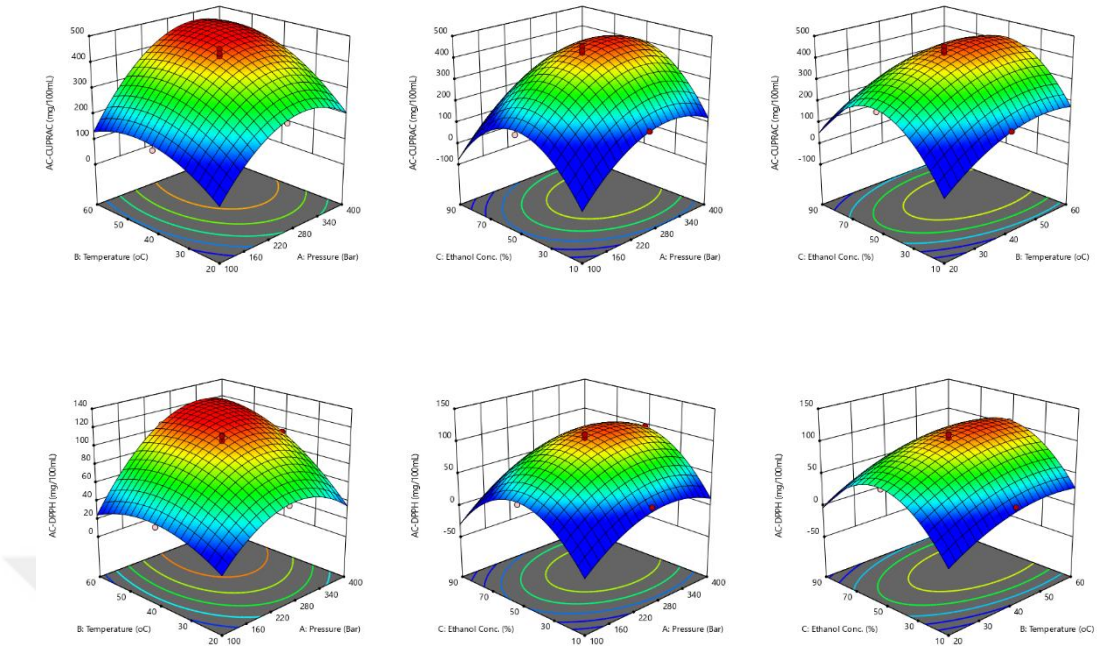

Figure 4.2 (Continued) : Response surfaces of AC-CUPRAC and AC-DPPH of black carrot extracts as a function of pressure, temperature and ethanol concentration (%) in ethanol-water mixture; other variables are held at the medium level.

The effect of extraction pressure on dry matter, TMAC, TPC, AC-DPPH and AC-CUPRAC were highly significant ($p < 0.0001$). Analysis also revealed that the TFC was affected significantly ($p < 0.0005$) with pressure at a high degree. The quadratic terms of the pressure effect were also significant for all responses at the degrees shown in the Table 4.5.

The pressure range was selected to cover a wide range between 100 and 400 bar in the study. The increased pressure levels gave higher dry matter content, and accordingly higher phenolic compounds and antioxidant activity in extracts. This is mainly due to the increase in the density of CO_2, i.e. increase in the solvating power with increasing pressure. It was previously explained in detail that, increased solvent density with pressure reduces the distance between the molecules by the rupturing effect and thus supports interactions between the solvent and feed matrix. Throughout the rupturing process, the chemical substances in the plant materials rapidly liberated into solvents, which enhances the solubility of the solute, mass transfer and diffusion of solvent into the feed material and increase the phenolics in extracts [103].

Table 4.5 : Coefficients and p-values of responses of the ternary solvent extraction.

	Dry Matter (%)		TMA (mg/L)		TPC (mg/100mL)		TFC (mg/ 100mL)		AC-CUPRAC (mg/100 mL)		AC-DPPH (mg/100 mL)	
		p values		p values		p values		p values		p values		p values
b_0	9.37		111.17		53.37		36.76		422.30		105.04	
b_1	1.70	< 0.0001	15.92	< 0.0001	9.67	< 0.0001	6.28	0.0004	59.10	< 0.0001	13.99	< 0.0001
b_2	1.70	< 0.0001	15.92	< 0.0001	9.67	< 0.0001	6.28	0.0004	59.10	< 0.0001	13.99	< 0.0001
b_3	0.22	0.3277	2.99	0.2556	2.10	0.1676	0.31	0.8014	8.65	0.2820	3.53	0.1113
b_{12}	1.08	0.0050	7.85	0.0493	3.59	0.1015	2.58	0.1594	9.21	0.4118	4.59	0.1397
b_{13}	0.21	0.4948	-2.98	0.4159	2.15	0.3059	1.37	0.4371	5.50	0.6204	1.48	0.6161
b_{23}	0.31	0.3373	2.13	0.5574	2.93	0.1726	0.99	0.5732	-3.69	0.7389	-0.06	0.9823
b_{11}	-0.93	0.0003	-10.81	0.0003	-5.26	0.0009	-3.21	0.0073	-33.93	0.0002	-9.07	0.0002
b_{22}	-0.93	0.0003	-11.04	0.0002	-4.47	0.0026	-2.25	0.0404	-20.14	0.0078	-5.20	0.0092
b_{33}	-1.61	< 0.0001	-15.87	< 0.0001	-9.91	< 0.0001	-4.81	0.0005	-60.45	< 0.0001	-17.97	< 0.0001

The density values of solvents at the experimental conditions were calculated and presented in Table 4.1. In contrast to significant effect of pressure on response variables, there was a weak correlation between density and response variables. An increase in response variables were determined when the density increased with pressure at constant temperature and ethanol-water ratio. It can be clearly seen when the experiments with numbers of 7-20, 8-17, 12-16 and 14-15 were compared between each other. The increase from 100 bar to 250 bar at 40°C and ethanol-water ratio of 50/50 also improved the extraction, however the further increase to 400 bar did not cause any change. This could be attributed to that the increase in the CO_2 density in those levels of pressure is not as high as the increase at lower pressures [122]. However, contradictory results are present in the literature. While a similar trend was observed by Adil et al. [122] for the extraction apple and peach pomaces, Paula et al. [123] and Mantell et al. [124] found a decrease in extraction rate of anthocyanins in red grape when the pressure was increased. They ascribed this to enhancement in the solubility of lipids and volatiles at high pressures which prevails over the extraction of anthocyanins. However, this could not be valid for black carrots in which trace amounts of lipids and volatiles are present [125].

The increased pressure was also observed to give higher bioactive compounds and antioxidant activity levels at higher temperature while a slight difference was observed between the minimum and maximum pressure levels at lower temperature values in the studied range (20-60°C). Presumably, it was related to CO_2 density i.e. solvating power exceeds at a higher degree when the extraction takes place at a higher temperature values for a constant pressure range.

4.3.4 Effect of extraction temperature on response variables

The results indicated that the linear and quadratic coefficients of extraction temperature were significant at the levels shown in Table 4.5. Three-dimensional (3D) plots showing the effect of extraction temperature on dry matter, anthocyanins, phenolics, flavonoids and antioxidant activity were given in Fig. 4.2.

The linear coefficients of the effect of temperature was positive (Table 4.5) which is in agreement with previous studies on the extraction with compressible CO_2 from various plants high in anthocyanins [103, 111, 126]. The studies conducted on the extraction of black carrots also confirmed the increase in yield with temperature [115,

117]. It was previously suggested that, increased temperature accelerates the mass transfer and thus provides a more efficient extraction in two ways: (1) lowering the viscosity of the solvent and surface tension leading to an enhancement its penetration into the matrix (2) decreasing the desorption activation energy of the compounds by breaking the solute-matrix interactions.

The optimum temperature values for individual response variables were specified using the numerical optimization technique by the software. The only relevant response variable was kept at maximum and the highest temperature value among the numerical optimized solutions was recorded. The dry matter content increased up to 60ºC, TMAC up to 55ºC, TPC up to 60ºC, TFC up to 60ºC, AC-CUPRAC up to 60ºC and AC-DPPH up to 60ºC. Similarly, Ahmadian-Kouchaksaraie and Niazmand [103] studied *Crocus sativus* petals extraction between 40-80ºC and observed an enhancement in TMAC up to 51ºC, TPC up to 63ºC, TFC up to 70ºC, and in antioxidant activity up to 67ºC. Our findings indicated that TMAC had a lower threshold value than those of other response variables. This was probably due to higher susceptibility of anthocyanins to high temperatures than that of other phenolic compounds [127, 128]. The mechanism behind the thermal degradation of anthocyanins was explained by the releasing of an aglycone by the hydrolysis of the glycosidic bond which results with a faster discoloration. The other mechanism presented was the hydrolysis of the heterocyclic ring leading to formation of chalcone which is the colorless structure of anthocyanins [129]. In the meantime, the threshold value for TMAC observed in our study was higher than some results found in the literature [101, 129, 130]. A reasonable explanation for this difference could be that the anthocyanins present in black carrots are in acylated form making them more resistant to elevated temperatures [131].

Regarding the temperature threshold values, it can be observed that antioxidant capacity measured by both CUPRAC and DPPH assays did not show a decrease at high temperature values as observed for TMAC. It seems that antioxidant capacity measured by DPPH and CUPRAC increased with TPA and TFA at higher temperatures which was supported by Garcia-Mendoza et al. [129]. They explained that, besides anthocyanins, phenolic acids and procyanidins present in feed material could be responsible for the enhancement of antioxidant capacity with temperature.

The negative quadratic terms and Fig. 4.2 depicted that the increase in response variables cease at a certain temperature. However, this was binding under a certain pressure level (~250 bar). At higher pressure levels, temperature had a positive effect on responses throughout the temperature range studied. These findings could be due to the 'cross-over effect' which was explained previously by the competing effects of the decrease in solvent density and the increase in solute vapor pressure with temperature. At lower pressure, the alteration of solvent density is more pronounced than the solute vapor pressure, as extraction rate increases with a reduction in temperature. In the meantime, at pressures above the cross-over pressure, the change of solvent density is lowered and thus the increase in solute vapor pressure becomes more effective on solubility [132, 133]. Thereby, it appears that the extraction rate is dependent on the solute vapor pressure and it increased with an increase in temperature at the pressure higher than about 250 bar in our study.

The susceptibility of anthocyanins to increased temperature also affected by ethanol-water ratio. As shown in Fig. 4.2, extracts had higher TMAC at the maximum temperatures used (60^{o}C) when the ethanol-water ratio 90/10 compared to those extracted by ethanol-water mixture at the ratios of 10/90 – 30/70. The results has similarity with the study of Garcia-Mendoza et al. [129] who found higher TMAC values in jujara residues-pressurized liquid extracts at 60^{o}C when using ethanol as a solvent instead of water.

4.3.5 The effect of ethanol concentration in co-solvent

The linear effects of ethanol concentration were not significant ($p > 0.05$) on response variables. However, the quadratic terms of ethanol concentration in co-solvent were highly significant at a level of $p \leq 0.0005$ on TFC and $p < 0.0001$ on all the other response variables. The quadratic terms were negative for all response variables indicating a reduction towards high and low level of ethanol.

The volume and molar ratios of solvent mixtures for each experiment was calculated and summarized in Table 4.1. As previously explained by Kühn and Temelli [109] the solvent mixture would be exist as a single phase or as multiple phases in equilibrium. Phase equilibrium data for CO_2-ethanol-water mixtures was represented in Fig. 4.3 where mixtures having the compositions that lie inside the binodal curve present in two phases while those with compositions that lie outside the curve will be exist as

one single phase. Single phase consists of a gas expanded liquid where the CO_2 dissolved in the liquid or a supercritical fluid, depending on the location of the mixture critical point. Binodal curves were drawn using the data at 40°C, 300 bar; 40°C, 200 bar [134]; 60°C, 101 bar and 50°C 101 bar [135]. Plotting the data at two different temperatures at constant pressure and vice versa allowed to observe the change in the location of binodal curve by increasing temperature and pressure. It was seen that decreasing temperature caused a large and increasing temperature caused a small shrinkage in binodal curves. The compositions of ternary mixtures used in our study were placed on the Fig. 4.3. Despite the shrinkage, the phase behavior of solvents used in experiments could be identified as two phases as the shrinkage can be assumed not to be large enough to re-identify the compositions of the solvents used in our study [109].

The results showed that the dry matter decreased towards high and low level of ethanol concentration co-solvent. Our results concur well with the Monroy et al. [111] who used 66% CO_2 + 34% of (EtOH 50% + H_2O 50%) mixture, and 68% CO_2+ 32% of (EtOH 70% / H_2O 30%) mixture for the extraction. They observed maximum extraction yields at 50 and 70% ethanol solutions while ethanol and water give the minimum yields when used individually with CO_2. Presumably, this was caused by the joint effect of viscosity, density and the polarity of resultant solvent mixture. The increase in ethanol concentration could enhance the penetration of solvent into the feed as it has a lower viscosity than water. Kerbstadt et al. [136] proposed that the presence of substantial amounts of water can decrease the extraction yield by disturbing the interaction between the solute and solvent. They also added that the presence of some water could improve the extraction yield by swelling the matrix and thereby facilitating the contact between the solute and solvent [136] by increasing the density and thus the solvating power. Moreover, decreased polarity with decreased water content had a negative impact on extraction efficiency [109]. On the other hand, previous works show that the phenolic yield increases significantly when low pH solvents are used, due to the disruption of cell membranes, especially at high temperatures, releasing low molecular weight phenols [129]. The formation of carbonic acid during extraction could decrease the pH of the solvent.

Apart from the effect on the extraction efficiency, the alteration in ethanol concentration may also impact the stability of phenolics. The presence of water in co-

solvent provides a pH reduction which happens due to the formation of in situ carbonic acid during the extraction. The increased water content in co-solvent could enhance the pH drop which leads an improved anthocyanin stability [104]. The low pH conditions present favorable conditions for anthocyanins to form flavillic ions which gives the red color to the monomeric anthocyanins [137]. On the other hand, it was suggested that, the increased water content in ethanol-water mixture leads to a higher water activity which reduce the anthocyanin stability [104].

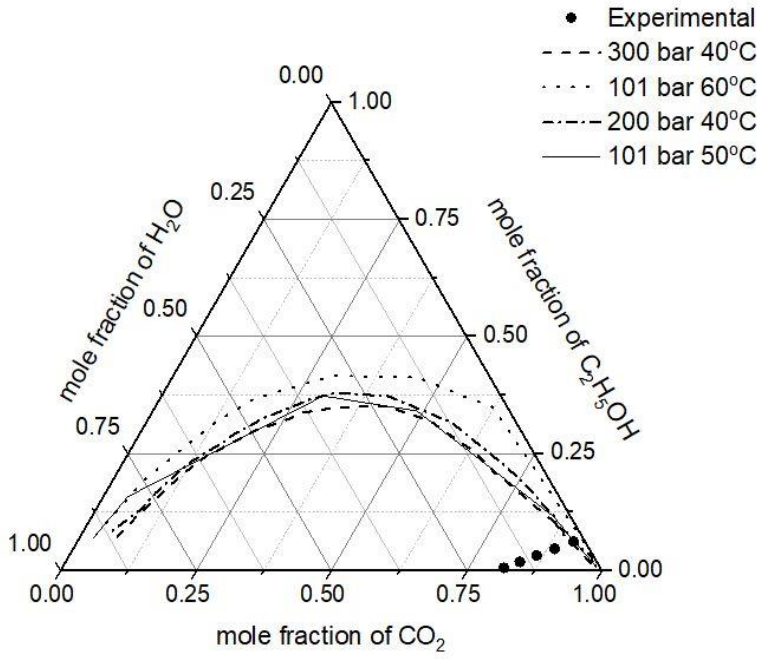

Figure 4.3 : Phase equilibrium data for the system CO_2-ethanol-water.

4.3.6 Determination and verification of optimal conditions

The optimal extraction parameters were found as 304.40 bar pressure, 51.54ºC temperature, and 47.63% ethanol concentration in ethanol-water mixture at a desirability value of 0.97. As it would be very difficult to conduct the experiment at the suggested conditions, optimum conditions were targeted as 304 bar pressure, 52ºC temperature and 48/52 ethanol-water ratio. The experiments were conducted under the targeted optimized conditions of process variables to verify the efficacy of the models. The observed results were in the range of 95% predicted interval and thus confirmed the accuracy of the models (Table 4.6). The values of optimum extracts were also compared to those obtained by conventional extraction and higher extraction efficiency was observed probably due to increased mass transfer in high pressure extraction (Table 4.6).

4.3.7 Characterization of anthocyanin profile of optimized extract

The determination of the anthocyanin profile of the obtained black carrot extract and commercial sample was performed by HPLC. The chromatogram of the black carrot extract prepared at the optimal conditions were shown in Fig. 4.4. Peak identifications of the compounds with no standard were conducted by consulting previous literature [99, 138] and quantified according to the external standard calibration curve because of the lacking anthocyanin standards. The commercial and extracted samples were compared based on the percentage peak areas of acylated and non-acylated anthocyanins which was shown in Table 4.7. Black carrot extract obtained in our study had a bit higher acylated anthocyanins than commercial one had which could make it more stable at elevated temperatures and prolonged storage periods [131]. The anthocyanin content of extract determined by HPLC was in good agreement with the pH-differential method (134.44 ± 11.74 mg/L).

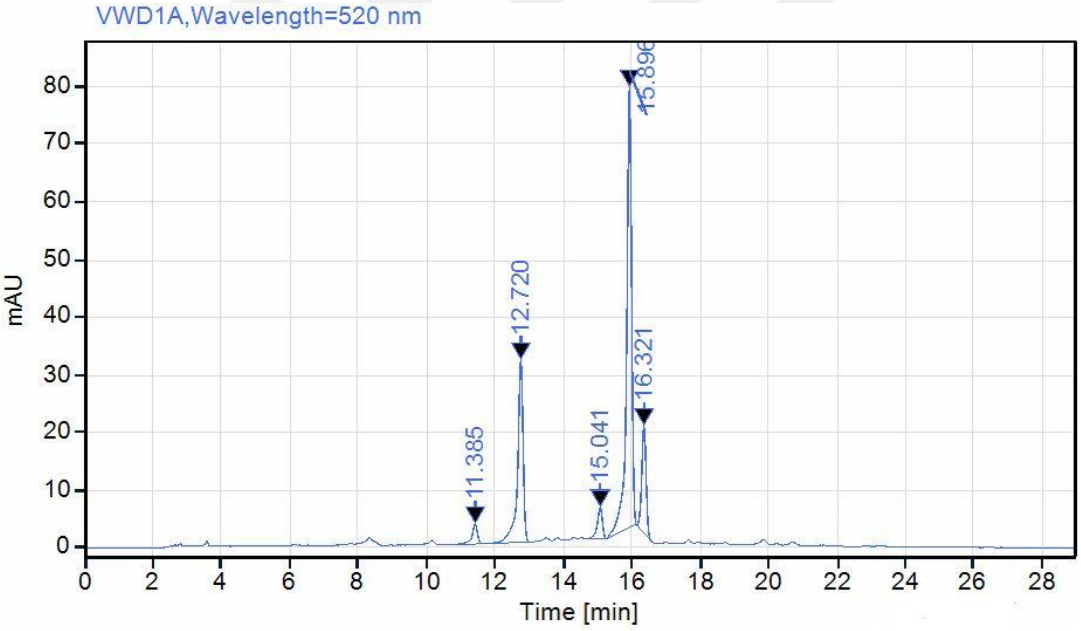

Figure 4.4 : Anthocyanin composition of extract obtained at optimum conditions.

4.4 Conclusion

The Central Composite design approach succeeded in the optimization of process variables and the results revealed that with the alteration of the extraction pressure, extraction temperature and ethanol-water ratio, a large range of changes in response variables could be procured. Based on the aim of the production of a health beneficial

Table 4.6 : Predicted and experimental values of the response variables at optimum conditions.

	Dry Matter (%)	TMAC (mg/100 mL)	TPC (mg/100 mL)	TFC (mg/100 mL)	AC-CUPRAC (mg/100 mL)	AC-DPPH (mg/100 mL)
Predicted	11.43	490.28	2486.00	1773.60	18910.40	4790.40
Experimental	11.25 ± 0.36	459.00 ± 52.32	2346.80 ± 51.20	1802.80 ± 126.40	19602.40 ± 475.60	4408.4 ± 178.40
Conventional	4.30 ± 0.01	148.29 ± 11.34	997.96 ± 64.86	693.74 ± 15.92	7975.46 ± 224.38	2021.30 ± 20.09

Table 4.7 : Peak area ratios of anthocyanins in the extract obtained in the study and the commercial extract.

	Cyanidin-3-xylosyl-glucosyl-galactoside	Cyanidin-3-xylosyl-galactoside	Cyanidin-3-xylosyl-glucosyl-galactoside acylated with sinapic acid	Cyanidin-3-xylosyl-glucosyl-galactoside acylated with coumaric acid	Cyanidin-3-xylosyl-glucosyl-galactoside acylated with ferulic acid	Non-acylated Anthocyanins	Acylated Anthocyanins
Extract obtained in the study	3.64	33.88	3.29	48.41	10.79	37.52	62.48
Commercial extract	10.70	28.10	13.68	41.98	4.69	38.81	60.34

coloring extract, an optimized condition for simultaneous maximum extraction of TMAC, TFC, TPC and antioxidant capacity was determined. Based on these models, the optimum conditions of extraction process were achieved (temperature of 52^{o}C, pressure of 304 bar and ethanol-water ratio of 48/52). TMAC, TPC, TFC, AC-CUPRAC and AC-DPPH presented a similar behavior in the extraction. Only small deviations were observed between the actual values and predicted values. Therefore, it is recommended the models obtained can be used to optimize the recovery of anthocyanin-rich extracts from the black carrots.

5. ENCAPSULATION OF ANTHOCYANIN-RICH BLACK CARROT EXTRACT IN POTATO PROTEIN-PECTIN COMPLEXES

5.1 Introduction

Black carrot anthocyanins have gained a large interest in food industry to be used as natural food colorant for confectionery, jellies, conserves, soft drinks, and fruit juices and nectars as an alternative to synthetic dyes [1]. Black carrots were determined to have anthocyanin content in the range of up to 1750 mg/kg fresh weight whereas 45.4 mg/kg to 17.4 g/kg dry matter [100]. However, the color and stability of anthocyanins could be affected by pH, temperature, light, presence of co-pigments, self-association, metallic ions, enzymes, oxygen, ascorbic acid, sugar and their degradation products, proteins and sulphur dioxide.

Encapsulation is a technique used to protect fragile compounds, by especially those sensitive to hydrolysis or oxidation. Microencapsulation for micrometric particles (1 to 1000 μm) are produced by microencapsulation which may contain compounds of various origins: active pharmaceutical ingredients [139], cosmetic active ingredients [140, 141], food additives [142], phyto-sanitary products [143], aromas [144], cells [145], inks [146], microorganisms, or catalysts of chemical reactions [147].

The microencapsulation process by complex coacervation mainly consists the deposition of a coacervate which composed of two polymers with opposite charges on the surface of a hydrophobic compound of an oil-in-water emulsion. Thereby, encapsulation by complex coacervation is typically used to protect aromatic oils, fish oils, hydrophobic vitamins, preservatives and enzymes [148]. Although it is mainly used for encapsulation of lipophilic compounds, it can also be used for the encapsulation of hydrophilic compounds. Encapsulation of ascorbic acid has been successfully carried out by using the double emulsion technique by Comunian et al. [149]. Furthermore, some studies also showed the possibility of increasing the stability of hydrophilic bioactive compounds using oppositely charged biopolymers without an emulsification process. In some part of studies, this procedure referred to complex coacervation [150, 151] , while in others defined as complexation [152-154]. In this

thesis, particles prepared by double emulsion – coacervation process called emulsified core-particles (ECP) and the particles prepared by complexation of BCE, PPI and CP called non-emulsified core-particles (NECP).

Vegetable proteins are an alternative to animal proteins for encapsulation by complex coacervation, because they are natural biodegradable polymers and biocompatible. In addition, plant proteins are known to be less allergenic than animal protein, which is an advantage for food applications [155]. Their disadvantage is that they present solubility problems due to presence of several fractions [3]. In this regard, potato proteins serve as an excellent alternative as they can be readily soluble in water.

As previously mentioned, potato proteins are by-products of starch production and its nutritional value has been shown to be greater than that of other vegetable or cereal proteins and casein while being comparable to that of egg protein [56-59]. Potato proteins are divided into three major fractions which are patatins, protease inhibitors and remainder proteins. Patatins (35–40%) are glycoproteins with a molecular weight around 40 kDa, having a pI at 4.8–5.2. The protease inhibitors (25–50%) are a diverse group of proteins with a molecular weight of 7–21 kDa and the pI varying between 5-8. The remainder proteins (~10%) are enzymes with different high molecular weight [60, 61].

Up to present, there is no study on the anthocyanin stabilization by complex coacervation consisting an emulsification process and complexation with these coacervates without an emulsification process. The aim of the study was to compare the effect of these two procedures on the final powder characteristics. The effect of core-to-wall ratio and the concentration of wall material was also investigated. It should be noted that, BCE loaded PPI particles without the addition CP were also produced and characterized to link the Section 5 to Section 6. The usage of individual PPI instead of PPI-CP complexes was explained in Section 6.

5.2 Material and Methods

5.2.1 Materials

Food grade PPI was donated by Döhler GmbH (Darmstadt, Germany). PPI contained (min.) 90% protein, (max.) 9% moisture, (max.) 5% ash, and (max.) 0.5% sulphite according to specification provided by manufacturer. Citrus pectin with 70% DE (CP

DE70, Pectin Classic CU-L 053/15) and citrus pectin with 35% DE (CP DE35, Pectin Classic CU-L 054/15) were supplied from Herbstreith & Fox KG (Neuenbürg, Germany) and used without further purification. Medium chain triacylglycerides (chain length C8 and C10) Miglyol 812 oil was donated by Sasol GmbH (Witten, Germany). For all analysis, distilled water was used and all other reagents used were of analytical grade.

5.2.2 Preparation of microcapsules

5.2.2.1 Formation of non-emulsified core-particles

PPI (10% w/w) and CP (4% w/w) were dissolved in double-distilled water and stirred at ambient temperature overnight to ensure complete hydration. The ratio of PPI-CP was selected based on the results of the Section 2. The maximum interaction was found at a PPI-CP ratio at 2.5. The range of wall material concentration and core-to-wall ratio was determined based on the literature. The protein to emulsified core ratio which was used in the literature was considered as it is important to form stable water in oil in water (W/O/W) emulsion.

The complexation procedure was initiated by dissolving black carrot extract in distilled water at a ratio of 1:2 (v/v). The prepared BCE solution was added to PPI solution (10%, w/w) and vigorously vortexed for 2 min. CP solution (4%, w/w) was added under agitation at 100 rpm. The final concentration of wall and core materials were shown in Table 5.1. The prepared samples were kept in 4^{o}C overnight to allow phases to separate and then freeze-dried at least for 16 hours.

5.2.2.2 Formation of emulsified core-particles

PPI and CP solutions were prepared as explained in previous section. The ratio of PPI-CP and the range of working parameters were also selected as indicated in previous section. Coacervated microcapsules was prepared according to the method of Calderón-Oliver et al. [150]. Primary (W/O) emulsion was prepared by homogenization of BCE in Miglyol oil at a ratio of 1:2 (v/v) using an Ultraturrax at 11000 rpm for 4 min. Secondary (W/O/W) emulsion was prepared by adding PPI (10%, w/w) solution to primary emulsion and homogenization at 7000 rpm for 2 min in an Ultraturrax. CP solution (4%, w/w) was added to secondary emulsion under agitation at 100 rpm. The final concentration of wall and core materials were shown

in Table 5.1. Similar to fabrication of non-emulsified core-particles, the prepared samples were kept in 4°C overnight to allow phases to separate and then freeze-dried at least for 16 hours.

Table 5.1 : Formulation of each run of the experimental design.

Exp. #	PPI (%, w/w)	CP (%, w/w)	BCE (%, w/w)	Miglyol oil (%, w/w)	Water (%, w/w)
E1	1.25	0.5	0.5	1	96.75
E2	1.25	0.5	1.25	2.5	94.5
E3	1.25	0.5	2	4	92.25
E4	2.5	1	1	2	93.5
E5	2.5	1	2.5	5	89
E6	2.5	1	4	8	84.5
E7	1.25	0.5	0.5	-	97.75
E8	1.25	0.5	1.25	-	97
E9	1.25	0.5	2	-	96.25
E10	2.5	1	1	-	95.5
E11	2.5	1	2.5	-	94
E12	2.5	1	4	-	92.5
E13	2.5	-	2.5	-	95

5.2.3 Residual moisture

About 0.5 g of sample was weighed and the moisture content was determined in triplicates using a UniBloc Halogen Moisture Analyzer (Shimadzu, Kyoto, Japan)

5.2.4 Hygroscopicity

About 0.5 g of sample was weighed in plastic dishes and stored for 7 days in climate chamber (HPP110, Memmert, Schwabach, Germany) at 75.2% RH at 25°C and then weigh the powders. The hygroscopicity was expressed as mass of water absorbed per 100 g of dry sample [156].

5.2.5 Particle size

The mean diameter of samples was measured by laser diffraction using a PSA1190 particle size analyzer (Anton Paar Physica, Austria) with liquid dispersion system. 75% ethanol solution was used as a dispersion medium. Particle size distributions in laser diffraction are calculated by Mie theory using the Kalliope™ software (Anton Paar, Austria). The measurement was carried out in triplicates.

5.2.6 Total monomeric anthocyanin determination

The total monomeric anthocyanin content was determined in duplicate using the pH differential method [157]. The appropriate dilution factor was determined by diluting with 0.025 M potassium chloride buffer, pH 1 until the absorbance of the sample at 520 nm is within the linear range of spectrophotometer (Biotek Instruments Inc., Vinooski, USA). Two dilutions of the samples were prepared, one with potassium chloride buffer, pH 1, and the other with sodium acetate buffer, pH 4.5, diluting each by the previously determined dilution factor. The samples were then equilibrated for 15 min and the absorbance of samples was measured at 520 nm and 700 nm.

5.2.7 Anthocyanin retention

Anthocyanin retention (%) was performed according to da Silva Carvalho et al. [158] with some modifications. Microparticles were then reconstituted in distilled water (1%, w/v). pH-differential method was used for the anthocyanin quantification. The anthocyanin retention (AR) was determined according to the equation 5.1 based on the quantification of these compounds in the feed solution and after the drying process.

$$AR\ (\%) = \left(\frac{A_{microparticle}}{A_{feed\ solution}}\right) \times 100 \quad (5.1)$$

where $A_{microparticle}$ corresponds to the anthocyanins in the microparticles (mg/g) and $A_{feed\ solution}$ to the anthocyanins in the feed (mg/g dry basis).

5.2.8 Encapsulation efficiency

The encapsulation efficiency of the produced particles was determined using the method of Davidov-Pardo et al. [159] with slight modifications and was calculated according to the Equation 5.2.

$$EE\ (\%) = \left(1 - \frac{S_A}{T_A}\right) \times 100 \quad (5.2)$$

where S_A and T_A are the surface and total anthocyanin content, respectively. In order to determine T_A, 0.1 g of sample was disintegrated in 10 mL of 50% methanol solution and then vigorously mixed using a vortex for 5 minute. The mixture was then filtered through a 0.45 μm non-pyrogenic filter. In order to determine the S_A, 0.1 g of sample was washed with 10 mL of anhydrous ethanol.

5.2.9 DSC

About 5 mg of prepared samples, PPI, CP and freeze-dried BCE were weight in aluminum pans and sealed hermetically. The thermal behavior was observed by a DSC (Q10 equipped with cooler; TA Instruments Inc., New Castle, DE, USA) where Universal Analysis 2000 Version 4.5A (TA Instruments Inc.) software was utilized. An empty pan was used as the reference [160]. Thermograms were obtained with a heat scanning from 20°C to 200°C at a rate of 10°C/min. The melting temperatures were calculated in the DSC thermogram.

5.2.10 FT-IR

FT-IR spectroscopy technique was used in order to identify characteristic organic groups in the PPI, CP, freeze-dried BCE and the prepared samples. FT-IR spectra of samples were recorded using the Bruker Tensor II FT-IR spectrometer equipped with the ATR diamond module (Bruker Optics, Germany). All the spectra were average of 18 scans from 4000 cm^{-1} to 400 cm^{-1} at a resolution of 4 cm^{-1}.

5.2.11 SEM

The samples were sprinkled onto adhesive coated an aluminum pin stub. The images were captured on a scanning electron microscope (Quanta FEG 250 SEM, ThermoFisher Scientific, Oregon, USA) at a magnification rate of 1000x and 8000x.

5.3 Results and Discussion

5.3.1 Hygroscopicity

Table 5.2 illustrated that hygroscopicity of NECP were ranged between 18.13 ± 0.54 - 28.65 ± 0.78 % (w/w, dry basis) while it was 10.15 ± 0.68 - 17.49 ± 1.61 % (w/w, dry basis) for ECP. Up to our knowledge, no literature was available on hygroscopicity of protein-based non-emulsified particles. Regarding the emulsified particles, the results were compatible with the findings of Rocha-Selmi et al. [161]. It was determined between 5.16 ± 0.26 - 16.11 ± 2.78 % (w/w, db.) for gelatin- gum Arabic coacervated particles which was used to encapsulate double emulsified sucralose. In their another study, hygroscopicity values were between 10.73 ± 0.25 - 13.43 ± 0.94 % (w/w, dry basis) for gelatin-gum Arabic coacervates around double emulsified aspartame particles. Furthermore, Mendanha et al. [53] used SPI-pectin coacervates to

encapsulate the casein hydrolysate in double emulsion and the hygroscopicity ranged between 20.08 ± 0.59 - 26.0 ± 0.73 (w/w). The hygroscopicity of free hydrolysate was found to be 53 ± 7.81 (%, w/w). On the other hand, Shaddel et al. [160] observed high hygroscopicity values for double emulsified black raspberry anthocyanins coacervated with gelatin and gum Arabic which varied from 36.00 ± 0.88 to 49.00 ± 0.38 % (w/w). The higher hygroscopicity results determined by Shaddel et al. [160] is probably due to high hygroscopicity value of core material (85.22 ± 1.02 % (w/w)). In comparison with this study, gelatin and gum Arabic also have higher hygroscopicity values (17.16 ± 0.08 and 46.51 ± 1.21, respectively) [160] than potato protein and pectin which possibly affect the hygroscopicity values.

The results highlighted the overall difference in hygroscopicity values between ECP and NECP. We suggest that the higher hygroscopicity in NECP was due to presence of some part of BCE on the surface even being entrapped in the matrix. The hygroscopicity of BCE-PPI particles was similar to the non-emulsified particles. It seems that, CP incorporation did not have any positive effect on hygroscopicity which is probably having higher hygroscopicity than PPI. Therefore, it would be assumed that the hygroscopicity of NECP depends on the hygroscopicity of individual PPI and BCE. In contrast, ECP had values between the hygroscopicity values of PPI and CP. This was probably due to core-shell type encapsulation in emulsified particles and the presence of oil in the structure which could also contribute to lower hygroscopicity values. In general, both ECP and NECP could be considered as non-hygroscopic according to classification method constructed by Callahan et al. [162]. The classification methods for hygroscopicity were represented in Table 5.3.

5.3.2 Particle size

As shown in Table 5.2, the mean particle diameter of powders ranged from 65.05 ± 0.97 to 152.47 ± 4.02 μm. Regarding the ECP, similar results were obtained with Shaddel et al. [160] which was between 45.25 ± 0.97 and 109.49 ± 4.77 μm for gelatin gum Arabic coacervates loaded with black raspberry anthocyanins. On the other hand, Calderón-Oliver et al. [150] found lower particle size values (37.95 and 39.39 μm) where they used alginate-collagen or pectin-collagen to complex with nisin and avocado extract without an emulsion step. It should be noted that the particle size of samples was measured before the drying process on the contrary to this study in which

Table 5.2 : Physicochemical properties of non-emulsified and emulsified core particles.

Run	PPI (%, w/w)	CP (%, w/w)	BCE (%, w/w)	Miglyol oil (%, w/w)	Moisture (%)	Hygroscopicity (%)	ζ-Potential (mV)	Particle size		
								D[4,3]	D[3,2]	span
NECP1	1.25	0.5	0.5	-	10.32 ± 0.3	18.13 ± 0.54 ef	-0.3 ± 0.18 c	68.76 ± 0.59 def	10.79 ± 0.94 d	2.06 ± 0.03 a
NECP2	1.25	0.5	1.25	-	10.24 ± 0.2	23.48 ± 0.32 c	0.43 ± 0.64 c	81.19 ± 4.56 cde	35.13 ± 0.23 cd	2.28 ± 0.05 a
NECP3	1.25	0.5	2	-	9.93 ± 0.11	26.72 ± 0.31bc	-7.03 ± 1.03 de	84.83 ± 2.83 bcd	43.15 ± 1.00 cd	1.2 ± 0.02 a
NECP4	2.5	1	1	-	9.47 ± 0.15	19.25 ± 0.31 de	-0.01 ± 0.08 c	77.38 ± 6.20 cdef	21.46 ± 11.78 cd	2.14 ± 0.06 a
NECP5	2.5	1	2.5	-	9.91 ± 0.36	22.93 ± 0.89 cd	-0.58 ± 0.22 c	76.1 ± 2.95 cdef	29.1 ± 17.27 cd	2.00 ± 0.15 a
NECP6	2.5	1	4	-	8.24 ± 0.06	28.65 ± 0.78 b	-8.48 ± 0.41 e	101.5 ± 3.04 bc	43.33 ± 1.32 bc	2.51 ± 0.06 a
ECP1	1.25	0.5	0.5	1	10.32 ± 0.4	12.32 ± 1.81 gh	-1.49 ± 0.58 c	107.83 ± 13.87 b	46.85 ± 2.04 bc	2.28 ± 0.25 a
ECP2	1.25	0.5	1.25	2.5	6.96 ± 0.5	14.76 ± 1.73 fg	-15.25 ± 1.48 f	152.47 ± 4.02 a	57.38 ± 0.36 a	2.94 ± 0.02 a
ECP3	1.25	0.5	2	4	6.34 ± 0.4	17.49 ± 1.61 ef	-17.77 ± 1.12 f	132.22 ± 17.23 a	42.42 ± 25.71 ab	2.67 ± 0.21 a
ECP4	2.5	1	1	2	8.11 ± 0.23	10.77 ± 1.00 gh	-0.32 ± 0.24 c	88.93 ± 24.36 cde	26.24 ± 18.65 cd	2.77 ± 1.22 a
ECP5	2.5	1	2.5	5	6.91 ± 0.4	10.15 ± 0.68 h	-5.5 ± 1.07 d	71.74 ± 3.49 ef	33.24 ± 1.23 d	2.29 ± 0.14 a
ECP6	2.5	1	4	8	6.23 ± 0.37	11.73 ± 0.79 gh	-6.31 ± 0.38 de	65.05 ± 0.97 f	29.83 ± 0.11 d	2.31 ± 0.05 a
PPI-BCE	2.5		2.5		7.23 ± 1.65	22.56 ± 1.09 cd	15.47 ± 0.57 b	9.73 ± 1.44 g	4.79 ± 2.75 e	1.18 ± 0.06 a
PPI						10.14 ± 0.79 h	28.40 ± 1.18 a	-	-	-
CP						17.82 ± 1.26 ef	-20.45 ± 0.90 g	-	-	-
FD-BCE						56.72 ± 1.01 a	-	-	-	-

Table 5.3 : Hygroscopicity classification methods proposed by Callahan et al. [162] and European Pharmacopoeia [163].

Conventional method		European pharmacopoeia	
Classification	Criteria	Classification	Criteria
Non-hygroscopic	Essentially no moisture increase below 90% RH; less than 20% (w/w) increase in moisture content above 90% RH in 1 week	-	-
Slightly hygroscopic	Essentially no moisture increase below 80% RH; less than 40% (w/w) increase in moisture content above 80% RH in 1 week	Slightly hygroscopic	Increase in mass < 2% - ≥ 0.2%
Moderately hygroscopic	Moisture content does not increase >5% (w/w) below 60% RH; less than 50% (w/w) increase in moisture content above 80% RH in 1 week	Hygroscopic	Increase in mass < 15% - ≥ 2%
Moderately hygroscopic	Moisture content does not increase > 5% (w/w) below 60% RH; less than 50% (w/w) increase in moisture content above 80% in 1 week.	Very Hygroscopic	Increase in mass ≥ 15%

the final characteristics of particles were investigated. The higher particle size values found in this study could be due to formation of agglomerations during the freeze-drying process. The high difference in mean volume particle diameter and mean surface particle diameter shows the occurrence of poly-disperses which was also determined by other researchers [80, 150]. High span values also supported the occurrence of agglomerations in freeze-dried particles.

Despite an increasing trend with increasing core-to-wall ratio for the NECP, the difference in measurements were not statistically significant ($p > 0.05$). However, ECP showed lower particle size values with increased wall concentration at the constant core-to-wall ratio. Especially the ECP2 and ECP3 had significantly higher ($p < 0.05$) particle size values. This was also coherent with ζ-potential values, higher ζ-potential was found for ECP2 and ECP3 which are the samples produced at low wall material concentrations and increasing core-to-wall ratio. This could be due to the inadequate wall material concentration which could not protect the emulsion and thus the BCE leaking from emulsion could cause stickiness in the structure. This could lead both the increase in the ζ-potential and particle size. Shaddel et al. [160], Comunian et al. [149] and Rocha-Selmi et al. [161] also found lower particle size values with

increased wall concentration where they encapsulate several hydrophilic cores with double emulsion-coacervation process. It was explained by protein surfactant properties, since enhancing protein concentration would result in a reduction of emulsion droplet size, improving encapsulation efficiency and the droplets' coalescence durability [3].

The effect of emulsion step was apparent at the low wall material concentration, the particle size values of ECP1, ECP2 and ECP3 were higher than the NECP1, NECP2 and NECP3, respectively, for the constant wall material concentration and core-to-wall ratio values. This was coherent with the findings of Calderón-Oliver et al. [150] where they also find higher particle size values when an emulsion step was added which was explained by the presence of oil droplets in emulsified coacervates.

5.3.3 Anthocyanin retention and encapsulation efficiency

The encapsulation efficiency is an important parameter showing the success of encapsulation process. High value of encapsulation efficiency indicates the suitability of procedure to encapsulate the desired core material as a significant amount of active substance as present inside of the particle with a low amount of core material which was on the surface.

As demonstrated in Fig. 5.1 EE of NECP and ECP was between 69.26 ± 2.57% - 82.84 ± 0.17% and 85.48 ± 0.55 - 90.15 ± 3.00%, respectively. The particles produced by BCE loaded PPI without CP also showed high encapsulation efficiency at 80.48 ± 1.49%. Shaddel et al. [160] measured the encapsulation efficiency on particles loaded with black raspberry anthocyanins double emulsified and coacervated with gelatin and gum Arabic at optimum pH (pH 4) and found a value of 81.12 ± 1.97% at a constant ratio of core-protein-polysaccharide (1:1:1) and 0.025 g/mL of the polymer. Moreover, Tao et al. [164] revealed EE in a range of 46.5 ± 0.6 - 97.1 ± 0.2% where they studied different combinations of wall materials which are maltodextrin, β-cyclodextrin, whey protein isolate and gum Arabic without an emulsification process. They found an EE at 76.4 ± 1.9% when they used whey protein isolate and gum Arabic at 1:1 ratio where they studied with more similar wall materials with those studied in this thesis.

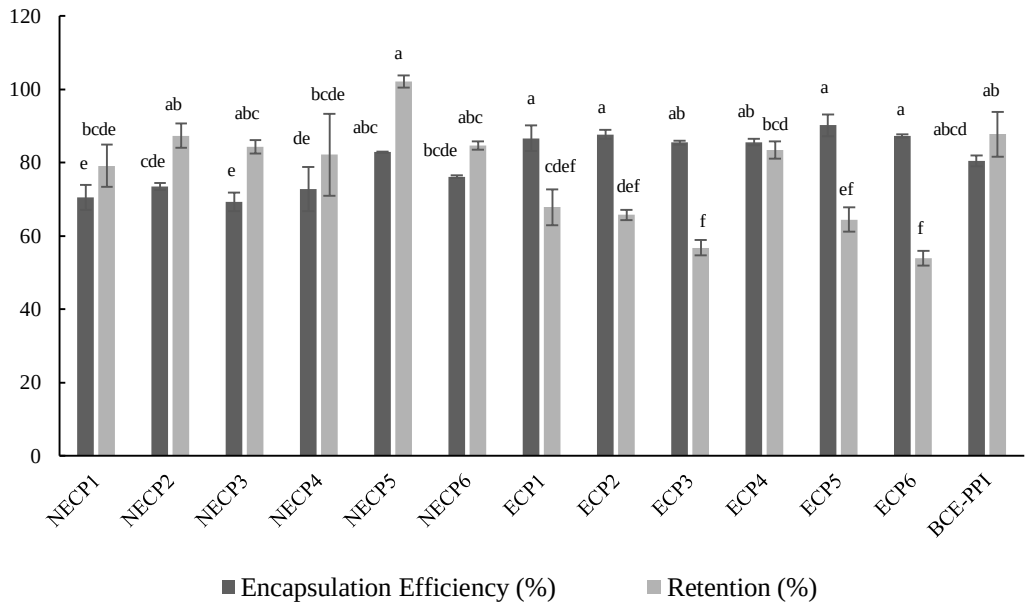

Figure 5.1 : Encapsulation efficiency (%) and anthocyanin retention (%) of NECP and ECP.

ECP had higher EE than NECP had which was probably due to higher protection of anthocyanin-rich extract in emulsified core preventing them to release onto the surface. In general, for both NECP and ECP, the increased core-to-wall ratio did not affect EE significantly ($p > 0.05$). Only a small increase observed at NECP5 in comparison to NECP4 where the core-to-wall ratio increased at the same wall material concentration.

Anthocyanin retention (%) is another important parameter describing the achievement of the high enough ANCs in certain weight of microcapsules required for the coacervated microcapsules to be functionality efficacious. It was also defined as loading capacity in the literature [172]. AR was between $79.08 \pm 5.78 – 102.16 \pm 1.65$ % and $53.90 \pm 2.03 – 83.37 \pm 2.35$ % for NECP and ECP, respectively. It was found 87.73 ± 6.11 % for freeze dried BCE loaded PPI particles. Regarding NECP, only NECP5 had a significant higher AR (%) than NECP4. In general, core-to-wall ratio and wall material concentration did not have a significant effect ($p > 0.05$) on AR. For ECP, a decreasing trend was observed at increasing core-to-wall ratio for both low and high wall material concentration. We observed that, despite the core-to-wall ratio, approximately same TMA concentration was obtained in these particles which lowers the AR. This trend was not significant at low wall material concentration, however, ECP5 and ECP6 with higher core-to wall ratio exhibited significantly ($p < 0.05$) lower

AR. It should be noted that, ζ-potential and particle size values also increased with core-to-wall ratio for ECP.

5.3.4 Thermal properties

A DSC analysis of samples was performed to reveal the information about the thermal behavior of samples that can be helpful in determining the storage conditions and shelf life of microparticles in various heating processes. This method enables a simultaneous assessment of physical and/or chemical changes in the sample by the action of heat. In this study, an endothermic peak (increase in enthalpy) was shown downward, while an exothermic peak is on the contrary direction. Generally, dehydration, phase transitions (from crystalline to amorphous state) and reduction produce endothermic effects, while oxidation, crystallization, and certain decomposition reactions produce exothermic effects. This technique also enables the glass transition of materials that can be observed as a gradual endothermic change in heat flow [165].

The qualitative thermograms of freeze dried BCE, native PPI, ECP and NECP were obtained. Microcapsules obtained with double emulsion showed a sharp and narrow peak while the non-emulsified microcapsules gave a large and broad peak. Moreover, a slight difference was observed in melting peak temperatures of ECP and NECP (Table 5.4). The melting peaks ranged between 133.38- 146.36 for ECP and 118.24–128.1 for NECP. It could be due to the complexation of protein – pectin with black carrot extract which could have a plasticizing effect on protein pectin complexes and decreasing the peak temperature. It was also seen that, both wall materials had high melting temperature, even when CP was not used in the microencapsulation process, particles had high melting peak temperature as can be seen Table 5.4.

The appearance of a single peak in thermograms indicated that the wall materials were homogeneously mixed [160]. The melting peak temperature of the microcapsules were between the peak temperatures seen in PPI and CP. Moreover, the endothermic phase transition peaks of BCE were not visible in DSC curve of microcapsules. Rutz et al. [165] stated that the displacement and/or disappearance of thermal profiles of the encapsulated and wall materials offer the occurrence of encapsulation.

Table 5.4 : Melting peak temperatures of emulsified and non-emulsified core loaded microcapsules, wall materials and freeze dried BCE loaded PPI particles.

	Melting Peak (°C)	
	ECP	NECP
1	133.38	127.62
2	145.44	128.1
3	140.58	118.24
4	138.71	123.28
5	139.27	128.65
6	146.36	135.32
PPI	224.52	
CP	145.56	
PPI-BCE	133.48	

5.3.5 FT-IR

The FT-IR spectra of PPI, CP, Miglyol oil, BCE, and ECP and NECP were shown in Fig. 5.1. Only one each from emulsified and non-emulsified microparticle treatment was shown because all treatments had similar behavior, differing only in the intensity of the peaks, which is associated with the amount of the compound used. The FT-IR spectra of ECP and NECP were shown in Appendix A- Figure A1 and Figure A2. The wavelength of peaks of the spectra of PPI, CP, Miglyol oil, BCE and produced particles were defined based on the studies of Akbari et al. [166], Einhorn-Stoll et al. [167] and Ge et al. [168] for PPI, CP and BCE, respectively.

The FT-IR spectra of PPI had peaks between 3700 - 2800 cm^{-1} and 1700- 800 cm^{-1}. In general, the spectral range between 1600–1700 cm^{-1} represents amide I (C=O stretching vibrations), 1480–1575 cm^{-1} amide II (N—H in plan bending vibration), and 1200–1400 cm^{-1} the amide III region (C—N stretching and N—H deformation vibration). It was also indicated that the conformation of the secondary structure of proteins comprises an α-helix (1650∼1660 cm^{-1}), a β-sheet (1610∼1640 cm^{-1}, 1670∼1690 cm^{-1}), a β-turn (1660∼1700 cm^{-1}), and a random coil (1640∼1650 cm^{-1}) [166]. Therefore, the peak at 1629 cm^{-1} could be attributed to be an indicative of a prevalence of β-sheets. The bands in the range of 2800–3000 cm^{-1} and 3200–3400 cm^{-1} are allocated to the stretching vibrations of the -CH and -OH groups, respectively [160]. Shaddel et al. [160] referred the peak at 3304 cm^{-1} as amine group of gelatin in their study on coacervated microencapsulation which could correspond to the peak 3272 cm^{-1} in our study.

The FTIR spectrum of CP showed a broad area of absorbance between 3000 cm^{-1} and 3600 cm^{-1}, of which corresponded to the O-H group. The FT-IR peak at 2944 cm^{-1}, 1733 cm^{-1} and 1603 cm^{-1} was ascribed to C-H, C=O and COO^- groups of pectin, respectively. The absorption pattern between 1000 cm^{-1} and 1400 cm^{-1} was referred to the fingerprinting region where C-H bending (pyranoid ring), C-O-C stretching (glycosidic bond), C-O stretching (alcohol), and CH_3 bending ($COOCH_3$) were found. Einhorn-Stoll et al. [167] defined the peak at 1723 cm^{-1} as free carboxyl group in their study. However, Shaddel et al. [160] and Saravanan and Rao [169] refer to peaks at 2925 cm^{-1} and 2927 cm^{-1} as carboxyl groups of Arabic gum and citrus pectin respectively, in their study on the complex coacervation between polysaccharides and proteins.

FT-IR spectra of ECP showed that the peaks at the wavenumber of 2961 cm^{-1}, 2931 cm^{-1} and 2874 cm^{-1} of PPI disappeared. This was coherent with the study of Muhoza et al. [170] where they also observed a disappearance of the peak at 2922 cm^{-1} in FT-IR spectrum of gelatin. We observed a new peak formed at 1539 cm^{-1} and a shift in amide I band of PPI from 1453 cm^{-1} to 1456 cm^{-1} in ECP. This new peak was also observed at the spectrum of BCE loaded PPI particles where the CP was not included. PPI could have been interacted both with CP and BCE forming this new peak. This was confirmed by the ζ-potential measurements, values were near zero or negative for the ECP and NECP while it was positive for PPI-BCE particles. However, ζ-potential decreased in case of PPI-BCE particles in comparison to individual PPI showing the interaction between PPI and BCE. There were two approaches in the literature regarding the formation of new peaks upon the interaction of carboxyl group of polysaccharide and amine group of protein. In the study of Shaddel et al. [160] the interaction between gelatin and gum Arabic was proved with the amide peak at 1453 cm^{-1}. On the other hand, Muhoza et al. [170] and Saravanan and Rao [169] remarked the formation of a new characteristic peak appeared at 1560 cm^{-1} and 1545 cm^{-1}, respectively. They attributed it to complex formation with the reaction between amino group of gelatin and carboxylic group of pectin. In the same study, amide I band of gelatin was shifted from 1404 cm^{-1} to 1405 cm^{-1} in gelatin-high methyl pectin coacervates.

FT-IR analysis also confirmed the cross-linking interactions between the wall materials and BCE regarding NECP. The wavelength band between 3082 - 2875 cm^{-1}

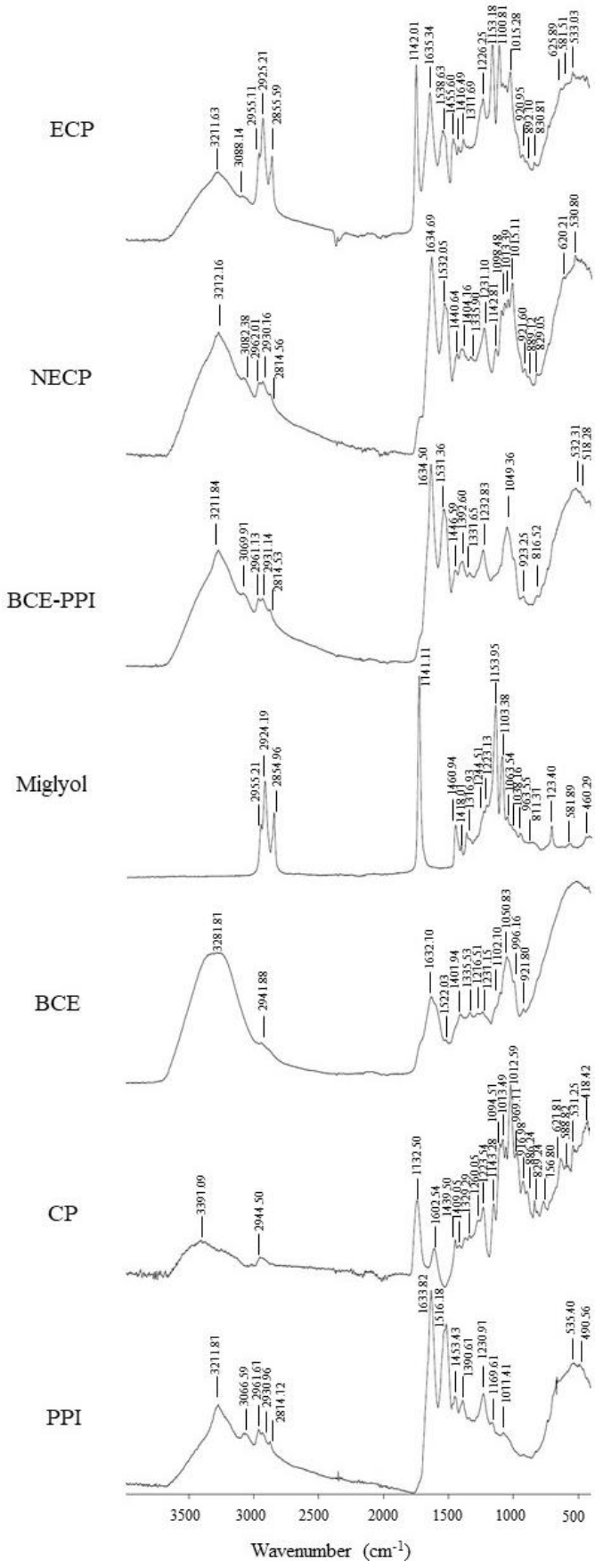

Figure 5.2 : FT-IR spectrums of core, wall and excipient materials and microcapsules.

which was disappeared in the spectra of ECP was visible in NECP. However, there were some shifts both in the region of stretching vibrations of the -CH and -OH groups and the amide I-II band indicating interactions between PPI and BCE. As it was observed in ECP, the spectra of NECP differed from the spectra of PPI, CP and BCE. The disappeared, formed or shifted peaks were analyzed based on the suggestions of Ge et al. [168] and Tan et al. [154] who studied the formation of anthocyanins-loaded polyelectrolyte complexes. Similar to ECP, it was observed that characteristic peak at 1516 cm^{-1} for $-NH_3$ on PPI and the characteristic peak of BCE at 1237 cm^{-1}, corresponding to stretching of pyran rings, has disappeared in NECP, suggesting the likelihood that amino groups have interacted with BCE. Furthermore, the peak at 1634 cm^{-1} derived from amide I band in the spectrum of PPI was shifted to 1635 cm^{-1} as it was also observed in ECP. Amine deformation was observed at 1539 cm^{-1} indicating that the amino group was in the form of NH^{3+} in NECP. The characteristic peak at 1409 cm^{-1} for COO- on CP shifted to 1405 cm^{-1} indicating the complexation of anthocyanins with CP. This peak was not observed in ECP, which was probably due to being captured of BCE inside the Miglyol oil while it could interact with wall materials in case of NECP. All these observations showed that the anthocyanins have been incorporated into PPI-CP complexes.

5.3.6 Morphology

The two representative micrographs of ECP and NECP and PPI-BCE particles were demonstrated in Fig. 5.2. Large and irregular particles were visible in ECP and NECP which was suitable with particle size measurements. Both ECP and NECP showed planar structures with flakey or scaly appearance. ECP presented alveolar structure which differs from the appearance of micrograph of NECP. BCE loaded PPI particles showed smaller planar structures in comparison to its counterpart produced by the incorporation of CP. Melgosa et al. [171] suggested that this alveolar structure could be formed during liquid nitrogen boiling during freezing of the O/W emulsion. In this study, freezing process took place at -80°C which also applies quick freezing before the freeze-drying process. In the case of NECP, a broken glass structure of variable sizes were clear, which are all common features of freeze-dried powders [153, 172-175]. Roos [176] suggested that this glassy structure, with an irregular shape, might protect the entrapped anthocyanins from exposure to heat and oxygen.

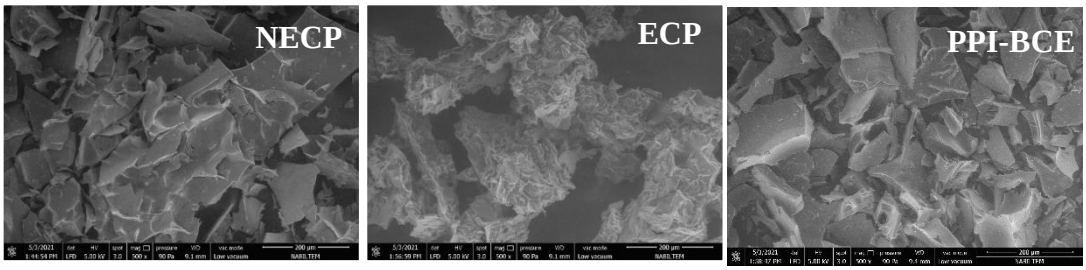

Figure 5.3 : Micrograph of freeze-dried emulsified, non-emulsified particles and BCE loaded PPI particles by scanning electron microscopy.

5.4 Conclusion

Anthocyanin-rich black carrot extract loaded potato protein-citrus pectin particles was produced using emulsified and non-emulsified core materials by freeze-drying. BCE loaded PPI particles was also produced by freeze-drying without the incorporation of CP. Wall material concentration had an effect on particle size of ECP, the higher concentration lowered the size and the ζ-potential of the particles. Encapsulation efficiency (%) was a bit higher when an emulsification procedure was incorporated, while the anthocyanin retention (%) decreased. The highest EE and AR value was found in NECP5 which was prepared at a wall material concentration of 3.5 % and a core material concentration of 2.5 %. Freeze-dried BCE loaded PPI particles produced at the same protein and core material concentration and no significant difference ($p > 0.05$) was found between NECP5 and BCE-PPI. FT-IR and ζ-potential values proved the complexation between PPI and CP in case of ECP and the interaction of PPI, CP and BCE for NECP. The DSC thermograms proved the success of encapsulation procedure and thermos-stability of the black carrot extract loaded particles.

6. THE EFFECT OF PROCESS PARAMETERS ON PHYSICO-CHEMICAL PROPERTIES OF BLACK CARROT EXTRACT LOADED POTATO PROTEIN PARTICLES PRODUCED BY PGSS-DRYING

6.1 Introduction

The PGSS-drying process (Particles from Gas Saturated Solutions) is a high pressure spray process, which is used for the direct generation of powders from solutions with simultaneous solvent separation and pulverization. It is possible to dry and pulverize the gentle substances with this process. In the PGSS drying process, the liquid to be pulverized mixed under high pressure with compressed carbon dioxide and this mixture then relaxed via nozzle in a spray tower. This is done with liquid carbon dioxide compressed by means of a metering pump, and heated by heat exchanger and conveyed to a mixing block. The substance to be pulverized is also fed to the mixing block with another metering pump promoted to the mixing block. In the mixing block, gas and liquid become intensively mixed under high pressure for a short time (milliseconds to seconds). The interfacial tension and viscosity of the substance are set by the carbon dioxide which favors a particularly effective mixing. Mixture is quickly brought to the pre-expansion temperature by the heated gas, part of the gas dissolves in the liquid and thus reduces its viscosity. Then the mixture adiabatically relaxed abruptly through a single-fluid nozzle in a spray tower (ST) operated at ambient pressure. When the pressure is released, the CO_2 suddenly goes from the liquid phase to gaseous phase. Due to strong increase in volume, the mixture torn into fine droplets. The droplets in the mixture are further broken up by the CO_2 escape in the nozzle so that a very fine mist of droplets is created. At the same time, the solvent of the feed solution also escapes during relaxation. The CO_2 cools down due to the Joule-Thomson effect when the pressure drops sharply. Because of this, the temperatures in spray tower are much lower than pre-expansion temperatures. Furthermore, an advantageous inert gas atmosphere is created that excludes oxidation processes in the fine liquid droplets and thus allows a very gentle pulverization [177].

The parameters which are pressure before expansion (pre-expansion pressure), temperature in front of the nozzle (pre-expansion temperature) and gas to liquid ratio (GLR) should be appropriately selected so that the state point of the gas atmosphere in the spray tower after expansion could be in the single-phase range above the dew point temperature of the mixture of feed solvent and CO_2. Gas to liquid ratio is defined as the mass flow of carbon dioxide and liquid to be pulverized. Too little CO_2 results in falling below the dew point and incomplete drying. When feed solvent and CO_2 in one phase, it could be taken from the spray tower via a cyclone. At the same time, a low-solvent-powder is produced which is deposited in the spray tower and in the cyclone. A simplified flow diagram of the process can be seen in Fig. 6.1. Fig. 6.2 shows a T-x, y diagram of CO_2 with a solvent at ambient pressure. The working range of the procedure should be above the dew line which has a light gray background [177].

The drying of solutions by means of PGSS-drying process takes place in three steps. The supercritical CO_2 phase already absorbs part of the moisture in between mixing and nozzle block. Another part of the moisture goes together with dissolved CO_2 with the quick relaxation in the nozzle and the rest is removed by evaporation from the particles released into the spray tower atmosphere [177].

The interest in plant-derived proteins is increasing because of rising awareness of healthy life and the fact that production is environmentally-friendly compared to that of animal sources. The use of plant proteins in encapsulation also emerges as a part of the 'green' trend rising in the pharmaceutical, cosmetic and food industries. Plant proteins are preferred by consumers also due to being less allergenic and not containing GMOs. Potato proteins are by-products of starch production and its nutritional value has been shown to be substantially high as it was previously mentioned.

Particle formation by commonly used drying techniques which are freeze-drying and spray-drying has some disadvantages. The disadvantages of freeze-drying are high energy input and long processing times. For the spray dryer, the most important drawback is degradation of bioactive component due to high temperature during processing [178]. It is possible to reduce these disadvantages by using supercritical systems for encapsulation purposes. Up to present, there is no available study investigating the use of PGSS-drying to generate bioactive compound loaded protein particles.

The aim of the study was to investigate feasibility of drying black carrot extract – potato protein complexes by using PGSS drying and to determine the effect of process parameters on the chemical and nutritional quality of powders. The results were also compared to powders produced by freeze drying and spray-drying techniques.

6.2 Material and Methods

6.2.1 Materials

Food grade potato protein isolate was donated by Döhler GmbH (Darmstadt, Germany). Potato protein isolate contained (min.) 90% protein, (max.) 9% moisture, (max.) 5% ash and (max.) 0.5% sulphite according to specification provided by manufacturer. Citrus pectin with 70% DE (CP DE70, Pectin Classic CU-L 053/15) and citrus pectin with 35% DE (CP DE35, Pectin Classic CU-L 054/15) were supplied from Herbstreith & Fox KG (Neuenbürg, Germany) and used without further purification. For the simulation of *in vitro* digestion, pepsin (from porcine gastric mucosa), pancreatin (from porcine pancreas), bile salts, KCl, KH_2PO_4, $NaHCO_3$, NaCl, $MgCl_2(H_2O)_6$, $(NH_4)_2CO_3$ and $CaCl_2(H_2O)_2$ were purchased from Sigma Aldrich Chemie GmbH (Steinheim, Germany). Hydrochloric acid was obtained from Merck Co (Darmstadt, Germany). For the spectrophotometric analyzes; 6-hydroxy-2,5,7,8-tetramethylchroman-2-carboxylic acid (Trolox) and 1,1-diphenyl-2-picrylhydrazyl (DPPH) were also obtained from Sigma-Aldrich Chemie GmbH (Steinheim, Germany). For all analysis, distilled water was used and all other reagents used were of analytical grade.

6.2.2 Preparation of feed

Potato protein isolate were dissolved in distilled water and stirred at ambient temperature overnight to ensure complete hydration. Afterwards, black carrot extract was added to prepared solution. The final concentration of PPI and BCE were 10% (w/w).

CP could not be included in the formation of complexes, as it gives a very dense structure with PPI which prevents to pump the feed material required for both spray-drying and PGSS-drying. The results of Section 5 showed that the PPI-BCE particles without the incorporation of CP had comparable hygroscopicity, encapsulation efficiency, anthocyanin retention and thermal properties with a lower particle size.

Thus, it was decided to continue the study with BCE loaded PPI without the incorporation of CP.

6.2.3 PGSS-drying

The flow chart of PGSS plant employed in this work was shown in Fig. 6.1. The CO_2 is pumped in liquid state from a storage tank (A). It is brought to the desired thermodynamic state using a three-head membrane pump (B) and a heat exchanger (C). CO_2 is pumped out of the liquid phase with a three-head diaphragm pump and compressed to the desired spray pressure. It is then fed into the laboratory and passes a mass flow device including an electronic evaluation unit where the mass flow rate of CO_2 is displayed. CO_2 continues to flow through a coil heat exchanger where it is heated up to its supercritical state before entering the mixing block. Marlotherm oil is applied as the heating medium, which can be heated to a maximum of 350 °C in an oil thermostat. CO_2 pipeline is heated up to the mixing block with a heating wire type. On the other hand, the pipe section between the heating cabinet and the mixing block is heated with a heating sleeve where temperature is adjustable up to 200°C.

In the mixing block (D) CO_2 meets the feed to be powderized. Up to the nozzle block (E), the two components are mixed within a heated pipeline before the solution is sprayed into the spray tower (F). Both mixing and nozzle blocks are heated with heating cartridges and insulated. An adapter for the nozzle is installed at the lower part of the block and the nozzle can be changed removing and re-installing this adapter. CO_2 which is gaseous after expansion, is extracted through a hole in the mid-part of the spray tower by means of suction and the solidified powder lands on the bottom of the spray tower in a plastic bag.

Fine particles that do not sediment in the spray tower are separated in a vacuum filter (G). The sample to be sprayed reaches the mixing block from a feed vessel (I), with an internal volume of approximately 16 liters. The vessel equipped with a mixer ensuring the uniform distribution throughout the process. The feed is conveyed from the feed vessel towards the mixing section by a four-head piston pump. The mass flow of the material is adjusted by setting the pump stroke, which reaches a maximum of 20 mm. This part of the plant is in a heating cabinet (H) to ensure a constant temperature for the feed. Table 6.1 summarizes the main characteristics of PGSS plant for the processing of thermal sensitive substances. Figure 6.3 and Figure 6.4 represents the

instrumentation inside the heating cabinet and instrumentation around the mixing and nozzle blocks as well as the spray tower, respectively.

Table 6.1 : Information on PGSS-Plant [179].

Characteristics of the PGSS-Plant	
Pressure	Up to 250 bars
Temperature	Up to 140°C
Maximum feed flow	100 g/min
Maximum feed tank pressure	6 bars
Heated plant units	Mixing section Nozzle Supply line CO_2 Feed pipeline of supply materials
Miscellaneous	Pumping of thermally sensitive substances

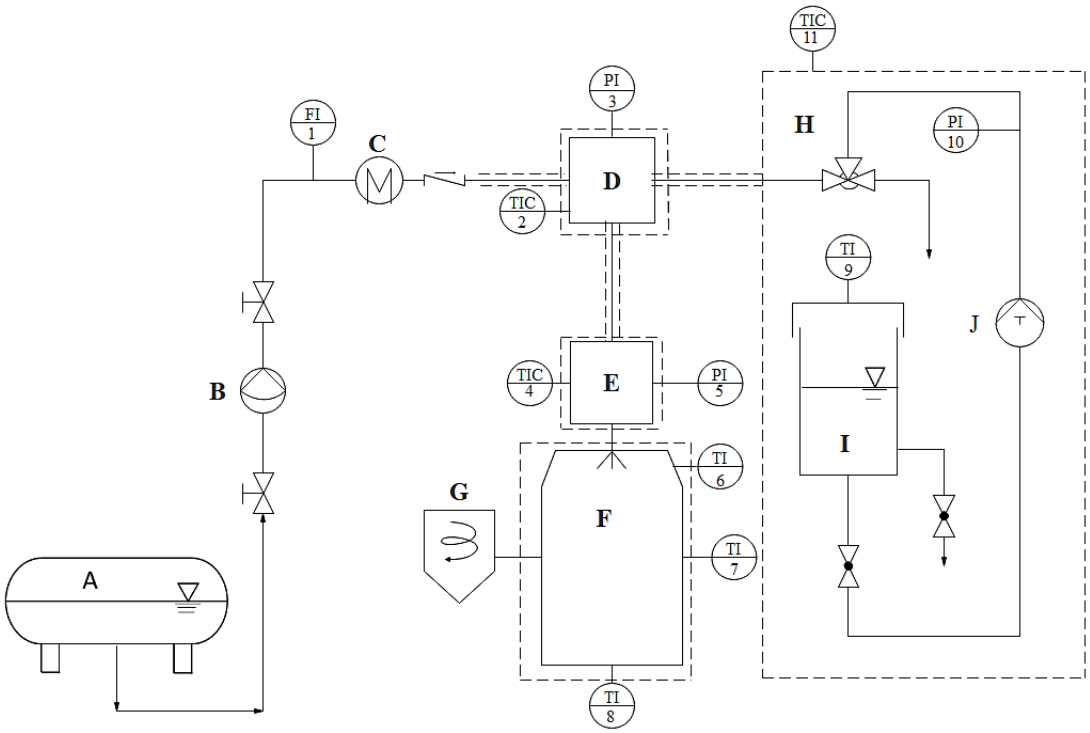

Figure 6.1 : P&I flow sheet for the PGSS-plant. (A) CO_2-Tank, (B) Three-head diaphragm pump, (C) Heat exchanger, (D) Mixing block, (E) Nozzle block, (F) Spray tower, (G) Filter/Cyclone, (H) Heat cabinet/Furnace, (J) Four-head piston pump; (FI) flow meter, (TI) Temperature sensor, (TIC) Temperature sensor and indicator, and (PI).

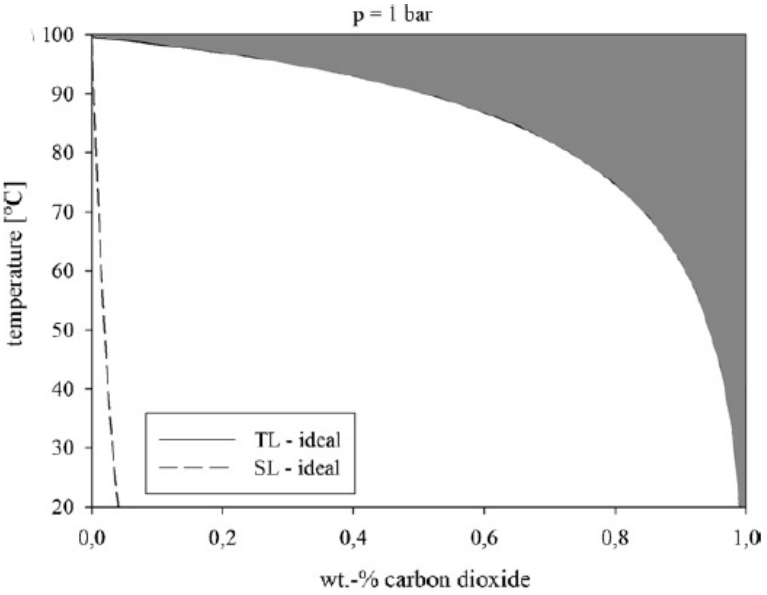

Figure 6.2 : Temperature (T)–composition (mass fraction of CO_2 in gas or liquid phase, m_{CO2}) diagram of CO_2–H_2O mixtures. The shaded area represents the region of suitable operating conditions for water removal in PGSS-drying.

Figure 6.3 : Furnace with substance-carrying parts of the PGSS plant: (1) Vessel, (2) Ball valve, (3) Ball valve for cleaning, (4) Four pump heads of the four-head piston pump, (5 and 6) Three-way valve, (7) Pressure sensor, (8) The plate, (9) Thermo-element type K, (10) Funnel, (11) Bypass-pipe, (12) Balance.

The PGSS system is equipped with various measuring instruments and control devices for recording and regulating the operating parameters. An overview of the positions of

the pressure, temperature and mass flow sensors can be seen in the flow sheet of the plant (Fig. 6.1). The dashed lines in Fig. 6.1 enclose the heated plant sections that require temperature control so that a constant operating temperature can be maintained throughout the process area before expansion.

The temperature is regulated by four controllers, which are installed outside the heating cabinet. The pipe heating and the heating cartridges in the mixing and nozzle block are also equipped with thermocouples. These thermocouples record the temperature of the heating conductors directly and transmit the actual temperature to the controllers.

The vessel is suspended in a frame, which in turn stands on a balance (12). The balance is placed outside the heating cabinet due to its temperature sensitivity. Accordingly, the four feet of the framework (8) are passed through openings in the bottom of the heating cabinet. Mass flow of the mixture, which is conveyed to the mixing block, is calculated by the weight loss of the feed vessel per time unit.

In order to detect the process temperatures before and especially after the nozzle, thermocouples are installed at six positions of the PGSS system. The temperature is regulated by four controllers which are installed outside the heating cabinet. The thermocouples record the temperature of the heating conductors directly and transmit the actual temperature to the controllers. Pressure in mixing and nozzle blocks are detected with gauge pressure sensors with a measuring range of 0 - 400 bar at a maximum temperature of 400 °C. The measurement technology in the front panel was displayed in the Figure 6.5.

6.2.4 Spray-drying and freeze-drying

Spray-drying was chosen to compare the characteristics of PGSS-dried particles as it is a conventional, well-known drying technique which is widely used in the pharmaceutical, cosmetic and food industries. The spray-drying process was carried out in a commercial Buchi B-290 mini spray-dryer. The BCE-PPI solution was fed into the spray-drying apparatus at an inlet temperature of 150 °C, and at a feed flow rate of 3.0 mL/min. Outlet temperature was 77-79 °C. The solution was dried under an air flow of 246 L/h.

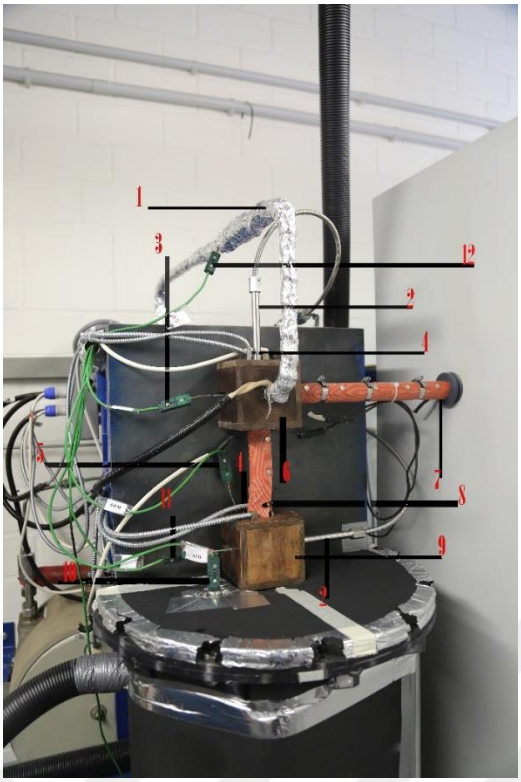

Figure 6.4 : Mixing and nozzle blocks of the PGSS-Plant and their instrumentation: (1) Heated CO_2-Pipe, (2) Pressure sensor, (3,5,10,11,12) Thermoelement Type K, (4) Heat cartridges, (6) Mixing unit, (7) Preheated pipe section connecting furnace with mixing unit, (8) Heated pipe section connecting the blocks, (9) Nozzle block.

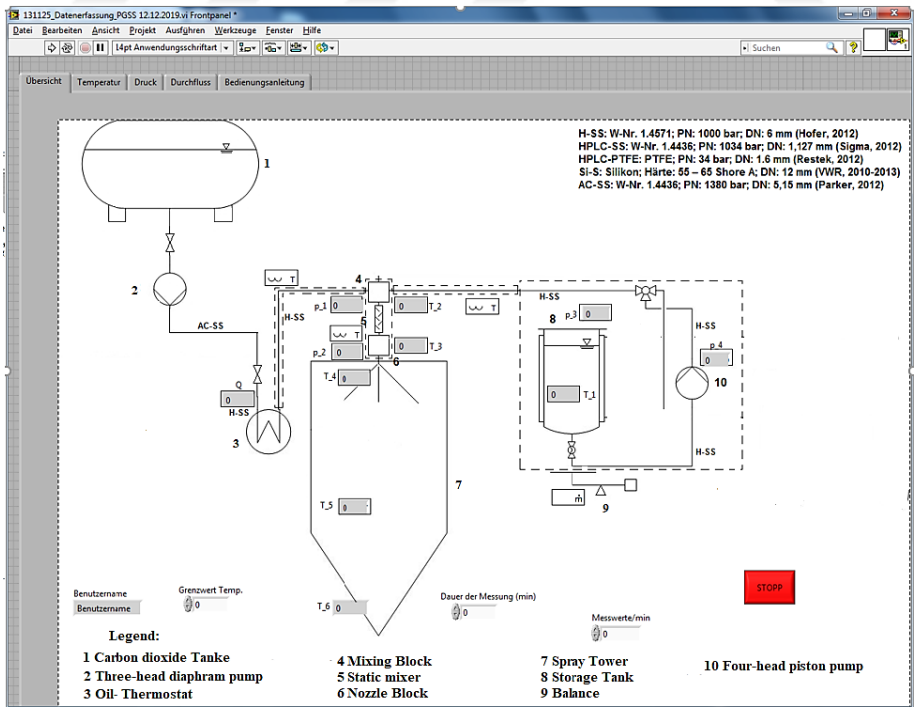

Figure 6.5 : Measurement technology in the front panel.

Freeze-drying was also applied to PPI-BCE solution. After the preparation of the PPI-BCE solution, samples were then frozen at −80 °C and then placed in freeze-dryer which is Labconco Freeze Dry System during at least 16 hours.

6.2.5 Particle characterization

Moisture, hygroscopicity, particle size, encapsulation efficiency, thermal properties, FT-IR characteristics and morphology of the SDP, FDP and PGSSDP observed with different process parameters were investigated using the methods explained in the Section 5.2.

6.2.6 *In vitro* bioaccessability

In vitro digestion model including sequential simulation of bucal, gastric and intestinal digestion, was adapted from Brodkorb et al. [180]. The compositions of the salivary, gastric and intestinal fluids were demonstrated in Table 6.2.

For simulated bucal digestion (SBD), 5 mL of gastric chyme samples were mixed with 2 mL of salivary fluid, 12.5 µL of 0.3 M $CaCl_2$ and 487.5 µL of distilled water to complete the volume to 5 mL. The mixture was incubated at 37 °C in a shaking water bath (Memmert SV 1422; Memmert GmbH & Co., Nürnberg, Germany) for 2 min.

For simulated gastric digestion (SGD), 4.24 mL of gastric fluid was added to 5 mL of oral bolus and the pH was adjusted to pH 3.0 using 3 M HCl. Then, 2.5 µL of 0.3 M $CaCl_2$ and 0.3335 mL of pepsin solution (25 000 U mL^{-1}) was added. Afterwards, the total volume of the mixture was completed to 10 mL with distilled water and the mixture was incubated in a shaking water bath (Memmert Co.) at 37 °C for 2 h. After SGD is completed, 5 mL aliquots were collected for each sample.

For simulated intestinal digestion (SID), 5 mL of gastric chime samples were mixed with 2 mL of intestinal fluid and pH of the mixture was adjusted to 7.0 using 1 M NaOH. Then, 0.75 mL of 160 mM bile, 0.1 mL of 0.3 M $CaCl_2$ and 1.25 mL of pancreatin (800 U mL^{-1}) was added. Afterwards, the total volume was completed to 10 mL using distilled water and the mixture was incubated in a shaking water bath (Memmert Co.) at 37 °C for another 2 h. After SID is completed, again 2 mL aliquots were collected for each sample.

The blank, without the addition of samples, was also incubated under the same conditions described above and used for the correction of interferences from the

digestive fluids. Samples collected from SGD and SID phases were centrifuged at 14000 rpm for 10 min, and the supernatants were kept at −20 °C until further analysis.

6.3 Results and Discussion

The effect of process parameters on the quality of particles were characterized in terms of moisture, hygroscopicity, particle size, thermal characteristics, morphology and FT-IR spectrum.

Table 6.2 : Composition of simulated salivary, gastric and intestinal fluids.

Constituents	Stock concentration (mol/L)	Volume of stock (mL)		
		Salivary fluid (pH 7)	Gastric fluid (pH 3)	Intestinal fluid (pH 7)
KCl	0.5	15.1	6.9	6.8
KH_2PO_4	0.5	3.7	0.9	0.8
$NaHCO_3$	1	6.8	12.5	42.5
NaCl	2	-	11.8	9.6
$MgCl_2(H_2O)_6$	0.15	0.5	0.4	1.1
$(NH_4)_2CO_3$	0.5	0.06	0.5	-
HCl	6	0.09	1.3	0.7

6.3.1 Moisture

As can be seen in Table 6.3, 11 different run was studied on PGSS system. One of the parameters from the nozzle diameter, pressure on CO_2 tank and thermostate temperature was changed in each experimental run. The experiments giving the particles with a moisture content ≤ 10 % were regarded as successful and the powders obtained from these experiments were characterized. Moisture content values were between 5.61 ± 0.06 % and 33.7 ± 5.06 %. We have only enumerated the successful experiments for the further discussion.

Moisture content was affected both by spray tower temperature and GLR. GLR is calculated by CO_2 and feed flow rates. Feed flow rate in our study was constant (15.53 ± 2.16 g/min) and so GLR was directly dependent on CO_2 flow rate. CO_2 flow was adjusted by changing the nozzles with different diameters and CO_2 tank pressure. The flow rate of CO_2 could be increased by using a nozzle at a larger diameter or by increasing the pressure. It was previously presented that GLR should be higher than a

Table 6.3 : The variables and dependent variables and moisture content values of PGSS-drying experiments.

Samples	Adjusted parameters			Variables			Dependent variables		Moisture
	Nozzle diameter (mm)	Pressure on CO_2 tank (bar)	Thermostate Temp (°C)	Pre spraying Pressure (bar)	Pre spraying Temp (°C)	CO_2 flow (kg/min)	Spray Tower Temp (°C)	GLR	
*	0.84	93	120	83.21 ± 3.40	126.30 ± 2.97	0.55	29.35 ± 3.09	38.76	18.45 ± 3.22
*	0.84	105	120	93.00 ± 2.10	125.93 ± 4.23	0.67	27.61 ±0.46	44.64	13.76 ± 2.83
PGSSDP1	1.02	105	120	90.17 ± 1.40	124.75 ± 3.87	1	26.59 ± 0.93	66.13	10.11 ± 2.31
*	1.02	93	120	79.50 ± 2.26	124.49 ± 5.14	0.94	24.89 ± 0.52	54.53	16.10 ± 0.48
PGSSDP2	1.02	105	130	91.06 ± 2.32	132.44 ± 4.90	1	29.43 ± 0.71	63.64	7.88 ± 0.94
PGSSDP3	1.02	93	130	79.63 ± 3.53	128.94 ± 3.78	0.9	32.59 ± 1.76	51.24	7.27 ± 0.75
PGSSDP4	1.02	80	130	67.19 ± 2.10	125.75 ± 3.08	0.68	36.63 ± 0.76	44.11	5.61 ± 0.06
*	1.2	105	130	85.78 ± 1.80	124.50 ± 4.74	1.39	20.55 ± 1.56	82.38	33.7 ± 5.06
PGSSDP5	1.2	105	140	86.9 ± 2.92	129.18 ± 2.56	1.36	32.61 ± 1.02	79.88	6.41 ± 0.08
PGSSDP6	1.2	93	140	74.05 ± 2.77	127.20 ± 4.39	1.19	37.50 ± 1.71	75.64	5.90 ± 0.10
PGSSDP7	1.2	80	140	59.77 ± 4.28	126.44 ± 3.67	0.8	42.73 ± 0.61	46.25	5.48 ± 0.72

certain value for a complete evaporation at a specific spray tower temperature.

A very low correlation between moisture content and GLR was (0.25, $p < 0.05$) found, however, lower moisture content was obtained at higher GLR values at similar spray tower temperature values.

In case of spray tower temperature, both pre-spraying pressure and pre-spraying temperature had an impact on spray tower temperature. It could be seen that, at constant pressure with the same nozzle size, spray tower temperature increases with pre-expansion temperature. It was simply explained by conservation of energy during the expansion by Martín et al. [181]. On the other hand, they continued that pre-expansion pressure has opposite effects on the spray tower temperature. When the pressure in the static mixer is increased above 8 MPa, where the minimum water solubility in CO_2 is observed, more water is extracted in this section and lower moisture can be achieved. At the same time, the saturation concentration of CO_2 in the liquid phase increases with increasing pressure. However, with increasing pre-expansion pressure, the cooling due to Joule-Thomson effect also increases and the spray tower temperature decreases. We found a high negative correlation with a Pearson coefficient of -0.78 ($p < 0.05$) between moisture and spray tower temperature.

6.3.2 Hygroscopicity

Hygroscopicity is the ability of materials to absorb moisture from the environment. It affects the storage and stability of powdered foods. Samples with less hygroscopicity are easier to handle and pack [182].

As can be observed from Table 6.4, the hygroscopicity of the produced particles were ranged from 18.79 ± 3.08 % (w/w, dry basis) to 24.94 ± 0.04 % (w/w, dry basis). It was observed that slightly hygroscopic black carrot extract-potato protein powders could be produced using PGSS Drying.

Up to our knowledge, no study available in literature investigating the hygroscopicity of powders obtained by PGSS. However, Correia et al. [183] concluded that polyphenol-protein matrices had low hygroscopicity (9.4–16.2 g H_2O/100 g) independent of the drying technique used where they studied the effect of spray-drying, freeze-drying, or vacuum oven drying on wild blueberry polyphenol – protein powders. It should also be noted that, these hygroscopicity values are much lower than

Table 6.4 : Physicochemical properties of unprocessed PPI, freeze dried BCE, FDP, SDP and PGSS-dried particles at different conditions.

Samples	Hygroscopicity (%)	ζ-potential (mV)	d50 (μm)	D[4,3] (μm)	D[3,2] (μm)	span
PGSSDP1	18.79 ± 3.08d	14.67 ± 1.74bc	8.18 ± 0.52ab	9.76 ± 0.67a	7.45 ± 0.45a	1.44 ± 0.03cd
PGSSDP2	21.93 ± 0.38bcd	14.97 ± 1.11bc	8.69 ± 0.32ab	11.49 ± 0.73a	2.59 ± 0.10a	2.34 ± 0.18ab
PGSSDP3	19.59 ± 0.99cd	15.63 ± 0.25bc	8.55 ± 0.32ab	10.04 ± 0.43a	6.4 ± 0.90a	1.44 ± 0.04cd
PGSSDP4	23.25 ± 1.79bcd	16.23 ± 1.40bc	10.09 ± 0.23ab	12.47 ± 0.32a	4.77 ± 1.24a	1.75 ± 0.04bcd
PGSSDP5	23.11 ± 0.39bcd	16.43 ± 1.16bc	10.01 ± 0.23ab	13.20 ± 0.23a	2.05 ± 0.08a	2.63 ± 0.03a
PGSSDP6	23.98 ± 1.06bc	13.27 ± 0.95c	12.33 ± 1.14a	14.97 ± 1.93a	3.31 ± 0.18a	1.87 ± 0.35bc
PGSSDP7	24.94 ± 0.04b	16.90 ± 0.87bc	8.04 ± 0.22b	9.28 ± 0.27a	7.48 ± 0.20a	1.25 ± 0.01d
FDP	24.41 ± 0.95bc	17.33 ± 0.97b	11.56 ± 3.28ab	13.34 ± 4.27a	7.3 ± 6.56a	1.58 ± 0.31bc
SDP	26.85 ± 0.97b	17.80 ± 0.69b	10.59 ± 2.59ab	11.88 ± 3.33a	4.48 ± 5.06a	1.66 ± 0.28cd
PPI	10.14 ± 0.79e	28.40 ± 1.18a	-	-	-	-
FD-BCE	56.72 ± 1.01a	-	-	-	-	-

those in the study of Bhusari et al. [184] where they determined the hygroscopicity of spray dried tamarind produced with maltodextrin, gum Arabic and whey protein isolate. Similarly, it has been observed that the hygroscopicity of spray dried cactus pear juice varied from 36.30 to 48.93g/100g dry solid [185]. The hygroscopic moisture of spray-dried betacyanin powders ranged from 45.4g/100g to 49.2g/100g dry solid [156] and the hygroscopicity values of spray-dried lulo powders showed values between 35 and 60g/100g dry solid [186]. Potato protein isolate proved to be efficient in lowering the hygroscopicity of polyphenol-protein matrices.

It was also observed that, hygroscopicity values increased with decreasing moisture content and increasing spray tower temperature as seen in Figure 6.6.

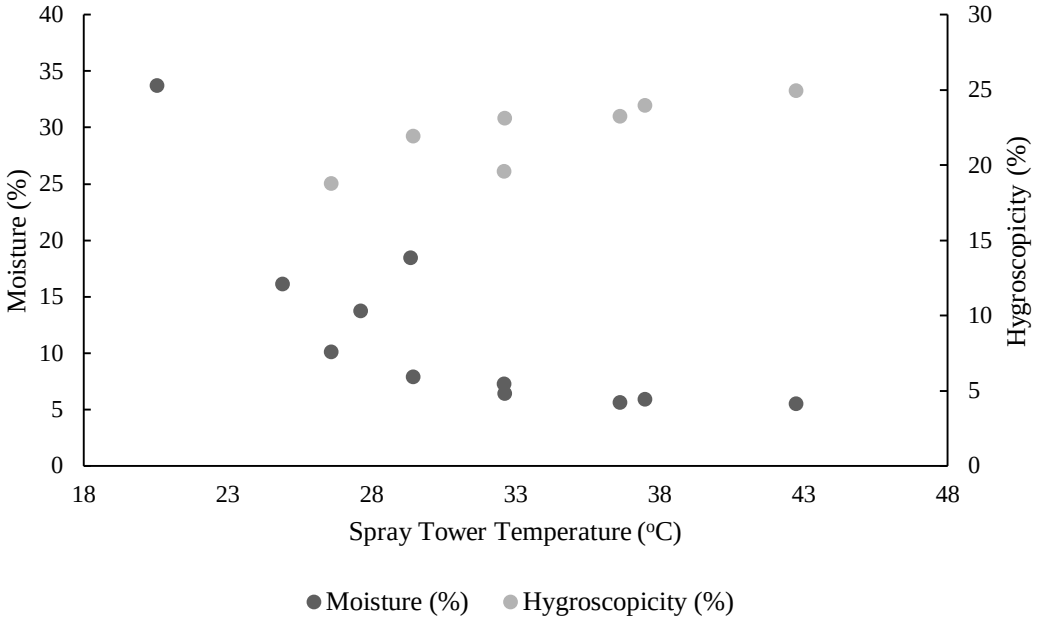

Figure 6.6 : The effect of spray tower temperature on moisture and hygroscopicity of PGSS-dried particles.

6.3.3 Encapsulation efficiency and TMA retention

Encapsulation efficiency of particles obtained at different parameters were between 69.49 ± 2.19 - 81.78 ± 1.52, while it was 78.58 ± 0.49 and 84.80 ± 1.27 for FDP and SDP, respectively (Fig. 6.7). Except the PGSSDP5 which was produced with the highest GLR, EE did not differ significantly ($p > 0.5$) between all samples including FDP and SDP. Up to our knowledge, no study available investigating the encapsulation efficiency of PGSS-dried particles in regards to surface and total bioactive compounds. The term of encapsulation efficiency was measured in different ways in the literature, in some studies, it refers to retention of bioactives after the applied process, while in

others, it was given as a result of the measurement of surface and total bioactives of the particles. Hence, the studies in which the EE was referred to measurement of surface and total bioactives was used for a literature comparison in this study. The results were comparable to spray dried anthocyanin-rich extract loaded particles. The encapsulation efficiency found between 45.4-74.4 % for maqui juice anthocyanin loaded particles [187], 86.07-96.21 % for barberry extract loaded particles [188], 44.79-64.69 % for sour cherry anthocyanin loaded particles [189], 97.13 % for elderberry bioactives loaded particles [190] and 99.64 % for blackcurrant concentrate [191] where they used inulin/sodium alginate, combinations of maltodextrin-gum Arabic, maltodextrin-gelatin and maltodextrin, β-lactoglobulin, whey proteins and whey protein isolate, respectively.

Only the PGSSDP5 differed significantly ($p < 0.05$) from the other PGSS-dried particles. However, encapsulation efficiency values showed a high negative Pearson correlation ($r = -0.75$) with GLR. Higher amount of CO_2 dissolved in feed solution could cause more porous structure in particles as the expansion in spray tower will be larger. Hence, the encapsulation efficiency could be lowered with a more porous structure.

Anthocyanin retention was found in a narrow range ($84.02 \pm 1.34 – 87.27 \pm 4.09\%$) for PGSS-dried particles which was probably due to the spray tower temperature lower than $42.73 \pm 0.61^{o}C$. There was no statistical difference ($p > 0.05$) between PGSS-dried particles and FDP. However, SDP had lower AR than other samples which was probably due to high temperature applied during the process which could damage the anthocyanins.

6.3.4 Particle size

Particle size measurements were given in Table 6.4. The mean particle size values D[4,3] and d50 were ranged between $9.28 \pm 0.27 – 14.97 \pm 1.93$μm and 8.04 ± 0.22 - 11.56 ± 3.28 μm, respectively. The samples presented low span values (1.25 ± 0.01 - 2.63 ± 0.03) showing a narrow size distribution. Gonçalves et al. [192] found much higher d50 values between 37.0 – 479.8 μm where they used OSA starch, lecithin and β-glucan as carriers to produce Epigallocatechin gallate-loaded particles. Martín and Weidner [37] studied the micronization of polyethylene glycol by PGSS-drying of aqueous solutions and measured a particle size range (d50) between 6-653 μm with a span range of 1.78 – 28.86 where they studied the effect of process parameters such as

pre-expansion pressure, pre-expansion temperature and GLR with a range of 85-121 bar, 70-151ºC and 19.6-139, respectively. Moreover, de Paz et al. [193] determine the mean size of β-carotene loaded soybean lecithin particles obtained by PGSS drying in between 20.8-449.8 μm which was also much higher than those found in this study. This shows potato protein is a good carrier for black carrot extract to produce dried particles. It should be also noted that the production of β-carotene-loaded soybean lecithin particles needed an emulsion step which could lead to formation of larger particles.

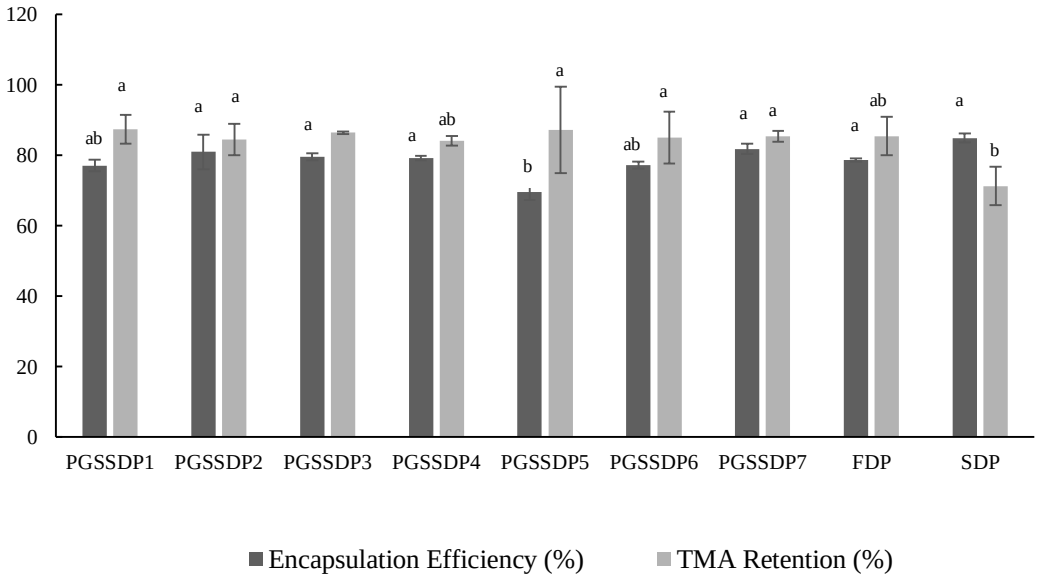

Figure 6.7 : Encapsulation efficiency and Anthocyanin retention of FDP, SDP and PGSS-dried particles using different process conditions.

Martín and Weidner [37] obtained that particles with a lower size could be produced with increased pre-expansion temperature and pre-expansion pressure. They explained that, when temperature or pressure increased, the solubility of CO_2 in the liquid phase increases as well, leading to more efficient atomization and smaller particle size. GLR was also revealed to have decreasing effect on particle size as the increased GLR indicates a more efficient atomization and a faster precipitation leading to smaller particles. It was also noted that experimental results are more dependent on the flow ratio than on the individual flow rates of solution and CO_2. Our results did not exhibit a correlation between the process parameters and particle size. However, the study conducted by Martín et al. [181] was in a wide range of parameters leading a particle size range of 20.8-449.8 μm as it was also written above. The small variation in mean size of PPI-BCE particles could hinder the effect of process parameters in this study.

Moreover, the same observation was reached when the correlationwas analyzed between parameters and particle size in a range of 6-12 μm in the study of Martín and Weidner [37].

PGSS-dried particles did not show any significant difference ($p > 0.05$) with SDP and FDP, indicating the possibility of powder production by PGSS with similar particle size values with commercial powder products.

6.3.5 Thermal properties

Qualitative DSC curves of freeze dried BCE, PPI, FDP, SDP and the one representative PGSSDP are presented in Fig. 6.9.

Freeze-dried black carrot extract showed various endothermic peaks between 115-190^{o}C which could be due to presence of different anthocyanin and sugar compounds. As the peaks are endothermic, it was shown that the black carrot extract is in the crystalline form and so showed different peaks for the transition from a crystalline to amorphous structure. These crystal transition peaks were not observed in PPI-BCE particles regardless of the applied drying process which was corroborating the amorphous state of the black carrot extract when it is complexed with PPI.

Native PPI showed three endothermic peaks at 124^{o}C, 156^{o}C and 224^{o}C. The firt two peaks could be attributed to two main subclasses of protease inhibitor, which explains the two separate denaturation events and the third one could be the melting. Du et al. [194] revealed the thermal characteristics of the same protein isolate and they found large endothermic peak spanning from 100^{o}C to 128^{o}C, and a broad, low intensity endothermic peak between 65^{o}C and 83^{o}C. The thermogram was similar to one obtained in this study, however, with the lower peak temperatures.

Freeze-dried PPI-BCE particles showed the most similar curve to that of native protein which was probably due to absence of high temperature during the drying process preserving the structure of the protein. Spray dried PPI-BCE particles showed one asymmetric broad peak which could be due to denaturation of one of the protease inhibitor during the process. On the other hand, the DSC curve of PGSS-dried PPI-BCE powder showed the denaturation of the second protease inhibitor as a plateau more than a peak which could be due to partial denaturation during the processing of the mixture in the part of nozzle and mixing block for a short time.

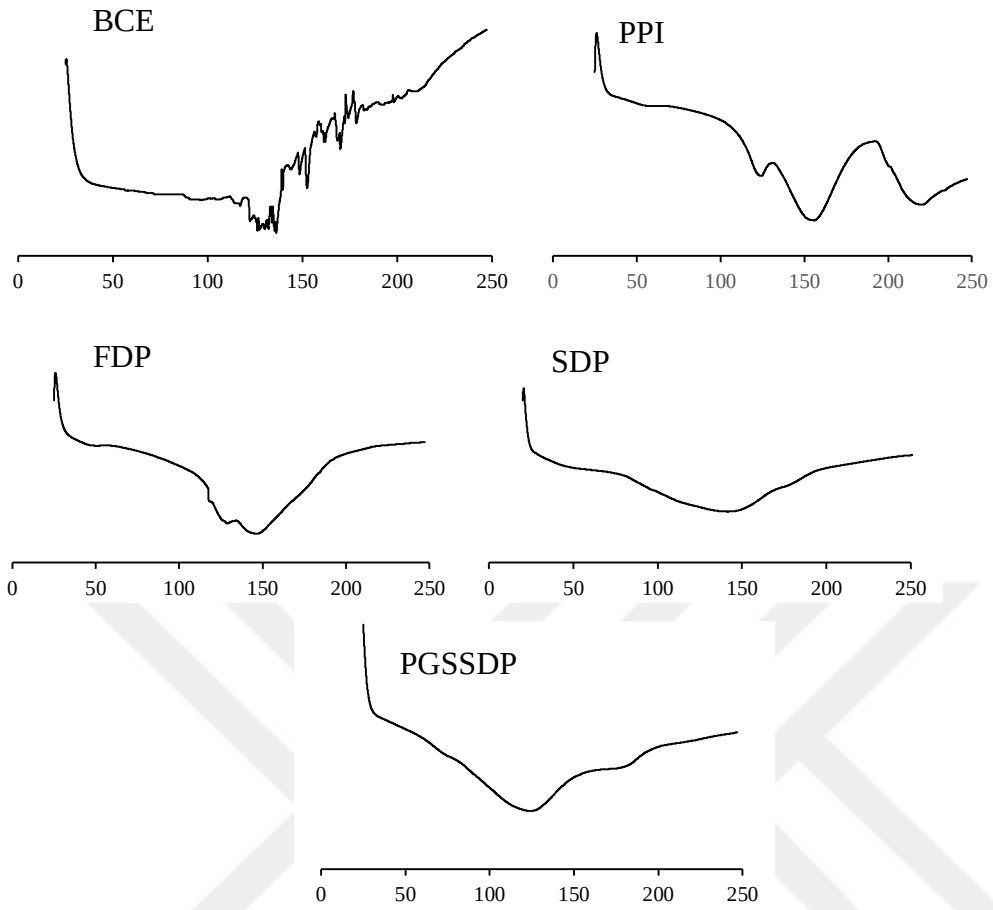

Figure 6.8 : DSC thermograms of freeze dried black carrot extract, PPI, freeze dried, spray dried and PGSS-dried PPI-BCE.

6.3.6 FT-IR

FTIR was used to verify whether BCE was successfully incorporated in the PPI matrix and their chemical interactions. The spectra of PPI and BCE was identified based on the literature as it was previously explained in the section of 5.3.5 FT-IR. Fig. 6.10 shows the infrared spectrum of PPI, BCE and the unprocessed mixture of BCE-PPI, freeze dried, spray dried and PGSS-dried BCE loaded PPI particles.

The characteristic peak at wavenumbers at 1051 cm^{-1} (aromatic ring C-H deformation) and 922 cm^{-1} were observed in the spectrum of FDP, SDP and all PGSSDP. However, the another characteristic peak of BCE at 1237 cm^{-1} (stretching of pyran rings) were shifted to 1232-1234 cm^{-1} in the spectra of particles indicating an interaction with PPI. Moreover, the characteristic peak of PPI at 1516 cm^{-1} for -NH_3 was disappeared and a new peak formed at a wavelength at 1530-1531 cm^{-1} for all particles. These results can suggest that BCE is not only incorporated in the carrier's matrix through physical interaction but also with the formation of chemical bond indicating a more efficient

encapsulation [192, 195]. This was confirmed by ζ-potential measurements, PPI- BCE particles had significantly lower values compared to individual PPI.

As it is seen in Figure 6.10, no difference was observed between the spectrums of FDP, SDP and PGSSDP suggesting the occurrence of same interactions for all processes between PPI and BCE. The spectrum of all of the particles was shown in Appendix A Figure A3.

6.3.7 Morphology

Visual morphology of the dried powders can be observed in the SEM micrographs (Fig. 6.11). Freeze-dried particles were found to be very large and irregular compared to spray and PGSS-drying. It presented a flakey or scaly appearance, forming planar structures with some particles being larger than 100 μm. Some dents were visible on the surface of particles, which was previously attributed to sublimation applied durimg freeze-drying. SDP exhibited a rougher surface with more imperfections or 'teeth' which was previously described by Melgosa et al. [171]. They associated these surface depressions to the collapse of the particle hollow core once the crust is formed during the initial stages of drying. Salgado et al. [196] and Melgosa et al. [171] observed very similar shape for both PGSS-dried and spray dried particles obtained in this study.

Based on the micrographs, PGSSDP were smaller than SDP, but they form agglomerates very easily composed by partially fused spheres, producing much larger clusters. This was supported by Comunian et al. [149] who detected an increase of the agglomeration of particles when drying at lower temperature. Salgado et al. [196] explained that the formation of small particles by PGSS-drying is a consequence of the desorption of CO_2 from the liquid when the pressure is suddenly reduced in the nozzle, which breaks the liquid.

The particle size values observed for SDP with particle size analyzer and micrographs were found to be coherent. The particles with a diameter of around 10 μm were able to be seen on the micrograph which was suitable with particle size measurements. In the case of PGSS-dried particles, despite the agglomerates around 20-40 μm seen on the micrographs, particle size values found between 9.28 ± 0.27 - 14.97 ± 1.93 μm. This could be due to partition of agglomerates due to the agitation and ultrasound applied in the particle size analyzer when the wet measurement method is used. It was

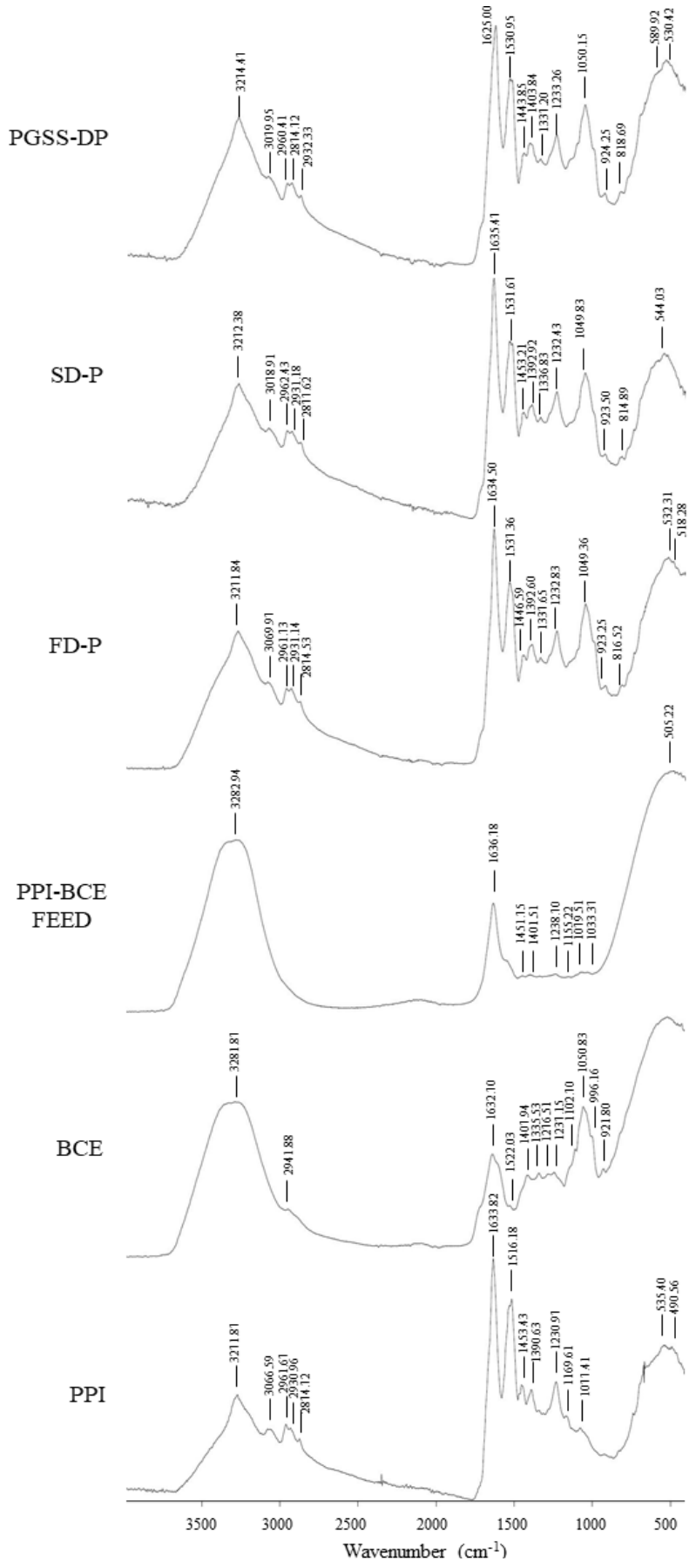

Figure 6.9 : FT-IR spectrums of unproccessed and processed materials.

size distribution diagrams. Freeze-drying also produced very large particles with irregular shape which was observed in SEM, however, the particle size found as 13.34 ± 4.27 μm. It would seem that, agglomerates have very loose structure which could break up to its structural units with mild physical force. Moreover, this agglomerates had a very porous structure while the SDP exhibit distinct shapes with indents on the surface. This loose and porous structure could be due the rapid evaporation of water with CO_2 escape through the nozzle during PGSS drying.

The spherical structural units of the agglomerates produced by PGSS-drying were more apparent for the experiments E3, E4, E5 and E8. This experiments were conducted under GLR and ST between 44.11 - 63.64 and 29.43 ± 0.71 – 42.73 ± 0.61ºC, respectively. The moisture content of particles obtained in these experiments were between 5.48 ± 0.72 - 7.88 ± 0.94 %. These spherical structural units were not visible for the particles with higher moisture content (E2) or higher GLR (E6 and E7).

Martín et al. [181] observed particles in the form of large agglomerates or flakes and with a broad dispersion of sizes when the moisture content was between 1–4 wt%. They pointed out that particle morphology is directly related to residual moisture content of particles. Lévai et al. [195] also stated the influence of moisture on morphology with regard to GLR. We observed similar morphologies at changing GLR with their study. A partial disappearance of spherical units within the agglomerates at higher GLR was also resulted in their study. However, they ascribed this to increased moisture content with increasing GLR. However, in our study, by means of adjustment of thermostate temperature, spray tower temperature was also high enough to obtain particles with low moisture content at higher GLR. Thus, the partial disappearance of these spherical units seem to be directly related to GLR in case of our study. It can thus be assumed that, higher CO_2 flow at the same feed flow could negatively affect the spherical structure of particles during the rapid depressurization through the nozzle.

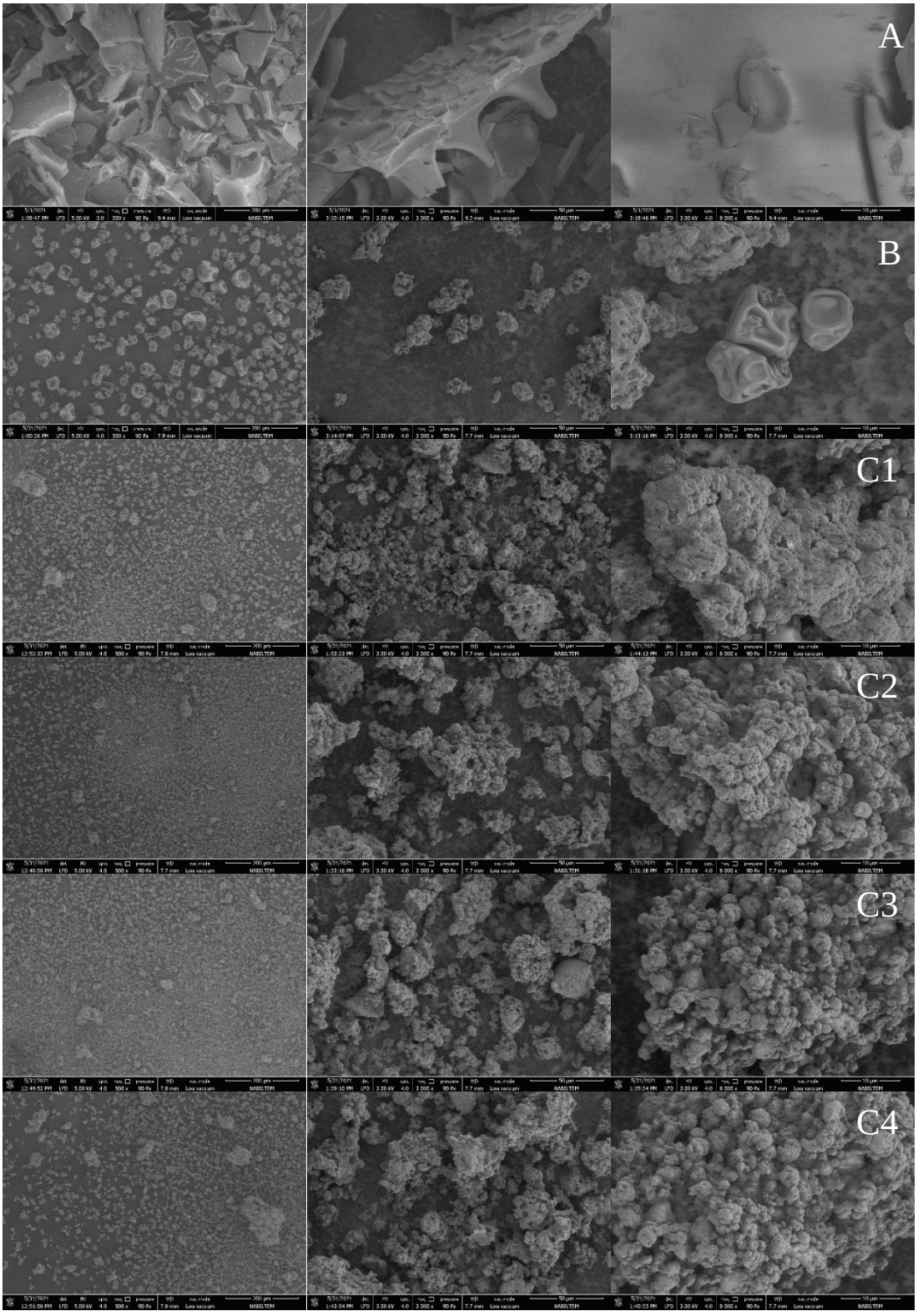

Figure 6.10 : Scanning electron micrographs of BCE loaded PPI particles produced by freeze-drying (A), spray-drying (B) and PGSS-Drying at different process conditions – Run R1 (C1), Run R2 (C2), Run R3 (C3), Run R4 (C4), Run R5 (C5), Run R6 (C6), Run R7 (C7) and Run R8 (C8).

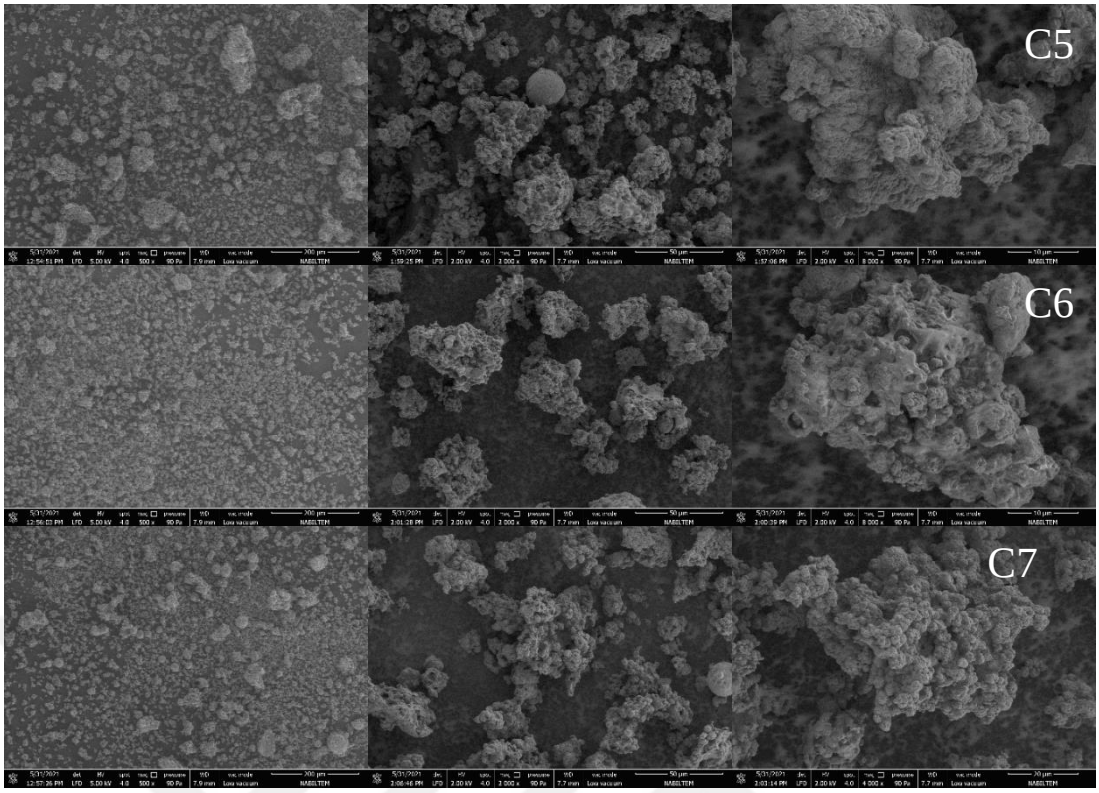

Figure 6.10 (Continued) : Scanning electron micrographs of BCE loaded PPI particles produced by PGSS-Drying at different process conditions – Run R5 (C5), Run R6 (C6), Run R7 (C7).

6.3.8 *In vitro* bioaccessability

The released total monomeric anthocyanin in gastric and intestinal digestion was revealed in Figure 6.12. The encapsulation with PPI via freeze-drying, spray-drying and PGSS-drying did not affect the anthocyanin release during the gastric digestion significantly ($p > 0.05$) as compared to release from black carrot extract. The stability during simulated gastric digestion could be expected due to chemical behavior of anthocyanins with pH. In aqueous solution, anthocyanins undergo structural re-arrangements with pH changes, leading to equilibria between four molecular structures: quinoidal base (blue), flavylium cation (red), carbinol (colorless) and chalcone (yellowish) forms [197]. Thus, it has been reported that the stability of anthocyanins under gastric conditions is most likely due to acidic conditions during the gastric phase under which anthocyanins are found in the flavylium cation stable form [198-200].

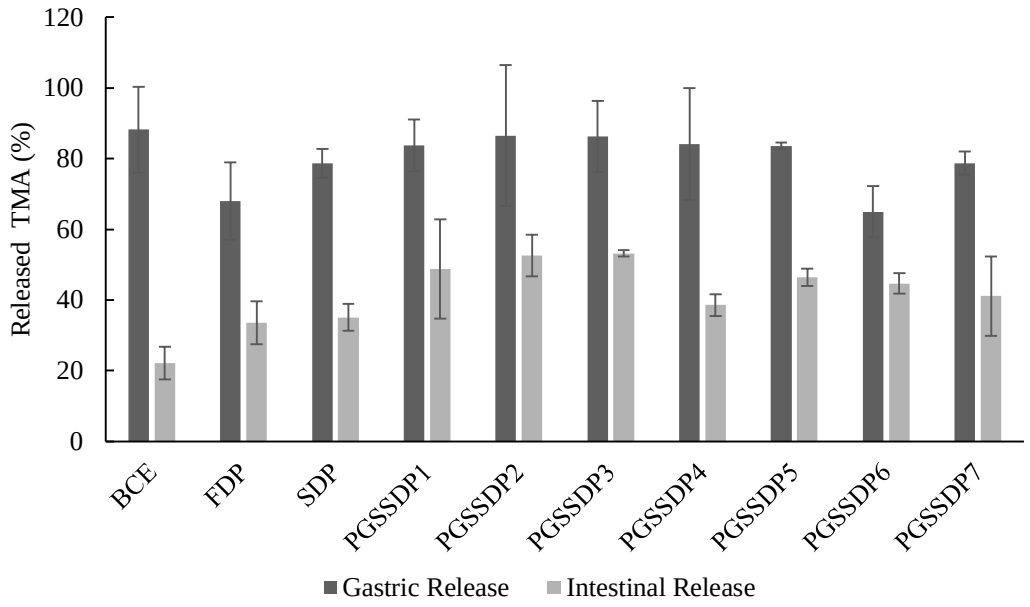

Figure 6.11 : Gastric and Intestinal Release (%) of unprocessed BCE, SDP, FDP and PGSSDP at different operating conditions.

Moreover, potato proteins used in this study are solubilized in water bringing the pH to between 3-4. Therefore, it could be regarded as stable at gastric conditions due to its high solubility and high ζ-potential values at acidic pH as it was previously explained in Section 3.2.4. and Section 3.2.5. Lang et al. [201] determined a slightly negative impact on anthocyanin stability with the addition of α-casein or β-casein and they ascribed this to denaturation and dissociation of casein molecules which could lead to slight loss of bound anthocyanins.

However, intestinal conditions caused a high decomposition of anthocyanins in un-encapsulated black carrot extract. It is due to the alkaline environment of intestinal juice that mainly causes the degradation and inferior accessibility of anthocyanins [202]. The *in vitro* bioaccessability of anthocyanins were studied by Ge et al. [168] with and without enzyme addition and they did not find any significant change ($p > 0.05$) between two applications. Encapsulation with PPI caused a slight increase in % released TMA for the particles produced by freeze-drying and spray-drying. Higher protection of anthocyanins was observed with some of the PGSS-drying runs which are PGSSDP1, PGSSDP2, PGSSDP3 and PGSSDP4. There are contradictory results in the literature on the bioaccessability of anthocyanins with protein complexation. Norkaew et al [203] studied *in vitro* gastric and intestinal release of black rice anthocyanins and they found a slight decrease in released anthocyanins in whey protein-black rice anthocyanin complexes compared to control. Regarding the

intestinal release, there was no statistical difference between the control and whey protein microcapsules after 4-hour intestinal digestion. On the other hand, Xiong et al. [204] found higher stability at 8-fold for blueberry and 3-fold for muscadine grape polyphenols delivered in protein-polyphenol aggregate particles during the simulated *in vitro* digestion. The higher stability values were observed than found in our study could be due to difference in the method applied. However, they used the precipitate in *in vitro* digestion model which was formed with the complexation of pea and rice proteins with polyphenolic extracts. In this study, protein anthocyanin complexes were relatively stable after the complexation and drying and the whole sample was subjected to *in vitro* digestion.

6.4 Conclusion

Anthocyanin-rich black carrot extract – potato protein isolate particles were successfully produced by PGSS-drying. GLR and spray tower temperature was two decisive parameters on the final moisture content of particles. Encapsulation efficiency decreased with increasing GLR, however, in general, particles showed high encapsulation efficiency values which are comparable to spray dried and freeze dried particles. Anthocyanin retention (%) of PGSSDP was similar with FDP and higher than SDP. The size of particles was about 10 μm which is acceptable regarding the food and drink applications. The ζ-potential values and FT-IR characteristics proved the interaction between BCE and PPI. The stability of proteins was not affected by the pressure applied in PGSS, as they exhibit similar ζ-potential values with FDP and SDP. DSC thermograms indicated the success of the encapsulation and improved thermal properties of particles. Higher protection was observed for PGSSDP than SDP and FDP at the intestinal conditions which could be due to alveolar structure of PGSS-dried particles obtained in SEM micrographs.

7. CONCLUSION AND RECOMMENDATIONS

In this thesis; the formation of potato protein based wall materials, the supercritical extraction of black carrot extracts to be used as core material, the encapsulation of black carrot extracts in potato protein based material using PGSS-drying was investigated through four work packages. In the first work package, potato protein isolate and pectins with different origins and degree of esterification was characterized. Potato protein was found to be highly soluble at acidic conditions, the isoelectric point was between 7-8. Pectins with different origins and degree of esterification were soluble and ζ-potential values were negative over the entire pH range. pH 3 was chosen for complexation, as the highest interaction could be achieved between proteins and pectins at this pH where absolute values of ζ-potential of polymers are similar. Viscosity of pectins with low degree of esterification was high preventing their utilization. Citrus pectin with high degree of esterification had the lowest viscosity values. Protein-pectin ratio (0.33-5) was tested for the protein pectin complexes, the highest interaction between protein and citrus pectin with high degree of esterification was found at the ratio of 2.5. The citrus pectin with high degree of esterification and potato protein complexes generated at pH 3 and protein-pectin ratio of 2.5 was chosen to be used wall materials for the encapsulation purposes. As a second work package, the ternary compressed CO_2-ethanol-water mixtures was employed to form core material to be used which is the black carrot extract. RSM was used to optimize pressure, temperature and ethanol-water ratio for the anthocyanin extraction. All the trials were found to be at two-phase region according phase equilibrium diagram of for CO_2-ethanol-water mixtures. The linear and quadratic effect of pressure and temperature were found to be significant, however, only the quadratic effect of ethanol-water ratio was found to be significant. The p values were given in the related sections. The observed results at the optimum points confirmed the accuracy of the models. The conventional extraction was also applied and it was found that higher extraction efficiencies are possible with pressurized extraction. As the produced extracts were not enough for the pilot plant PGSS-drying system, commercial extracts were used in the further work packages. Therefore, the characterization of extract

obtained at optimum conditions and the commercial extract were compared based on the HPLC measurements and similar anthocyanin profiles were found. The third work package included the investigation of encapsulation of black carrot extract in potato protein pectin complexes. Black carrot extract was also encapsulated in the matrix of potato protein without the citrus pectin to compare the effect of citrus pectin incorporation in the powder production. Hygroscopicity was substantially decreased in encapsulated black carrot extract powders compared to freeze dried black carrot extract. Emulsified core-particles had even lower hygroscopicity levels than non-emulsified core particles, however all particles were considered as non-hygroscopic according commercial criteria. Wall material concentration had an effect on particle size of emulsified core-particles, the higher concentration lowered the size and the ζ-potential of the particles. Encapsulation efficiency (%) was a bit higher when an emulsification procedure was incorporated, while the anthocyanin retention (%) decreased. The highest EE and AR value was found in NECP5 which was prepared at a wall material concentration of 3.5 % and a core material concentration of 2.5 %. Freeze dried BCE loaded PPI particles produced at the same protein and core material concentration and no significant difference ($p > 0.05$) was found between NECP5 and BCE-PPI. This was probably due to the interaction between potato protein and black carrot extract which was proved by the FT-IR characteristics. The DSC thermograms showed that, thermo-stability could be increased by the encapsulation of black carrot extract. Particle size value of black carrot extract loaded potato protein particles were much lower than that of particles formed with citrus pectin incorporation. In the last work package, PGSS-drying system was employed to produce black carrot extract loaded potato protein particles. Citrus pectin could not be incorporated in the encapsulation procedure as it almost solidifies the feed material which is not machinable. Moreover, the characterization results showed that the black carrot extract loaded potato protein particles were comparable for all characteristics to particles produced with citrus pectin incorporation and they had lower particle size values. This was probably due to chemical interaction between potato protein and black carrot extracts proved by the FT-IR spectra. The PGSS-drying was conducted under different independent variables which are nozzle size, pressure and temperature values. GLR and spray tower temperature was two independent variables affecting the characteristics of particles. Moisture decreased by increasing spray tower temperature, GLR was also effective to decrease the moisture content at similar spray tower

temperature values. Encapsulation efficiency decreased with increasing GLR, however, in general, particles showed high encapsulation efficiency values which are comparable to spray dried and freeze dried particles. Anthocyanin retention (%) of PGSS-dried particles was similar with freeze dried particles and higher than spray dried particles. The size of particles was about 10 μm which is acceptable regarding the food and drink applications. In general, PGSS-dried particles had more spherical shape than spray-dried particles. High GLR values negatively affected the spherical shape of PGSS-dried particles. Higher protection was observed for PGSS-dried particles than freeze and spray dried particles at the intestinal conditions which could be due to spherical structure of PGSS-dried particles obtained in SEM micrographs. The particles obtained with the highest GLR showed the lowest intestinal stability which was probably due to damaged spherical structure of particles.

In general, it was observed that sub- and supercritical CO_2 was employed successfully to derive black carrot extracts efficiently in comparison to conventional extraction and to encapsulate these extracts in the potato protein matrix with higher anthocyanin retention, a more spherical structure and higher bioavailability.

Further studies could be conducted on bioavailability of emulsified and non-emulsified core-particles formed with the incorporation of pectin. The produced powders could be incorporated in food models to determine the effect on texture, color and sensorial properties. The bioavailability of powders when incorporated in foods could also be studied. The shelf life kinetics could be revealed in further studies to observe the effect of encapsulation procedures on the storage stability of produced particles. Regarding the usage of PGSS-drying, high GLR values which leads to high CO_2 amounts could be a limitation. A feasibility study could be conducted to state the advantages of PGSS-drying over traditional spray-drying. However, it should be noted that, spray-drying used in this study was a lab scale system while the PGSS-drying was a pilot plant which could also affect the characteristics of particles. A spray-drying pilot plant system could be also employed to compare characteristics of PGSS-dried and spray dried particles especially the anthocyanin retention, particle morphology and particle size values.

REFERENCES

[1] **Kırca, A., Özkan, M., & Cemeroğlu, B.** (2007). Effects of temperature, solid content and pH on the stability of black carrot anthocyanins, *Food Chemistry, 101*(1), 212-218.

[2] **Santos, D.T. & Meireles, M.a.A.** (2011). Optimization of bioactive compounds extraction from jabuticaba (Myrciaria cauliflora) skins assisted by high pressure CO2, *Innovative Food Science & Emerging Technologies, 12*(3), 398-406.

[3] **Nesterenko, A., Alric, I., Silvestre, F., & Durrieu, V.** (2013). Vegetable proteins in microencapsulation: A review of recent interventions and their effectiveness, *Industrial Crops and Products, 42*, 469-479.

[4] **Charlton, A.J., Baxter, N.J., Khan, M.L., Moir, A.J., Haslam, E., Davies, A.P., & Williamson, M.P.** (2002). Polyphenol/peptide binding and precipitation, *Journal of Agricultural and Food Chemistry, 50*(6), 1593-1601.

[5] **Prigent, S., Voragen, A., Van Koningsveld, G., Baron, A., Renard, C., & Gruppen, H.** (2009). Interactions between globular proteins and procyanidins of different degrees of polymerization, *Journal of Dairy Science, 92*(12), 5843-5853.

[6] **Haslam, E.** (1996). Natural polyphenols (vegetable tannins) as drugs: possible modes of action, *Journal of Natural Products, 59*(2), 205-215.

[7] **Pasquali, I. & Bettini, R.** (2008). Are pharmaceutics really going supercritical?, *International Journal of Pharmaceutics, 364*(2), 176-187.

[8] **Cocero, M.J., Martín, Á., Mattea, F., & Varona, S.** (2009). Encapsulation and co-precipitation processes with supercritical fluids: fundamentals and applications, *The Journal of Supercritical Fluids, 47*(3), 546-555.

[9] **Knez, Z. & Weidner, E.** (2003). Particles formation and particle design using supercritical fluids, *Current Opinion in Solid State and Materials Science, 7*(4-5), 353-361.

[10] **Karaca, A.C., Low, N., & Nickerson, M.** (2015). Potential use of plant proteins in the microencapsulation of lipophilic materials in foods, *Trends in Food Science & Technology, 42*(1), 5-12.

[11] **Erkey, C.** (2011). *Supercritical fluids and organometallic compounds: from recovery of trace metals to synthesis of nanostructured materials*: Elsevier.

[12] **Witkowski, A., Majkut, M., & Rulik, S.** (2014). Analysis of pipeline transportation systems for carbon dioxide sequestration, *Archives of Thermodynamics, 35*(1), 117--140.

[13] **Reid, R.C., Prausnitz, J.M., & Poling, B.E.** (1987). *The properties of gases and liquids.*

[14] **Pascual, C.D. & Subra-Paternault, P.** (2015). *Supercritical Fluid Nano-technology: Advances and Applications in Composites and Hybrid Nanomaterials*: CRC Press.

[15] **Perrut, M.** (2000). Supercritical fluid applications: industrial developments and economic issues, *Industrial & Engineering Chemistry Research, 39*(12), 4531-4535.

[16] **Da Ponte, M.N. & Zakrzewska, M.E.** (2016). Volumetric and phase behaviour of mixtures of fluoroalkylphosphate-based ionic liquids with high pressure carbon dioxide, *The Journal of Supercritical Fluids, 113*, 61-65.

[17] **Budisa, N. & Schulze-Makuch, D.** (2014). Supercritical carbon dioxide and its potential as a life-sustaining solvent in a planetary environment, *Life, 4*(3), 331-340.

[18] **Celiktas, O.Y., Bedir, E., & Sukan, F.V.** (2007). In vitro antioxidant activities of Rosmarinus officinalis extracts treated with supercritical carbon dioxide, *Food Chemistry, 101*(4), 1457-1464.

[19] **Sapkale, G., Patil, S., Surwase, U., & Bhatbhage, P.** (2010). Supercritical fluid extraction, *International Journal of Chemical Science, 8*(2), 729-743.

[20] **Mohamed, R.S. & Mansoori, G.A.** (2002). The use of supercritical fluid extraction technology in food processing, *Food Technology Magazine, 20*(7), 134-139.

[21] **Eggers, R., Ambrogi, A., & Schnitzler, J.V.** (2000). Special features of SCF solid extraction of natural products: deoiling of wheat gluten and extraction of rose hip oil, *Brazilian Journal of Chemical Engineering, 17*, 329-334.

[22] **Lang, Q. & Wai, C.M.** (2001). Supercritical fluid extraction in herbal and natural product studies—a practical review, *Talanta, 53*(4), 771-782.

[23] **González, J.C., Fontal, O.I., Vieytes, M.R., Vieites, J.M., & Botana, L.M.** (2002). Basis for a new procedure to eliminate diarrheic shellfish toxins from a contaminated matrix, *Journal of Agricultural and Food Chemistry, 50*(2), 400-405.

[24] **Ibanez, E., Palacios, J., Senorans, F., Santa-Maria, G., Tabera, J., & Reglero, G.** (2000). Isolation and separation of tocopherols from olive by-products with supercritical fluids, *Journal of the American Oil Chemists' Society, 77*(2), 187-190.

[25] **Osborne, J.** (2014). *Handbook on Supercritical Fluids:Fundamentals, Properties and Applications*: Nova Science Publishers, Incorporated.

[26] **Gaonkar, A., Vasisht, N., Khare, A., & Sobel, R.** (2014). *Microencapsulation in the Food Industry*: Elsevier.

[27]**Zuidam, N.J. & Nedovic, V.** (2010). Encapsulation technologies for active food ingredients and food processing.

[28] **Gibbs, F., Kermesha, S., Alli, I., Catherina, N., & Mulligan, B.** (1999). Encapsulation in the food industry: a review, *International Journal of Food Sciences and Nutrition, 50*(3), 213-224. doi:10.1080/096374899101256

[29] **Jyothi, N.V.N., Prasanna, P.M., Sakarkar, S.N., Prabha, K.S., Ramaiah, P.S., & Srawan, G.** (2010). Microencapsulation techniques, factors influencing encapsulation efficiency, *Journal of Microencapsulation, 27*(3), 187-197.

[30] **Timilsena, Y.P., Akanbi, T.O., Khalid, N., Adhikari, B., & Barrow, C.J.** (2019). Complex coacervation: Principles, mechanisms and applications in microencapsulation, *International journal of biological macromolecules, 121*, 1276-1286.

[31] **Piacentini, E.** (2016). Coacervation, *Encyclopedia of Membranes*, 422-424.

[32] **Fahrurrozi, M. & Wirawan, S.** (2016). Microencapsulation technology of ginger oleoresin with chitosan as wall material: A review, *Journal of Applied Pharmaceutical Science, 6*(12), 209-223.

[33] **Tayebi, L. & Moharamzadeh, K.** (2017). *Biomaterials for oral and dental tissue engineering*: Woodhead Publishing.

[34] **Feguš, U., Žigon, U., Petermann, M., & Knez, Ž.** (2015). Effect of drying parameters on physiochemical and sensory properties of fruit powders processed by PGSS-, Vacuum-and Spray-drying, *Acta Chimica Slovenica, 62*(2), 479-487.

[35] **Đorđević, V., Balanč, B., Belščak-Cvitanović, A., Lević, S., Trifković, K., Kalušević, A., . . . Nedović, V.** (2015). Trends in encapsulation technologies for delivery of food bioactive compounds, *Food Engineering Reviews, 7*(4), 452-490.

[36] **Assadpour, E. & Jafari, S.M.** (2019). Advances in spray-drying encapsulation of food bioactive ingredients: From microcapsules to nanocapsules, *Annual Review of Food Science and Technology, 10*, 103-131.

[37] **Martín, Á. & Weidner, E.** (2010). PGSS-drying: Mechanisms and modeling, *The Journal of Supercritical Fluids, 55*(1), 271-281.

[38] **Baranski, R., Maksylewicz-Kaul, A., Nothnagel, T., Cavagnaro, P.F., Simon, P.W., & Grzebelus, D.** (2012). Genetic diversity of carrot (Daucus carota L.) cultivars revealed by analysis of SSR loci, *Genetic resources and crop evolution, 59*(2), 163-170.

[39] **Simon, P., Rubatzky, V., Bassett, M., Strandberg, J., & White, J.** (1997). B7262, purple carrot inbred, *HortScience, 32*(1), 146-147.

[40] **Montilla, E.C., Arzaba, M.R., Hillebrand, S., & Winterhalter, P.** (2011). Anthocyanin composition of black carrot (Daucus carota ssp. sativus var. atrorubens Alef.) cultivars Antonina, Beta Sweet, Deep Purple, and Purple Haze, *Journal of Agricultural and Food Chemistry, 59*(7), 3385-3390.

[41] **Kirca, A., Özkan, M., & Cemeroglu, B.** (2003). Thermal stability of black carrot anthocyanins in blond orange juice, *Journal of Food Quality, 26*(5), 361-366.

[42] **Waglay, A., Karboune, S., & Alli, I.** (2014). Potato protein isolates: Recovery and characterization of their properties, *Food Chemistry, 142*, 373-382.

[43] **Schäfer, D., Reinelt, M., Stäbler, A., & Schmid, M.** (2018). Mechanical and barrier properties of potato protein isolate-based films, *Coatings, 8*(2), 58.

[44] **Schols, H.A. & Voragen, A.G.** (1994). Occurrence of pectic hairy regions in various plant cell wall materials and their degradability by rhamnogalacturonase, *Carbohydrate Research, 256*(1), 83-95.

[45] **Willats, W.G., Knox, J.P., & Mikkelsen, J.D.** (2006). Pectin: new insights into an old polymer are starting to gel, *Trends in Food Science & Technology, 17*(3), 97-104.

[46] **Salminen, H. & Weiss, J.** (2014). Effect of pectin type on association and pH stability of whey protein—pectin complexes, *Food Biophysics, 9*(1), 29-38.

[47] **Daas, P.J., Meyer-Hansen, K., Schols, H.A., De Ruiter, G.A., & Voragen, A.G.** (1999). Investigation of the non-esterified galacturonic acid distribution in pectin with endopolygalacturonase, *Carbohydrate Research, 318*(1-4), 135-145.

[48] **Chang, P.G., Gupta, R., Timilsena, Y.P., & Adhikari, B.** (2016). Optimisation of the complex coacervation between canola protein isolate and chitosan, *Journal of Food Engineering, 191*, 58-66.

[49] **Schmitt, C. & Turgeon, S.L.** (2011). Protein/polysaccharide complexes and coacervates in food systems, *Advances in Colloid and Interface Science, 167*(1-2), 63-70.

[50] **Liu, S., Cao, Y.-L., Ghosh, S., Rousseau, D., Low, N.H., & Nickerson, M.T.** (2010). Intermolecular interactions during complex coacervation of pea protein isolate and gum Arabic, *Journal of Agricultural and Food Chemistry, 58*(1), 552-556.

[51] **Moschakis, T. & Biliaderis, C.G.** (2017). Biopolymer-based coacervates: Structures, functionality and applications in food products, *Current Opinion in Colloid & Interface Science, 28*, 96-109.

[52] **Zeeb, B., Yavuz-Düzgun, M., Dreher, J., Evert, J., Stressler, T., Fischer, L., . . . Weiss, J.** (2018). Modulation of the bitterness of pea and potato proteins by a complex coacervation method, *Food & function, 9*(4), 2261-2269.

[53] **Mendanha, D.V., Ortiz, S.E.M., Favaro-Trindade, C.S., Mauri, A., Monterrey-Quintero, E.S., & Thomazini, M.** (2009). Microencapsulation of casein hydrolysate by complex coacervation with SPI/pectin, *Food Research International, 42*(8), 1099-1104.

[54] **Sipos, E. & Foster, L.** (1992). Dietary Trends for Vegetable Proteins in Foods. In *Dietary Proteins* (pp. 243-282): AOCS Publishing.

[55] **Young, V.R. & Pellett, P.L.** (1994). Plant proteins in relation to human protein and amino acid nutrition, *The American journal of clinical nutrition, 59*(5), 1203S-1212S.

[56] **Friedman, M.** (1996). Nutritional value of proteins from different food sources. A review, *Journal of Agricultural and Food Chemistry, 44*(1), 6-29.

[57] **Jackman, R.L. & Yada, R.Y.** (1988). Functional properties of whey-potato protein composite blends in a model system, *Journal of Food Science, 53*(5), 1427-1432.

[58] **Kaldy, M.S.** (1972). Protein yield of various crops as related to protein value, *Economic Botany, 26*(2), 142-144. doi:10.1007/bf02860775

[59] **Kapoor, A.C., Desborough, S.L., & Li, P.H.** (1975). Potato tuber proteins and their nutritional quality, *Potato Research, 18*(3), 469-478. doi:10.1007/bf02361913

[60] **Stounbjerg, L., Vestergaard, C., Andreasen, B., & Ipsen, R.** (2019). Associative phase separation of potato protein and anionic polysaccharides, *Colloids and Surfaces A: Physicochemical and Engineering Aspects, 566*, 104-112.

[61] **Løkra, S. & Strætkvern, K.O.** (2009). Industrial proteins from potato juice. A review, *Food, 3*(1), 88-95.

[62] **Schols, H.A. & Voragen, A.G.J.** (1994). Occurrence of pectic hairy regions in various plant cell wall materials and their degradability by rhamnogalacturonase, *Carbohydrate Research, 256*(1), 83-95.

[63] **Willats, W.G.T., Knox, P., & Mikkelsen, J.D.** (2006). Pectin: new insights into an old polymer are starting to gel, *Trends in Food Science & Technology, 17*(3), 97-104.

[64] **Morr, C., German, B., Kinsella, J., Regenstein, J., Buren, J.V., Kilara, A., . . . Mangino, M.** (1985). A collaborative study to develop a standardized food protein solubility procedure, *Journal of Food Science, 50*(6), 1715-1718.

[65] **Bradford, M.M.** (1976). A rapid and sensitive method for the quantitation of microgram quantities of protein utilizing the principle of protein-dye binding, *Analytical Biochemistry, 72*(1), 248-254.

[66] **Tang, C. H. & Sun, X.** (2011). A comparative study of physicochemical and conformational properties in three vicilins from Phaseolus legumes: Implications for the structure–function relationship, *Food Hydrocolloids, 25*(3), 315-324.

[67] **Du, Y., Chen, F., Zhang, Y., Rempel, C., Thompson, M.R., & Liu, Q.** (2015). Potato protein isolate-based biopolymers, *Journal of Applied Polymer Science, 132*(44).

[68] **Yin, S.-W., Chen, J.C., Sun, S.D., Tang, C.-H., Yang, X.Q., Wen, Q.B., & Qi, J.R.** (2011). Physicochemical and structural characterisation of protein isolate, globulin and albumin from soapnut seeds (Sapindus mukorossi Gaertn.), *Food Chemistry, 128*(2), 420-426.

[69] **Mcclements, D.J.** (2004). Protein-stabilized emulsions, *Current Opinion in Colloid & Interface Science, 9*(5), 305-313.

[70] **Townend, R., Winterbottom, R.J., & Timasheff, S.N.** (1960). Molecular Interactions in β-Lactoglobulin. II. Ultracentrifugal and Electrophoretic Studies of the Association of β-Lactoglobulin below its Isoelectric Point, *Journal of the American Chemical Society, 82*(12), 3161-3168.

[71] **Yang, Y., Leser, M.E., Sher, A.A., & Mcclements, D.J.** (2013). Formation and stability of emulsions using a natural small molecule surfactant: Quillaja saponin (Q-Naturale®), *Food Hydrocolloids, 30*(2), 589-596.

[72] **Krzeminski, A., Prell, K.A., Weiss, J., & Hinrichs, J.** (2014). Environmental response of pectin-stabilized whey protein aggregates, *Food Hydrocolloids, 35*, 332-340.

[73] **Wang, X., Chen, Q., & Lü, X.** (2014). Pectin extracted from apple pomace and citrus peel by subcritical water, *Food Hydrocolloids, 38*, 129-137.

[74] **Lutz, R., Aserin, A., Wicker, L., & Garti, N.** (2009). Structure and physical properties of pectins with block-wise distribution of carboxylic acid groups, *Food Hydrocolloids, 23*(3), 786-794.

[75] **Turgeon, S., Schmitt, C., & Sanchez, C.** (2007). Protein–polysaccharide complexes and coacervates, *Current Opinion in Colloid & Interface Science, 12*(4-5), 166-178.

[76] **Weinbreck, F., De Vries, R., Schrooyen, P., & De Kruif, C.** (2003). Complex coacervation of whey proteins and gum arabic, *Biomacromolecules, 4*(2), 293-303.

[77] **Ye, A.** (2008). Complexation between milk proteins and polysaccharides via electrostatic interaction: principles and applications–a review, *International Journal of Food Science & Technology, 43*(3), 406-415.

[78] **Sanchez, C., Mekhloufi, G., Schmitt, C., Renard, D., Robert, P., Lehr, C.-M., . . . Hardy, J.** (2002). Self-assembly of β-lactoglobulin and acacia gum in aqueous solvent: structure and phase-ordering kinetics, *Langmuir, 18*(26), 10323-10333.

[79] **Kim, Y. & Wicker, L.** (2011). Charge domain of modified pectins influence interaction with acidified caseins, *Food Hydrocolloids, 25*(3), 419-425.

[80] **Ducel, V., Richard, J., Saulnier, P., Popineau, Y., & Boury, F.** (2004). Evidence and characterization of complex coacervates containing plant proteins: application to the microencapsulation of oil droplets, *Colloids and Surfaces A: Physicochemical and Engineering Aspects, 232*(2-3), 239-247.

[81] **Einhorn-Stoll, U., Salazar, T., Jaafar, B., & Kunzek, H.** (2001). Thermodynamic compatibility of sodium caseinate with different pectins. Influence of the milieu conditions and pectin modifications, *Food/Nahrung, 45*(5), 332-337.

[82] **Nordmark, T. & Ziegler, G.R.** (2000). Quantitative assessment of phase composition and morphology of two-phase gelatin–pectin gels using fluorescence microscopy, *Food Hydrocolloids, 14*(6), 579-590.

[83] **Einhorn-Stoll, U., Salazar, T., Jaafar, B., & Kunzek, H.** (2001). Thermodynamic compatibility of sodium caseinate with, different pectins. Influence of the milieu conditions and pectin modifications, *Nahrung-Food, 45*(5), 332-337.

[84] **Hans-Ulrich, E., Frank, M., & Karl, N.** (2005). Pectins. In *Handbook of Food Science, Technology, and Engineering*: CRC Press.

[85] **Antonov, Y.A., Celus, M., Kyomugasho, C., Hendrickx, M., Moldenaers, P., & Cardinaels, R.** (2019). Complexation of pectins varying in overall charge with lysozyme in aqueous buffered solutions, *Food Hydrocolloids, 94*, 268-278.

[86] **Powell, D., Morris, E., Gidley, M., & Rees, D.** (1982). Conformations and interactions of pectins: II. Influence of residue sequence on chain association in calcium pectate gels, *Journal of Molecular Biology, 155*(4), 517-531.

[87] **Kohn, R., Markovič, O., & Machová, E.** (1983). Deesterification mode of pectin by pectin esterases of Aspergillus foetidus, tomatoes and alfalfa, *Collection of Czechoslovak Chemical Communications, 48*(3), 790-797.

[88] **Thibault, J. & Rinaudo, M.** (1985). Interactions of mono-and divalent counterions with alkali-and enzyme-deesterified pectins in salt-free solutions, *Biopolymers: Original Research on Biomolecules, 24*(11), 2131-2143.

[89] **Ralet, M.-C., Dronnet, V., Buchholt, H.C., & Thibault, J.-F.** (2001). Enzymatically and chemically de-esterified lime pectins: characterisation, polyelectrolyte behaviour and calcium binding properties, *Carbohydrate Research, 336*(2), 117-125.

[90] **Löfgren, C., Guillotin, S., Evenbratt, H., Schols, H., & Hermansson, A.-M.** (2005). Effects of calcium, pH, and blockiness on kinetic rheological behavior and microstructure of HM pectin gels, *Biomacromolecules, 6*(2), 646-652.

[91] **Limberg, G., Körner, R., Buchholt, H.C., Christensen, T.M., Roepstorff, P., & Mikkelsen, J.D.** (2000). Analysis of different de-esterification mechanisms for pectin by enzymatic fingerprinting using endopectin lyase and endopolygalacturonase II from A. niger, *Carbohydrate Research, 327*(3), 293-307.

[92] **Rolin, C.** (2002). Commercial pectin preparations, Pectins and their manipulation, 222-241.

[93] **Sperber, B.L., Schols, H.A., Stuart, M.a.C., Norde, W., & Voragen, A.G.** (2009). Influence of the overall charge and local charge density of pectin on the complex formation between pectin and β-lactoglobulin, *Food Hydrocolloids, 23*(3), 765-772.

[94] **Warnakulasuriya, S., Pillai, P.K., Stone, A.K., & Nickerson, M.T.** (2018). Effect of the degree of esterification and blockiness on the complex coacervation of pea protein isolate and commercial pectic polysaccharides, *Food Chemistry, 264*, 180-188.

[95] **Zeeb, B., Mi-Yeon, L., Gibis, M., & Weiss, J.** (2018). Growth phenomena in biopolymer complexes composed of heated WPI and pectin, *Food Hydrocolloids, 74*, 53-61.

[96] **Buchweitz, M., Speth, M., Kammerer, D., & Carle, R.** (2013). Impact of pectin type on the storage stability of black currant (Ribes nigrum L.) anthocyanins in pectic model solutions, *Food Chemistry, 139*(1-4), 1168-1178.

[97] **Nasseri, A.T., Thibault, J.-F., & Ralet, M.-C.** (2008). Citrus Pectin: Structure and Application in Acid Dairy Drinks, *Tree Science and Biotechnology, 2*, 60-70.

[98] **Renard, C.M., Crépeau, M.-J., & Thibault, J.-F.** (1995). Structure of the repeating units in the rhamnogalacturonic backbone of apple, beet and citrus pectins, *Carbohydrate Research, 275*(1), 155-165.

[99] **Kammerer, D., Carle, R., & Schieber, A.** (2004). Quantification of anthocyanins in black carrot extracts (Daucus carota ssp. sativus var. atrorubens Alef.) and evaluation of their color properties, *European Food Research and Technology, 219*(5), 479-486.

[100] **Pala, C., Sevimli-Gur, C., & Yesil-Celiktas, O.** (2017). Green extraction processes focusing on maximization of black carrot anthocyanins along with cytotoxic activities, *Food Analytical Methods, 10*(2), 529-538.

[101] **Ghafoor, K., Park, J., & Choi, Y.-H.** (2010). Optimization of supercritical fluid extraction of bioactive compounds from grape (Vitis labrusca B.) peel by using response surface methodology, *Innovative Food Science & Emerging Technologies, 11*(3), 485-490.

[102] **Da Porto, C., Natolino, A., & Decorti, D.** (2014). Extraction of proanthocyanidins from grape marc by supercritical fluid extraction using CO2 as solvent and ethanol–water mixture as co-solvent, *The Journal of Supercritical Fluids, 87*, 59-64.

[103] **Ahmadian-Kouchaksaraie, Z. & Niazmand, R.** (2017). Supercritical carbon dioxide extraction of antioxidants from Crocus sativus petals of saffron industry residues: Optimization using response surface methodology, *The Journal of Supercritical Fluids, 121*, 19-31.

[104] **Seabra, I.J., Braga, M.E.M., Batista, M.T., & De Sousa, H.C.** (2010). Effect of solvent (CO2/ethanol/H2O) on the fractionated enhanced solvent extraction of anthocyanins from elderberry pomace, *The Journal of Supercritical Fluids, 54*(2), 145-152.

[105] **Shi, J., Xue, S.J., & Quek, S.Y.** (2015). Solubility of Food Components in the Supercritical-CO2 Fluid Process, *Functional Food Ingredients and Nutraceuticals: Processing Technologies, 13*, 53.

[106] **Serra, A.T., Seabra, I.J., Braga, M.E., Bronze, M., De Sousa, H.C., & Duarte, C.M.** (2010). Processing cherries (Prunus avium) using supercritical fluid technology. Part 1: Recovery of extract fractions rich in bioactive compounds, *The Journal of Supercritical Fluids, 55*(1), 184-191.

[107] **Silva, S., Costa, E., Calhau, C., Morais, R., & Pintado, M.** (2017). Anthocyanin extraction from plant tissues: A review, *Critical Reviews in Food Science and Nutrition*, *57*(14), 3072-3083.

[108] **Paes, J., Dotta, R., Barbero, G.F., & Martínez, J.** (2014). Extraction of phenolic compounds and anthocyanins from blueberry (Vaccinium myrtillus L.) residues using supercritical CO2 and pressurized liquids, *The Journal of Supercritical Fluids, 95*, 8-16.

[109] **Kühn, S. & Temelli, F.** (2017). Recovery of bioactive compounds from cranberry pomace using ternary mixtures of CO2+ ethanol+ water, *The Journal of Supercritical Fluids, 130*, 147-155.

[110] **Chatterjee, D., Jadhav, N.T., & Bhattacharjee, P.** (2013). Solvent and supercritical carbon dioxide extraction of color from eggplants: Characterization and food applications, *LWT-Food Science and Technology*, *51*(1), 319-324.

[111] **Monroy, Y.M., Rodrigues, R.A., Sartoratto, A., & Cabral, F.A.** (2016). Influence of ethanol, water, and their mixtures as co-solvents of the supercritical carbon dioxide in the extraction of phenolics from purple corn cob (Zea mays L.), *The Journal of Supercritical Fluids, 118*, 11-18.

[112] **Paula, J.T., Paviani, L.C., Foglio, M.A., Sousa, I.M., & Cabral, F.A.** (2013). Extraction of anthocyanins from Arrabidaea chica in fixed bed using CO2 and CO2/ethanol/water mixtures as solvents, *The Journal of Supercritical Fluids, 81*, 33-41.

[113] **Reátegui, J.L.P., Da Fonseca Machado, A.P., Barbero, G.F., Rezende, C.A., & Martínez, J.** (2014). Extraction of antioxidant compounds from blackberry (Rubus sp.) bagasse using supercritical CO2 assisted by ultrasound, *The Journal of Supercritical Fluids, 94*, 223-233.

[114] **Vatai, T., Škerget, M., & Knez, Ž.** (2009). Extraction of phenolic compounds from elder berry and different grape marc varieties using organic solvents and/or supercritical carbon dioxide, *Journal of Food Engineering, 90*(2), 246-254.

[115] **Guldiken, B., Boyacioglu, D., & Capanoglu, E.** (2016). Optimization of extraction of bioactive compounds from black carrot using response surface methodology (RSM), *Food Analytical Methods, 9*(7), 1876-1886.

[116] **Span, R., Beckmüller, R., Eckermann, T., Herrig, S., Hielscher, S., Jäger, A., . . . Semrau, B.** (2019). *TREND. Thermodynamic Reference and Engineering Data 4.0.*

[117] **Agcam, E., Akyıldız, A., & Balasubramaniam, V.** (2017). Optimization of anthocyanins extraction from black carrot pomace with thermosonication, *Food Chemistry, 237*, 461-470.

[118] **Chandra, A., Rana, J., & Li, Y.** (2001). Separation, identification, quantification, and method validation of anthocyanins in botanical supplement raw materials by HPLC and HPLC− MS, *Journal of Agricultural and Food Chemistry*, *49*(8), 3515-3521.

[119] **Bouayed, J., Hoffmann, L., & Bohn, T.** (2011). Total phenolics, flavonoids, anthocyanins and antioxidant activity following simulated gastro-intestinal digestion and dialysis of apple varieties: Bioaccessibility and potential uptake, *Food Chemistry, 128*(1), 14-21.

[120] **Kumaran, A. & Karunakaran, R.J.** (2006). Nitric oxide radical scavenging active components from Phyllanthus emblica L, *Plant Foods for Human Nutrition, 61*(1), 1.

[121] **Apak, R., Güçlü, K., Özyürek, M., & Karademir, S.E.** (2004). Novel total antioxidant capacity index for dietary polyphenols and vitamins C and E, using their cupric ion reducing capability in the presence of neocuproine: CUPRAC method, *Journal of Agricultural And Food Chemistry, 52*(26), 7970-7981.

[122] **Adil, I.H., Cetin, H., Yener, M., & Bayındırlı, A.** (2007). Subcritical (carbon dioxide+ ethanol) extraction of polyphenols from apple and peach pomaces, and determination of the antioxidant activities of the extracts, *The Journal Of Supercritical Fluids, 43*(1), 55-63.

[123] **Paula, J.T., Paviani, L.C., Foglio, M.A., Sousa, I.M., Duarte, G.H., Jorge, M.P., . . . Cabral, F.A.** (2014). Extraction of anthocyanins and luteolin from Arrabidaea chica by sequential extraction in fixed bed using supercritical CO2, ethanol and water as solvents, *The Journal of Supercritical Fluids, 86*, 100-107.

[124] **Mantell, C., Rodríguez, M., & Martinez De La Ossa, E.** (2003). A screening analysis of the high-pressure extraction of anthocyanins from red grape pomace with carbon dioxide and cosolvent, *Engineering in Life Sciences, 3*(1), 38-42.

[125] **Goyal, M.R. & Suleria, H.a.R.** (2019). *Human health benefits of plant bioactive compounds: potentials and prospects*: CRC Press.

[126] **Maran, J.P., Priya, B., & Manikandan, S.** (2014). Modeling and optimization of supercritical fluid extraction of anthocyanin and phenolic compounds from Syzygium cumini fruit pulp, *Journal of Food Science and Technology, 51*(9), 1938-1946.

[127] **He, B., Zhang, L.-L., Yue, X.-Y., Liang, J., Jiang, J., Gao, X.-L., & Yue, P.-X.** (2016). Optimization of Ultrasound-Assisted Extraction of phenolic compounds and anthocyanins from blueberry (Vaccinium ashei) wine pomace, *Food Chemistry, 204*, 70-76.

[128] **Espada-Bellido, E., Ferreiro-González, M., Carrera, C., Palma, M., Barroso, C.G., & Barbero, G.F.** (2017). Optimization of the ultrasound-assisted extraction of anthocyanins and total phenolic compounds in mulberry (Morus nigra) pulp, *Food Chemistry, 219*, 23-32.

[129] **Garcia-Mendoza, M., Espinosa-Pardo, F.A., Baseggio, A.M., Barbero, G.F., Marostica, M., Rostagno, M.A., & Martinez, J.** (2017). Extraction of phenolic compounds and anthocyanins from juçara (Euterpe edulis Mart.) residues using pressurized liquids and supercritical fluids, *Journal of Supercritical Fluids, 119*, 9-16.

[130] **Cacace, J. & Mazza, G.** (2003). Mass transfer process during extraction of phenolic compounds from milled berries, *Journal of Food Engineering, 59*(4), 379-389.

[131] **Yılmaz, F.M. & Ersus Bilek, S.** (2018). Ultrasound-assisted vacuum impregnation on the fortification of fresh-cut apple with calcium and black carrot phenolics, *Ultrasonics Sonochemistry, 48*, 509-516.

[132] **Roy, B.C., Goto, M., & Hirose, T.** (1996). Extraction of Ginger Oil with Supercritical Carbon Dioxide: Experiments and Modeling, *Industrial & Engineering Chemistry Research, 35*(2), 607-612.

[133] **Murga, R., Sanz, M.a.T., Beltrán, S., & Cabezas, J.L.** (2003). Solubility of three hydroxycinnamic acids in supercritical carbon dioxide, *The Journal of Supercritical Fluids, 27*(3), 239-245.

[134] **Durling, N.E., Catchpole, O.J., Tallon, S.J., & Grey, J.B.** (2007). Measurement and modelling of the ternary phase equilibria for high pressure carbon dioxide–ethanol–water mixtures, *Fluid Phase Equilibria, 252*(1-2), 103-113.

[135] **Lim, J.S., Lee, Y.Y., & Chun, H.S.** (1994). Phase equilibria for carbon dioxide-ethanol-water system at elevated pressures, *The Journal of Supercritical Fluids, 7*(4), 219-230.

[136] **Kerbstadt, S., Eliasson, L., Mustafa, A., & Ahrné, L.** (2015). Effect of novel drying techniques on the extraction of anthocyanins from bilberry press cake using supercritical carbon dioxide, *Innovative Food Science & Emerging Technologies, 29*, 209-214.

[137] **Truong, V.D., Hu, Z., Thompson, R.L., Yencho, G.C., & Pecota, K.V.** (2012). Pressurized liquid extraction and quantification of anthocyanins in purple-fleshed sweet potato genotypes, *Journal of Food Composition and Analysis, 26*(1), 96-103.

[138] **Bilek, S.E., Yılmaz, F.M., & Özkan, G.** (2017). The effects of industrial production on black carrot concentrate quality and encapsulation of anthocyanins in whey protein hydrogels, *Food and Bioproducts Processing, 102*, 72-80.

[139] **Jizomoto, H., Kanaoka, E., Sugita, K., & Hirano, K.** (1993). Gelatin-acacia microcapsules for trapping micro oil droplets containing lipophilic drugs and ready disintegration in the gastrointestinal tract, *Pharmaceutical Research, 10*(8), 1115-1122.

[140] **Junyaprasert, V.B., Mitrevej, A., Sinchaipanid, N., Boonme, P., & Wurster, D.E.** (2001). Effect of process variables on the microencapsulation of vitamin A palmitate by gelatin-acacia coacervation, *Drug Development and Industrial Pharmacy, 27*(6), 561-566.

[141] **Ammala, A.** (2013). Biodegradable polymers as encapsulation materials for cosmetics and personal care markets, *International Journal of Cosmetic Science, 35*(2), 113-124.

[142] **Wang, B., Adhikari, B., & Barrow, C.J.** (2014). Optimisation of the microencapsulation of tuna oil in gelatin–sodium hexametaphosphate using complex coacervation, *Food Chemistry, 158*, 358-365.

[143] **Gu, X.-L., Zhu, X., Kong, X.-Z., & Tan, Y.** (2010). Comparisons of simple and complex coacervations for preparation of sprayable insect sex pheromone microcapsules and release control of the encapsulated pheromone molecule, *Journal of Microencapsulation, 27*(4), 355-364.

[144] **Leclercq, S., Harlander, K.R., & Reineccius, G.A.** (2009). Formation and characterization of microcapsules by complex coacervation with liquid or solid aroma cores, *Flavour and Fragrance Journal, 24*(1), 17-24.

[145] **Kang, A., Park, J., Ju, J., Jeong, G.S., & Lee, S.-H.** (2014). Cell encapsulation via microtechnologies, *Biomaterials, 35*(9), 2651-2663.

[146] **Guo, H., Zhao, X., & Wang, J.** (2005). The relation between narrow-dispersed microcapsules and surfactants, *Journal of Microencapsulation, 22*(8), 853-862.

[147] **Zaera, F.** (2013). Nanostructured materials for applications in heterogeneous catalysis, *Chemical Society Reviews, 42*(7), 2746-2762.

[148] **Gouin, S.** (2004). Microencapsulation: industrial appraisal of existing technologies and trends, *Trends in Food Science & Technology, 15*(7-8), 330-347.

[149] **Comunian, T.A., Thomazini, M., Alves, A.J.G., De Matos Junior, F.E., De Carvalho Balieiro, J.C., & Favaro-Trindade, C.S.** (2013). Microencapsulation of ascorbic acid by complex coacervation: Protection and controlled release, *Food Research International, 52*(1), 373-379.

[150] **Calderón-Oliver, M., Pedroza-Islas, R., Escalona-Buendía, H.B., Pedraza-Chaverri, J., & Ponce-Alquicira, E.** (2017). Comparative study of the microencapsulation by complex coacervation of nisin in combination with an avocado antioxidant extract, *Food Hydrocolloids, 62*, 49-57.

[151] **De Souza, V.B., Thomazini, M., Barrientos, M.a.E., Nalin, C.M., Ferro-Furtado, R., Genovese, M.I., & Favaro-Trindade, C.S.** (2018). Functional properties and encapsulation of a proanthocyanidin-rich cinnamon extract (Cinnamomum zeylanicum) by complex coacervation using gelatin and different polysaccharides, *Food Hydrocolloids, 77*, 297-306.

[152] **Ge, J., Yue, P., Chi, J., Liang, J., & Gao, X.** (2018). Formation and stability of anthocyanins-loaded nanocomplexes prepared with chitosan hydrochloride and carboxymethyl chitosan, *Food Hydrocolloids, 74*, 23-31.

[153] **Yamashita, C., Chung, M.M.S., Dos Santos, C., Mayer, C.R.M., Moraes, I.C.F., & Branco, I.G.** (2017). Microencapsulation of an anthocyanin-rich blackberry (Rubus spp.) by-product extract by freeze-drying, *LWT, 84*, 256-262.

[154] **Tan, C., Celli, G.B., & Abbaspourrad, A.** (2018). Copigment-polyelectrolyte complexes (PECs) composite systems for anthocyanin stabilization, *Food Hydrocolloids, 81*, 371-379.

[155] **Li, H., Zhu, K., Zhou, H., & Peng, W.** (2012). Effects of high hydrostatic pressure treatment on allergenicity and structural properties of soybean protein isolate for infant formula, *Food Chemistry, 132*(2), 808-814.

[156] **Cai, Y.-Z. & Corke, H.** (2000). Production and properties of spray-dried Amaranthus betacyanin pigments, *Journal of Food Science, 65*(7), 1248-1252.

[157] **Giusti, M.M. & Wrolstad, R.E.** (2001). Characterization and measurement of anthocyanins by UV-visible spectroscopy, *Current Protocols In Food Analytical Chemistry* (1), F1. 2.1-F1. 2.13.

[158] **Da Silva Carvalho, A.G., Da Costa Machado, M.T., Da Silva, V.M., Sartoratto, A., Rodrigues, R.a.F., & Hubinger, M.D.** (2016). Physical properties and morphology of spray dried microparticles containing anthocyanins of jussara (Euterpe edulis Martius) extract, *Powder Technology, 294*, 421-428.

[159] **Davidov-Pardo, G., Arozarena, I., & Marín-Arroyo, M.R.** (2013). Optimization of a wall material formulation to microencapsulate a grape seed extract using a mixture design of experiments, *Food and Bioprocess Technology, 6*(4), 941-951.

[160] **Shaddel, R., Hesari, J., Azadmard-Damirchi, S., Hamishehkar, H., Fathi-Achachlouei, B., & Huang, Q.** (2018). Double emulsion followed by complex coacervation as a promising method for protection of black raspberry anthocyanins, *Food Hydrocolloids, 77*, 803-816.

[161] **Rocha-Selmi, G.A., Theodoro, A.C., Thomazini, M., Bolini, H.M., & Favaro-Trindade, C.S.** (2013). Double emulsion stage prior to complex coacervation process for microencapsulation of sweetener sucralose, *Journal of Food Engineering, 119*(1), 28-32.

[162] **Callahan, J., Cleary, G., Elefant, M., Kaplan, G., Kensler, T., & Nash, R.** (1982). Equilibrium moisture content of pharmaceutical excipients, *Drug Development and Industrial Pharmacy, 8*(3), 355-369.

[163] **Murikipudi, V., Gupta, P., & Sihorkar, V.** (2013). Efficient throughput method for hygroscopicity classification of active and inactive pharmaceutical ingredients by water vapor sorption analysis, *Pharmaceutical Development and Technology, 18*(2), 348-358.

[164] **Tao, Y., Wang, P., Wang, J., Wu, Y., Han, Y., & Zhou, J.** (2017). Combining various wall materials for encapsulation of blueberry anthocyanin extracts: Optimization by artificial neural network and genetic algorithm and a comprehensive analysis of anthocyanin powder properties, *Powder Technology, 311*, 77-87.

[165] **Rutz, J.K., Borges, C.D., Zambiazi, R.C., Da Rosa, C.G., & Da Silva, M.M.** (2016). Elaboration of microparticles of carotenoids from natural and synthetic sources for applications in food, *Food Chemistry, 202*, 324-333.

[166] **Akbari, N., Mohammadzadeh Milani, J., & Biparva, P.** (2020). Functional and conformational properties of proteolytic enzyme-modified potato

protein isolate, *Journal of the Science of Food and Agriculture, 100*(3), 1320-1327.

[167] **Einhorn-Stoll, U., Kastner, H., Fatouros, A., Krähmer, A., Kroh, L.W., & Drusch, S.** (2020). Thermal degradation of citrus pectin in low-moisture environment–Investigation of backbone depolymerisation, *Food Hydrocolloids, 107*, 105937.

[168] **Ge, J., Yue, X., Wang, S., Chi, J., Liang, J., Sun, Y., . . . Yue, P.** (2019). Nanocomplexes composed of chitosan derivatives and β-Lactoglobulin as a carrier for anthocyanins: Preparation, stability and bioavailability in vitro, *Food Research International, 116*, 336-345.

[169] **Saravanan, M. & Rao, K.P.** (2010). Pectin–gelatin and alginate–gelatin complex coacervation for controlled drug delivery: Influence of anionic polysaccharides and drugs being encapsulated on physicochemical properties of microcapsules, *Carbohydrate Polymers, 80*(3), 808-816.

[170] **Muhoza, B., Xia, S., Cai, J., Zhang, X., Duhoranimana, E., & Su, J.** (2019). Gelatin and pectin complex coacervates as carriers for cinnamaldehyde: Effect of pectin esterification degree on coacervate formation, and enhanced thermal stability, *Food Hydrocolloids, 87*, 712-722.

[171] **Melgosa, R., Benito-Román, Ó., Sanz, M.T., De Paz, E., & Beltrán, S.** (2019). Omega–3 encapsulation by PGSS-drying and conventional drying methods. Particle characterization and oxidative stability, *Food Chemistry, 270*, 138-148.

[172] **Franceschinis, L., Salvatori, D.M., Sosa, N., & Schebor, C.** (2014). Physical and functional properties of blackberry freeze-and spray-dried powders, *Drying Technology, 32*(2), 197-207.

[173] **Kuck, L.S. & Noreña, C.P.Z.** (2016). Microencapsulation of grape (Vitis labrusca var. Bordo) skin phenolic extract using gum Arabic, polydextrose, and partially hydrolyzed guar gum as encapsulating agents, *Food Chemistry, 194*, 569-576.

[174] **Rocha-Parra, D.F., Lanari, M.C., Zamora, M.C., & Chirife, J.** (2016). Influence of storage conditions on phenolic compounds stability, antioxidant capacity and colour of freeze-dried encapsulated red wine, *LWT, 70*, 162-170.

[175] **Saikia, S., Mahnot, N.K., & Mahanta, C.L.** (2015). Optimisation of phenolic extraction from Averrhoa carambola pomace by response surface methodology and its microencapsulation by spray and freeze drying, *Food Chemistry, 171*, 144-152.

[176] **Roos, Y.** (1997). Frozen state transitions in relation to freeze drying, *Journal of Thermal Analysis and Calorimetry, 48*(3), 535-544.

[177] **Weidner, E.** (2009). High pressure micronization for food applications, *The Journal of Supercritical Fluids, 47*(3), 556-565.

[178] **Ray, S., Raychaudhuri, U., & Chakraborty, R.** (2016). An overview of encapsulation of active compounds used in food products by drying technology, *Food Bioscience, 13*, 76-83.

[179] **Hanu, L., Alessi, P., Kilzer, A., & Kareth, S.** (2012). Manufacturing and characterization of water filled micro-composites, *The Journal of Supercritical Fluids, 66*, 274-281.

[180] **Brodkorb, A., Egger, L., Alminger, M., Alvito, P., Assunção, R., Ballance, S., . . . Carrière, F.** (2019). INFOGEST static in vitro simulation of gastrointestinal food digestion, *Nature Protocols, 14*(4), 991-1014.

[181] **Martín, Á., Pham, H.M., Kilzer, A., Kareth, S., & Weidner, E.** (2010). Micronization of polyethylene glycol by PGSS (Particles from Gas Saturated Solutions)-drying of aqueous solutions, *Chemical Engineering and Processing: Process Intensification, 49*(12), 1259-1266.

[182] **Wang, H., Tong, X., Yuan, Y., Peng, X., Zhang, Q., Zhang, S., . . . Xu, J.** (2020). Effect of spray-drying and freeze-drying on the properties of soybean hydrolysates, *Journal of Chemistry, 2020*.

[183] **Correia, R., Grace, M.H., Esposito, D., & Lila, M.A.** (2017). Wild blueberry polyphenol-protein food ingredients produced by three drying methods: Comparative physico-chemical properties, phytochemical content, and stability during storage, *Food Chemistry, 235*, 76-85.

[184] **Bhusari, S., Muzaffar, K., & Kumar, P.** (2014). Effect of carrier agents on physical and microstructural properties of spray dried tamarind pulp powder, *Powder Technology, 266*, 354-364.

[185] **Rodríguez-Hernández, G., González-García, R., Grajales-Lagunes, A., Ruiz-Cabrera*, M., & Abud-Archila, M.** (2005). Spray-drying of cactus pear juice (Opuntia streptacantha): effect on the physicochemical properties of powder and reconstituted product, *Drying Technology, 23*(4), 955-973.

[186] **Igual, M., Ramires, S., Mosquera, L., & Martínez-Navarrete, N.** (2014). Optimization of spray drying conditions for lulo (Solanum quitoense L.) pulp, *Powder Technology, 256*, 233-238.

[187] **Fredes, C., Becerra, C., Parada, J., & Robert, P.** (2018). The microencapsulation of maqui (Aristotelia chilensis (Mol.) Stuntz) juice by spray-drying and freeze-drying produces powders with similar anthocyanin stability and bioaccessibility, *Molecules, 23*(5), 1227.

[188] **Mahdavi, S.A., Jafari, S.M., Assadpoor, E., & Dehnad, D.** (2016). Microencapsulation optimization of natural anthocyanins with maltodextrin, gum Arabic and gelatin, *International Journal of Biological Macromolecules, 85*, 379-385.

[189] **Oancea, A.-M., Turturică, M., Bahrim, G., Râpeanu, G., & Stănciuc, N.** (2017). Phytochemicals and antioxidant activity degradation kinetics during thermal treatments of sour cherry extract, *LWT-Food Science and Technology, 82*, 139-146.

[190] **Stănciuc, N., Oancea, A.M., Aprodu, I., Turturică, M., Barbu, V., Ioniţă, E., . . . Bahrim, G.** (2018). Investigations on binding mechanism of bioactives from elderberry (Sambucus nigra L.) by whey proteins for

efficient microencapsulation, *Journal of Food Engineering, 223*, 197-207.

[191] **Wu, G., Hui, X., Mu, J., Brennan, M.A., & Brennan, C.S.** (2021). Functionalization of whey protein isolate fortified with blackcurrant concentrate by spray-drying and freeze-drying strategies, *Food Research International, 141*, 110025.

[192] **Gonçalves, V., Poejo, J., Matias, A., Rodríguez-Rojo, S., Cocero, M., & Duarte, C.** (2016). Using different natural origin carriers for development of epigallocatechin gallate (EGCG) solid formulations with improved antioxidant activity by PGSS-drying, *RSC Advances, 6*(72), 67599-67609.

[193] **De Paz, E., Martín, Á., Duarte, C.M., & Cocero, M.J.** (2012). Formulation of β-carotene with poly-(ε-caprolactones) by PGSS process, *Powder Technology, 217*, 77-83.

[194] **Du, Y.-L., Huang, G.-Q., Wang, H.-O., & Xiao, J.-X.** (2018). Effect of high coacervation temperature on the physicochemical properties of resultant microcapsules through induction of Maillard reaction between soybean protein isolate and chitosan, *Journal of Food Engineering, 234*, 91-97.

[195] **Lévai, G., Martín, Á., Moro, A., Matias, A.A., Gonçalves, V.S., Bronze, M., . . . Cocero, M.J.** (2017). Production of encapsulated quercetin particles using supercritical fluid technologies, *Powder Technology, 317*, 142-153.

[196] **Salgado, M., Rodríguez-Rojo, S., Alves-Santos, F.M., & Cocero, M.J.** (2015). Encapsulation of resveratrol on lecithin and β-glucans to enhance its action against Botrytis cinerea, *Journal of Food Engineering, 165*, 13-21.

[197] **Andersen, O.M. & Markham, K.R.** (2005). *Flavonoids: Chemistry, Biochemistry and Applications*: CRC press.

[198] **Castañeda-Ovando, A., De Lourdes Pacheco-Hernández, M., Páez-Hernández, M.E., Rodríguez, J.A., & Galán-Vidal, C.A.** (2009). Chemical studies of anthocyanins: A review, *Food Chemistry, 113*(4), 859-871.

[199] **Fernandes, I., Faria, A., Calhau, C., De Freitas, V., & Mateus, N.** (2014). Bioavailability of anthocyanins and derivatives, *Journal of Functional Foods, 7*, 54-66.

[200] **Carrillo, C., Kamiloglu, S., Grootaert, C., Van Camp, J., & Hendrickx, M.** (2020). Co-Ingestion of Black Carrot and Strawberry. Effects on Anthocyanin Stability, Bioaccessibility and Uptake, *Foods, 9*(11), 1595.

[201] **Lang, Y., Li, B., Gong, E., Shu, C., Si, X., Gao, N., . . . Meng, X.** (2021). Effects of α-casein and β-casein on the stability, antioxidant activity and bioaccessibility of blueberry anthocyanins with an in vitro simulated digestion, *Food Chemistry, 334*, 127526.

[202] **Jiao, X., Li, B., Zhang, Q., Gao, N., Zhang, X., & Meng, X.** (2018). Effect of in vitro-simulated gastrointestinal digestion on the stability and antioxidant activity of blueberry polyphenols and their cellular antioxidant activity towards HepG2 cells, *International Journal of Food Science & Technology, 53*(1), 61-71.

[203] **Norkaew, O., Thitisut, P., Mahatheeranont, S., Pawin, B., Sookwong, P., Yodpitak, S., & Lungkaphin, A.** (2019). Effect of wall materials on some physicochemical properties and release characteristics of encapsulated black rice anthocyanin microcapsules, *Food Chemistry, 294*, 493-502.

[204] **Xiong, J., Chan, Y.H., Rathinasabapathy, T., Grace, M.H., Komarnytsky, S., & Lila, M.A.** (2020). Enhanced stability of berry pomace polyphenols delivered in protein-polyphenol aggregate particles to an in vitro gastrointestinal digestion model, *Food Chemistry, 331*, 127279.

APPENDICES

APPENDIX A: FT-IR Spectrums

APPENDIX A: FT-IR Spectrums

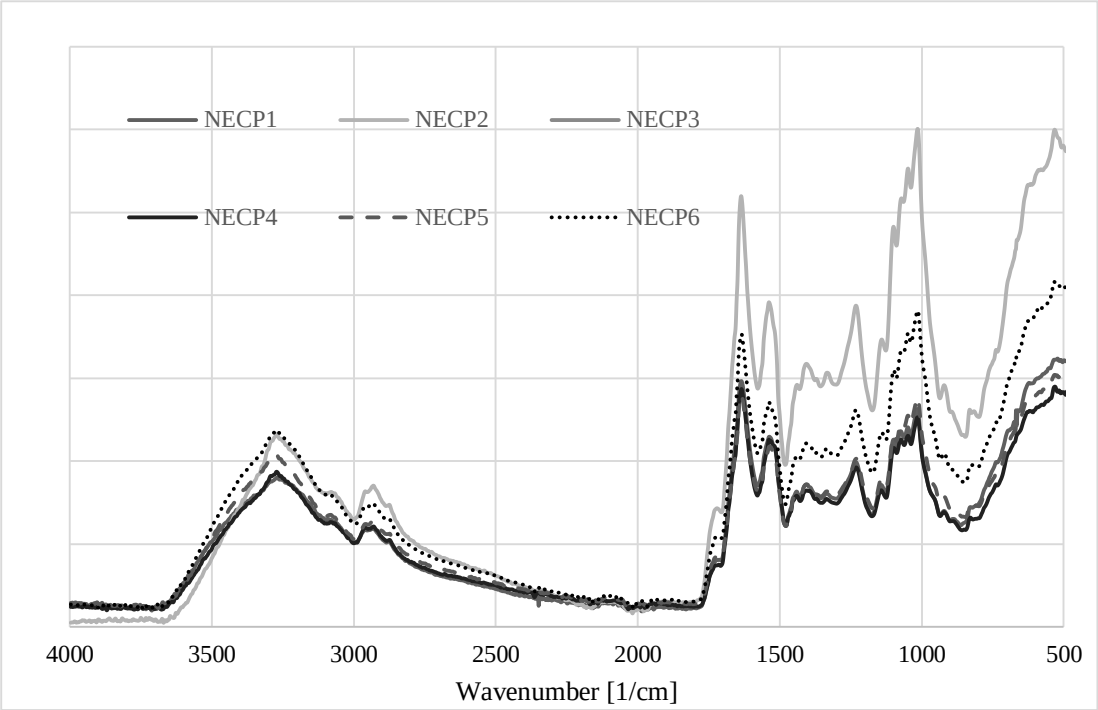

Figure A.1 : FT-IR spectra of non-emulsified BCE loaded PPI-CP particles prepared at different core-to-wall ratio and wall material concentration.

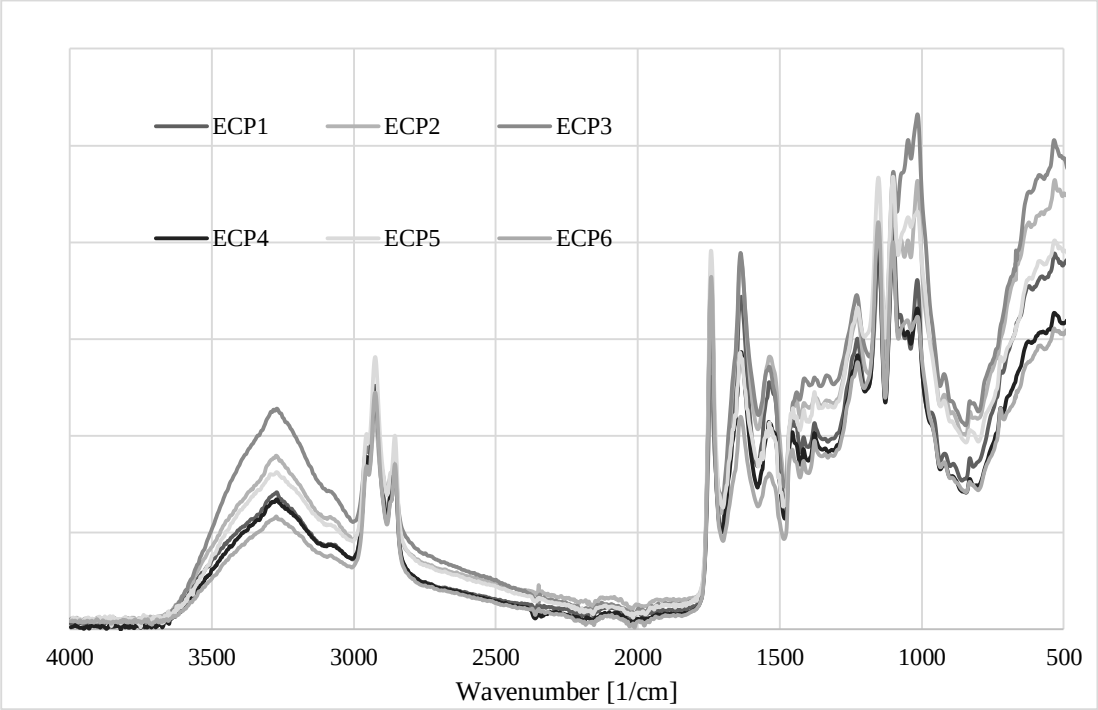

Figure A.2 : FT-IR spectra of emulsified BCE loaded PPI-CP particles prepared at different core-to-wall ratio and wall material concentration.

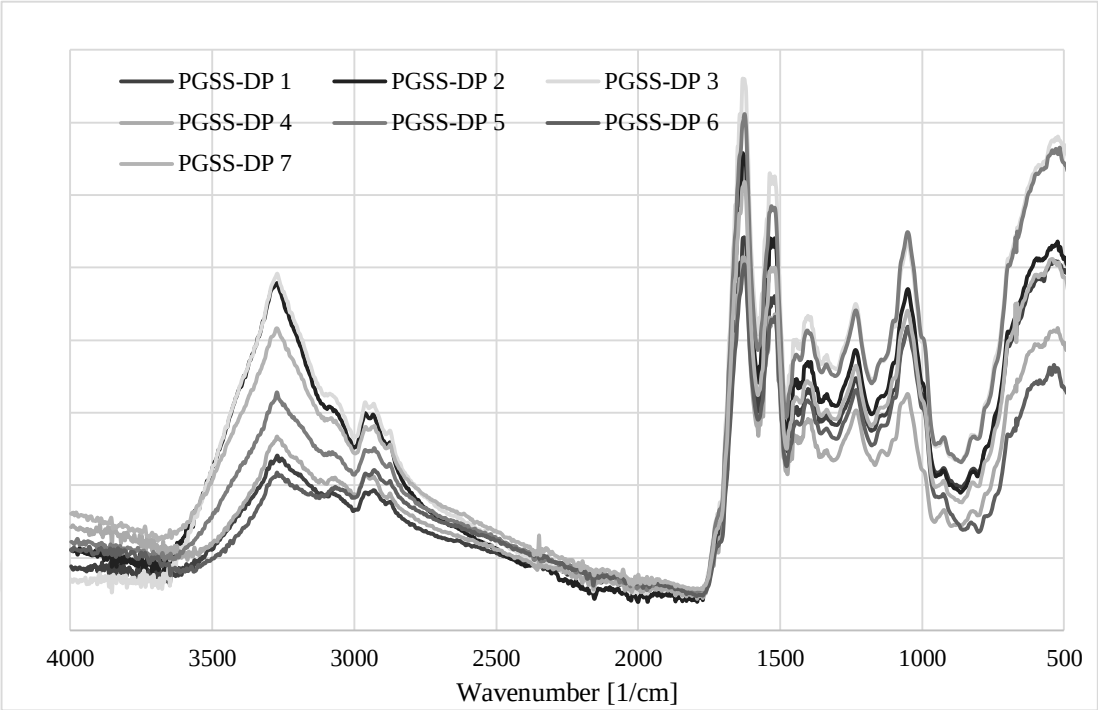

Figure A.3: FT-IR spectra of BCE loaded PPI particles produced by PGSS-Drying with different processing conditions.

CURRICULUM VITAE

Name Surname **:** Merve YAVUZ DÜZGÜN

EDUCATION **:**

- **B.Sc.** **:** 2011, ITU, Food Engineering Department
- **M.Sc.** **:** 2014, METU, Food Engineering Department

PROFESSIONAL EXPERIENCE AND REWARDS:

- 2013-2021 Research and Teaching Assistant, ITU Food Engineering Department
- 2015-2016 ERASMUS Scholarship
- 2019-2020 DAAD German Academic Exchange Service - One Year Research Grant
- 2020 TUBITAK International Research Fellowship Programme – International Doctoral Research Grant

PUBLICATIONS, PRESENTATIONS AND PATENTS ON THE THESIS:

- **Yavuz-Düzgün, M.,** Zeeb, B., Dreher, J., Özçelik, B., & Weiss, J**.** 2020. The Impact of Esterification Degree and Source of Pectins on Complex Coacervation as a Tool to Mask the Bitterness of Potato Protein Isolates. *Food Biophysics*, 15, 376-385.

OTHER PUBLICATIONS, PRESENTATIONS AND PATENTS:

Uluslararası hakemli dergilerde yayınlanan makaleler (SCI & SSCI & Arts and Humanities)

Zeeb, B., **Yavuz-Düzgun, M.,** Dreher, J., Evert, J., Stressler, T., Fischer, L., ... & Weiss, J. 2018. Modulation of the bitterness of pea and potato proteins by a complex coacervation method. *Food & Function*, 9(4), 2261-2269.

Pasli, A. A., **Yavuz-Düzgün, M.,** Altuntas, U., Altin, G., Özçelik, B., Firatligil, E. 2019. In vitro bioaccessibility of phenolics and flavonoids in various dried vegetables, and the determination of their antioxidant capacity via different spectrophotometric assays. *International Food Research Journal*, 26(3), 793-800.

Yücetepe, A., **Yavuz-Düzgün, M.,** Şensu, E., Bildik, F., Demircan, E., & Özçelik, B. 2021. The impact of pH and biopolymer ratio on the complex coacervation of Spirulina platensis protein concentrate with chitosan. *Journal of Food Science and Technology*, 58(4), 1274-1285.

Aĝirbaş, H. E. T., **Yavuz-Düzgün, M.,** & Özçelik, B. 2021. The effect of fruit seed flours on Farinograph characteristics of composite dough and shelf life of cake products. *Journal of Food Measurement and Characterization*, 1-12.

Uluslararası kitaplardaki bölümler:

Ozcelik, O., & **Yavuz, M.** 2016. Watermelon juice. In *Handbook of Functional Beverages and Human Health* (pp. 553-562): CRC Press.

Yavuz-Duzgun, M., Altuntas, U., Gultekin-Ozguven, M., & Ozcelik, B. 2018. Communicating Food Safety: Ethical Issues in Risk Communication. In *Food Ethics Education* (pp. 157-166). Springer, Cham.

Kasapoğlu, K. N., Daşkaya-Dikmen, C., **Yavuz-Düzgün, M.,** Karaça, A. C., & Özçelik, B. 2019. Enrichment of Beverages with Health Beneficial Ingredients. In *Value-Added Ingredients and Enrichments of Beverages* (pp. 63-99). Academic Press.

Ulusal hakemli dergilerde yayınlanan makaleler:

Yavuz, M. & Ozcelik, B. 2016. Functional properties of plant protein isolates. *Academic Food Journal*, 14(4), 424-430.

Diğer ulusal dergilerde yayınlanan makaleler

Yavuz, M. & Ozcelik, B. 2013. Toxic compounds formed after heat processes. *Dünya Gıda Dergisi,* 2013-*09*, 33-36.

Altuntas, U., **Yavuz, M.,** Yücetepe, A. & Ozcelik., B. 2014.Safety of Food Packages and Migration of Toxic Substances to Food. *Dünya Gıda Dergisi,* 2014-09, 90-97.

Yavuz, M. & Ozcelik B. (2015) The effects of novel technologies on quality and health effects of watermelon juice. *Drink İçecek ve Teknolojileri Dergisi,* 92, 76-79.

International Oral Presentations

Yavuz-Duzgun, M., Gulkirpik, E., Ozel, N., & Ozcelik, B. (2017) Supercritical CO_2 extraction of anthocyanins from black carrots. Journal of Food Processing Technology, 8:9(Suppl), 19th International Conference on Food Processing & Technology. Paris, France, October 23-25, 2017, DOI:10.4172/2157-7110-C1-068.

International Poster Presentations

Yavuz Düzgün M., Kapci B. , Özçelik B., " 3-MCPD and Glycidyl Esters Formation During Food Processing: Presence in Foods, Toxicity, Legal Regulations and Mitigation Strategies ", 2nd International Conference on Advanced Engineering Technologies, Bayburt, Türkiye, September 21-23, 2017, pp.1651-1658

Özçelik B., Altın G., **Yavuz Düzgün M.,** Daşkaya Dikmen C., Kasapoğlu K.N., "Nano and Micro Encapsulation of Bioactive Compounds", 2nd International Conference on

Advanced Engineering Technologies, Bayburt, Türkiye, September 21-23i 2017, pp.1329-1340

Yavuz, M., Altuntas, U., Paslı, A., Karateke, C., Taskiran, O., Ozcelik, B. (2017) Dried Leafy Green Vegetables: Investigation of In Vitro Bioaccessability Of Total Phenolic And Total Flavonoid Content. 5th International Conference on Food Digestion. Rennes, France, April 4-6, 2017, Abstract No. P25; p.85

Yavuz, M., Altuntas, U., Pasli, A., Karateke, C, Taskiran, Ö. & Özçelik, B. (2016) In vitro bioaccessability of phenolics and antioxidant capacity in various dried vegetables. Black Sea Association of Food Science and Technology Congress. Ohrid, Macedonia, September 22-24, 2016, p.72.

Yavuz, M., Sensoy, I. & Ozcelik, B. (2014) Effect of some health-promoting ingredients on the quality of wheat flour extrudates. EFFOST Innovations in Attractive and Sustainable Food for Health. Uppsala, Sweden, November 25-28, 2014, Abstract No. P1.066.

Yavuz, M., Sensoy, I. & Ozcelik, B. (2014) Acrylamide Level and Quality of Extrudates After Quercetin Addition. ISNFF Functional Foods, Nutraceuticals, Natural Health Products and Dietary Supplements. Istanbul, Turkey, October 14-17, 2014, Abstract No. 21.

Tok, E., **Yavuz, M.,** & Ozcelik, B. (2014) Effect Of Map And Hıgh Pressure Homogenızer On The B-Caroten Level Of Carrots. ISNFF Functional Foods, Nutraceuticals, Natural Health Products and Dietary Supplements. Istanbul, Turkey, October 14-17, 2014, Abstract No. 32.

Altin, G., **Yavuz, M.,** & Ozcelik, B. (2014) Encapsulation of Cocoa Phenolics in Chitosan-Coated Liposomes. ISNFF Functional Foods, Nutraceuticals, Natural Health Products and Dietary Supplements. Istanbul, Turkey, October 14-17, 2014, Abstract No. 320.

Kapci, B., **Yavuz, M.,** Saygun, A., & Aran, N. (2011) The effects of different carbon and nitrogen sources on sporulation in Bacillus indicus HU36. 2011 IFT Annual Meeting and Food Expo, Abstracts of Papers Presented New Orleans, Louisiana, USA, June 11-14, 2011, Abstract No. 198-19; p. 158.

National Poster Presentations

Yavuz, M., Ozel, N., Gulkirpik, E., & Ozcelik, B. (2016) Natural Colour Production from Plant Wastes by Supercritical CO_2 Extraction. National Food, Metabolism and Health: Bioactive Components and Natural Food Ingredients Congress. Istanbul, November 28, 2016, p.192.

Tuna, H. E., **Yavuz, M.,** & Ozcelik, B. (2016) Volarization of Pomagranade Seeds in Cake Production. National Food, Metabolism and Health: Bioactive Components and Natural Food Ingredients Congress. Istanbul, November 28, 2016, p.199.

Kavassan, D., Kayacan, S., Ercan, S., Dogal, S., **Yavuz, M.,** Erdil., D. N. & Ozcelik, B. (2016) The taste profile of water kefir (Turkish traditional beverage) produced with different fruits. National Food, Metabolism and Health: Bioactive Components and Natural Food Ingredients Congress. Istanbul, November 28, 2016. p.200.

Yavuz, M. & Ozcelik B. (2013) Reduction of acrylamide level in potato strips covered with cowpea flour. II. International Food R&D Congress. Izmir, June 3-4, 2013, Abstract No. P61

Yavuz, M. & Ozcelik, B. (2013) Acrylamide formation in breakfast cereals. 4th Food Safety Congress, Istanbul, May 14-15, 2013, Abstract No. P105; s. 135.